UNDERSTANDING THE PHYSIOLOGY OF PSEUDOMONAS AERUGINOSA BIOFILMS IN AN IN VITRO CHRONIC WOUND MODEL

by

Benjamin Michael White

A thesis submitted in partial fulfillment
of the requirements for the degree

of

Master of Science

in

Microbiology

MONTANA STATE UNIVERSITY
Bozeman, Montana

November 2016

©COPYRIGHT

by

Benjamin Michael White

2016

All Rights Reserved

DEDICATION

To my wife and best friend Alyssa ReNae White, you've carried me so far. I couldn't have asked for better friend. Thank you for all of your sacrifice and support. To my friend and colleague Tatsuya 'Tats' Akiyama, your encouragement and advice were essential. Thank you. You gave me new direction, challenged the way I think, and helped me grow intellectually.

ACKNOWLEDGEMENTS

I greatly appreciate Tim Hamerly for his help and his mass spectrometry mastery. Tim is responsible for the liquid chromatography mass spectrometry section of this thesis. The training and assistance of Kerry Williamson were indispensable. Because of her expertise and mentorship, our RNA-related work was successful. Thank you for instilling in me the deep paranoia that RNases are everywhere. I'm thankful for the help of my lab mates in both the Franklin and Voyich-Kane labs. Thank you Voyich-Kane lab members, you accommodated me and welcomed me as part of your lab. It meant a lot to me. Thank you.

TABLE OF CONTENTS

1. INTRODUCTION 1

2. MATERIALS AND METHODS 5

Bacterial Strain and Culture Medium 5
Growth in CWE Medium 6
Minimum Inhibitory Concentration of Ciprofloxacin 7
Growth Conditions 7
Quantification of Protein, Carbohydrates, and DNA in Biofilms 9
Preparation of RNA 11
Hybridization, Scanning and Analysis 15
Collection of Metabolic Data 15
Liquid Chromatography Mass Spectrometry 17

3. RESULTS AND DISCUSSION 19

Growth and Biomass of *P. aeruginosa* in CWE Medium 19
Analysis of Expression Data 19
Differential Gene Regulation Upon Biofilm Growth 22
Branched-Chain Amino Acid Degradation 23
Regulation of the TCA Cycle and the Glyoxylate Bypass 27
Isoleucine, Valine, Propionyl-CoA and the TCA Cycle 31
Siderophore Biosynthesis in Biofilms 34
Ciprofloxacin Treatment Alters the Transcriptome of Biofilms 35
DNA Repair, Prophage Genes, and Ciprofloxacin Treatment 39
Expression Upon Ciprofloxacin Treatment and Previous Work 39
Phenazine Biosynthesis and Ciprofloxacin Treatment 42
The Type VI Secretion System is Differentially Expressed 43
The Roles of the T6SS Remain Elusive 44
T6SS Loci are Regulated Differently in *P. aeruginosa* 53
Possible Gene Targets for Resensitizing Biofilms to Ciprofloxacin 61

REFERENCES CITED 65

APPENDICES 78

APPENDIX A: Supplementary Tables 79
APPENDIX B: Supplementary Figures 115

LIST OF TABLES

Table Page

1. Biofilm Functional Annotation Clustering 25

2. Biofilm Gene Enrichment Analysis 36

3. Ciprofloxacin-Treated Biofilm Functional Annotation Clustering 38

4. Ciprofloxacin-Treated Biofilm Gene Enrichment Analysis 40

5. Biofilm T6SS Gene Expression 44

6. Ciprofloxacin-Treated Biofilm T6SS Gene Expression 44

LIST OF FIGURES

Figure Page

1. *P. aeruginosa* Biofilm 21

2. Biofilm Biomass 22

3. Principle Component Analysis of GC-RMA Normalized Data 23

4. Bubble Plot of Gene Expression 24

5. TCA Cycle, Valine Degradation, and Connected Pathways 32

6. Chorismate Metabolism 37

ABSTRACT

Pseudomonas aeruginosa is a common colonizer of cutaneous abrasions and burns. These Gram-negative, aerobic bacteria are problematic due to their natural resilience to antibiotics and their metabolic versatility. *P. aeruginosa* can produce a prodigious extracellular matrix. Within this matrix *P. aeruginosa* can divide and form a multicellular community called a biofilm. Biofilms have become a health concern worldwide, as these communities are highly resistant to antibiotics. This thesis reports the effort to model the wound environment. A chronic wound exudate medium was designed and *P. aeruginosa* was grown at 33˚C under low flow in a drip-flow biofilm reactor. Bacterial cells were grown planktonically and in biofilms. Biofilms were treated with the fluoroquinone, ciprofloxacin for 24 hours and transcriptomic and metabolomic data were collected from treated and untreated biofilms and planktonic cells. Cells growing in biofilms demonstrated a shift in in the regulation of their tricarboxylic acid cycle, amino acid degradation, and siderophore biosynthesis genes as compared to planktonic cells. Ciprofloxacin treatment altered the transcriptomic landscape within the biofilm. Changes were observed in the transcription of DNA repair, prophage, and phenazine biosynthesis genes. An important virulence factor, the type VI secretion system, was also differently regulated in these samples and is likely important for the persistent infection of wounds. From the information collected, target genes have been identified for future gene-knockout and ciprofloxacin susceptibility assays. A reduction in fitness may indicate genes that are relevant drug targets to enhance antibiotic treatment of these resilient communities.

INTRODUCTION

Increased antibiotic resistance is well documented in *Pseudomonas aeruginosa* cells growing in multicellular communities, or biofilms, as compared to planktonic cells[1–14]. The mechanisms responsible for the reduction in antibiotic susceptibility of biofilm inhabiting cells are not well understood. Because of the complexity and heterogeneity of the biofilm community, there are a number of factors that appear to contribute to antibiotic resistance. The first factor that must be considered is that antibiotic diffusion into the biofilm is impaired. Stewart theoretically modeled antibiotic penetration and realized that it did not appear to account for the increased resistance of biofilms to antibiotics[15]. Instead he proposed that differences in metabolism and nutrients could play an important role. Experimental data demonstrate that although some antibiotics, especially aminoglycosides such as amikacin and gentamycin, exhibit slower penetration through biofilms, it does not appear that it is the main mechanism the biofilm's increased resistance[16–21]. Even though slower penetration of some antibiotics may give bacteria time to adapt, this does not explain the increased resistance of biofilm cells to antibiotics that exhibit rapid penetration into biofilms such as ciprofloxacin[19,22]. It has also been considered that genetic differences arise between individuals in the biofilm community and that heterogeneity at the genetic level may contribute to the resilience of biofilms. This does not appear to be the case, Folsom et al. demonstrated that resistance was not due to the selection of genetic mutants when biofilm cells were resuspended in a planktonic state and displayed an increased susceptibility[14]. The reversibility of antibiotic resistance points instead to environmental and physiological factors such as available

oxygen concentrations, nutrient availability, and growth rate as determinants of resistance.

Walters et al. demonstrated the roles of antibiotic penetration, oxygen gradients, and stratified metabolic activity in the biofilm[20]. Oxygen concentrations plummet within the first 50 μm of a mature biofilm[14,20,23] and differences in oxygen concentration can greatly affect the tolerance of *P. aeruginosa* to antibiotics[5,11,23]. Oxygen limitation can lead to slower metabolic processes. In fact, heterogeneity within the biofilm is determined, in part, by available oxygen[24]. Rani et al. reported that, spatially, the availability of oxygen, DNA replication activity, and active protein synthesis all correspond in *Staphylococcus* biofilms[25]. Heterogeneity in protein synthesis had been previously noted in *P. aeruginosa* biofilms, and also corresponded with oxygen penetration[26]. Not only is there heterogeneity in oxygen concentration, DNA replication, and protein synthesis, but differences have been demonstrated in transcription levels in *P. aeruginosa* biofilms[27–29].

The realization of phenotypically different subpopulations in the biofilms has directed focus to understanding biofilm phenotypes. Genes important for antibiotic resistance in biofilms are, in fact, different than those important in planktonic cells. De Kievit and colleagues investigated the role of multidrug efflux pumps in the antibiotic resistance of *P. aeruginosa* biofilms. The efflux pumps MexAB-OprM, MexCD-OprJ, MexEF-OprN, and MexXY are important for antibiotic resistance in planktonic cells; however, they did not account for increased resistance in biofilms[30]. A number of other genes have been implicated as important for biofilm antibiotic resistance[4,7,31,32]. These

different genes may each provide different paths to resistance. This leads to the realization that an in-depth understanding of gene regulation and metabolism is needed to fully appreciate these complex communities and aid in the understanding of their inherently antibiotic-resistant nature.

Over $25 billion is spent every year in United States on the treatment of chronic wounds[33]. In fact, a majority of chronically infected wounds host biofilms[34]. These infections in compromised hosts often persist and wound healing can be delayed indefinitely. It's not just that bacterial cells cause delayed healing, but cells living in the biofilm state have found to be inhibitors of wound healing[35,36]. Biofilm cells are phenotypically different than cells living planktonically and affect wound healing differently than their planktonic counterparts. Decreased cell viability and increased apoptosis in human keratinocytes have been observed after treatment with biofilm-conditioned media compared with planktonically-conditioned media[37]. It was also found that biofilm-conditioned media caused differential transcriptional responses in human keratinocytes including upregulation of pro-inflammatory transcription factors, cytokines, and apoptosis-related genes and down regulation of genes associated with transcription and metabolism[38]. This highlights the importance of not just understanding bacterial infections in wounds, but rather biofilm infections. It is crucial to understand the physiology of bacterial cells involved in infections.

This thesis reports the creation of an *in vitro* system that mimics the abiotic environment of a wound, the growth of *P. aeruginosa* PAO1 in the system, and the analysis of transcriptomic and metabolomics data obtained. The model system employs

the use of a defined medium that mimics the exudates of chronically infected wounds[39–41] in a drip-flow reactor (DFR) at a physiologically relevant temperature and flow rate. The goal of this work was to identify possible biofilm-specific gene targets and metabolic pathways that may participate in antibiotic resistance of *P. aeruginosa* in chronic wounds.

MATERIALS AND METHODS

Bacterial Strain and Culture Medium

P. aeruginosa PAO1 WT was selected for use in this project. A chemically defined chronic wound exudates (CWE) medium was designed for the model. CWE medium was made by mixing 7 solutions. The salt solution contained KCl (4.89 mM), NaCl (110.97 mM), Na_2SO_4 (333 μM), Na_2HPO_4 (1.41 mM), urea (10.66 mM), $NaNO_2$ (64 μM), and TRIS (11.11 mM). HCl (1 N) was added to the salt solution until a pH of 7.5 was reached. The salt solution was then autoclaved. The glucose/lactate solution consisted of sodium L-lactate (334.64 mM) and glucose (45.02 mM) and was sterilized by PES bottle-top filters with 0.2 μm pore size (Fisher Scientific, Waltham, MA). Two amino acid solutions were made. The first consisted of L-alanine (62.86 mM), L-arginine (7.03 mM), L-asparagine (3.57 mM), L-aspartate (36.02 mM), L-cysteine (39.62 mM), L-glutamate (36.81 mM), L-glutamine (47.13 mM), L-glycine (51.26 mM), L-histidine (13.35 mM), L-isoleucine (22.50 mM), L-leucine (44.88 mM), L-lysine (50.51 mM), L-methionine (6.17 mM), L-phenylalanine (22.42 mM), L-proline (137.57 mM), L-serine (25.35 mM), L-threonine (23.30 mM), and L-valine (40.15 mM). The amino acid solution was sterilized using Whatman™ PES syringe filters with 0.2 μm pore size (GE Healthcare). The second amino acid solution, Trp/Tyr solution, was composed of L-tryptophan (2.57 mM) and L-tyrosine (12.45 mM). To dissolve the two amino acids, the pH of the solution was adjusted to 11 with NaOH. The divalent cation solution contained $MgCl_2$ (94.00 mM) and $CaCl_2$ (55.75 mM) and was sterilized by autoclave. The

supplemental solution was created with thiamine (7.54 mM) and nicotinic acid (16.25 mM). An iron solution was added and contains $FeSO_4 \cdot 7H_2O$ (360 μM). Both the supplemental and iron solutions were sterilized using Whatman™ PES syringe filters. Each solution was added to the salt solution in the order that they are listed. The final molarities of the media are as follows: KCl (4.40 mM), NaCl (99.93 mM), Na_2SO_4 (300 μM), Na_2HPO_4 (1.27 mM), urea (9.60 mM), $NaNO_2$ (58 μM), TRIS (10 mM), sodium L-lactate (13.39 mM), glucose (1.80 mM), L-alanine (786 μM), L-arginine (88 μM), L-asparagine (45 μM), L-aspartate (451 μM), L-cysteine (495 μM), L-glutamate (460 μM), L-glutamine (589 μM), L-glycine (641 μM), L-histidine (167 μM), L-isoleucine (281 μM), L-leucine (561 μM), L-lysine (631 μM), L-methionine (77 μM), L-phenylalanine (280 μM), L-proline (1,720 μM), L-serine (317 μM), L-threonine (291 μM), L-valine (502 μM), L-tryptophan (64 μM), L-tyrosine (311 μM), $MgCl_2$ (940 μM), $CaCl_2$ (557 μM), thiamine (7.5 μM), nicotinic acid (16 μM), and $FeSO_4 \cdot 7H_2O$ (0.36 μM). Medium used for antibiotic treatment contained 1 mg/L ciprofloxacin.

Growth in CWE Medium

To start a culture, 3 mL CWE medium is inoculated by stick from the *P. aeruginosa* PAO1 freezer stock and grown overnight at 33˚C shaking at 250 rotations per minute (rpm). The overnight culture is added to 25 mL CWE medium to an optical density (OD) of 0.010 at 600 nm. The culture is then grown at 33˚C shaking at 250 rpm. For DFR biofilm experiments, CWE medium with 10 mM Tris was used.

Minimum Inhibitory Concentration of Ciprofloxacin

An overnight culture of PAO1 was started by inoculating 3 mL of CWE medium in a 15 mL test tube using a stick from the freezer stock. The culture was incubated at 33˚C and shaken at 250 rpm overnight. A starter culture for determining the MIC was started by adding 250 µL of overnight culture to 25 mL of CWE medium in a 125 mL beveled Erlenmeyer flask. The culture was grown until it reached an OD600 of 0.271 (approximately 1.2E8 CFU/mL). The culture was diluted by a factor of 100 with fresh CWE medium. From the diluted culture, 100 µL were added to each well in columns 2-10 in rows D-G in a sterile, clear, 96-well flat-bottom microtiter plate (Evergreen Scientific, Los Angeles, CA). Each culture-loaded well in the microtiter plate contained approximately 1.2E5 cells. Ciprofloxacin was serially diluted and added to each well for final concentrations of 1.00, 0.50, 0.25, 0.13, 0.06, 0.03, 0.02, 0.01, and 0 mg/L. Blanks for each ciprofloxacin concentration were loaded in were loaded in rows B-C. Columns A and H and rows 1 and 12 were loaded with medium to help prevent evaporation in the SpectraMax® Paradigm® plate reader (Molecular Devices LLC, Sunnyvale, CA). The microtiter plate was placed in the plate reader and incubated at 33˚C shaking in a circular path with readings at every 30 minutes for 20 hours.

Growth Conditions

P. aeruginosa planktonic cultures were started by a 1:100 dilution from overnight cultures. Planktonic cultures were grown in 100 mL CWE medium in 500 mL beveled Erlenmeyer flasks in triplicate. Once cultures had reached early logarithmic growth (O.D.

0.250, 1E8 CFU), cultures were harvested. Two samples of 45 mL were collected from each flask in 50 mL Falcon Tubes (Corning Inc., Corning, NY). Samples were spun at 5,125 g for 5 minutes at 4˚C in an Allegra® X-15R Centrifuge (Beckman Coulter, Brea, CA). Supernatant was decanted and frozen. Cell pellets were frozen in the -80˚C freezer. *P. aeruginosa* biofilms were grown in a drip flow reactor (DFR) designed by Biosurface Technologies Corp., Bozeman, MT. One hydroxyapatite-coated glass slide (Clarkson Chromatography, South Williamsport, PA) was placed into each DFR channel. DFR and all connecting input and output connectors and tubes were autoclaved. *P. aeruginosa* PAO1 was started from the freezer stock and grown overnight in CWE medium at 33˚C shaking at 250 rpm. A 1:100 dilution of overnight culture was made and allowed to grow to an OD of 1.0, mid-logarithmic growth. The effluent tubes of the DFR were clamped and the angle of the DFR was adjusted from 10˚ to 0˚. A 1:10 dilution was made of the culture and 5 mL were added to each channel of the DFR. The DFR was incubated for 40 minutes at room temperature (RT) and 20 minutes at 33˚C. Once the DFR had incubated for a total of one hour, the angle was readjusted to 10˚, the effluent tubes were unclamped, the MasterFlex® L/S™ model 7519-20 peristaltic pump (Cole-Parmer, Vernon Hills, IL) was started at a flow rate of 10 mL/hour, and the incubator was set to 33˚C. After the DFR was run for 72 hours, the CWE medium containing 1 mg/L ciprofloxacin was attached to the influent tubes for the ciprofloxacin treatment chambers. The pump was allowed to flow for 24 hours. After a total of 96 hours of growth the *P. aeruginosa* PAO1 biofilms were harvested. Each slide was removed from its chamber using sterile forceps and placed in a 50 mL Falcon Tube (Corning Inc., Corning, NY)

containing 10 mL phosphate buffered saline (PBS) buffer. Slides were scraped using sterile GeneMate 18 cm Cell Lifters (BioExpress, Kaysville, UT). The cell suspension was homogenized by vortexing and passing the suspension through an 18 gauge, 1.5 inch long, Precisionglide® needle and 20 mL syringe (Beckton Dickinson and Co., Franklin Lakes, NJ) twice slowly. Aliquots of 1 mL were collected from the suspension and spun at 10,000 g for 1 minute. The supernatant was removed by pipetting and discarded. Cell pellets were placed into the -80˚C freezer.

Quantification of Protein, Carbohydrates, and DNA in Biofilms

Total protein amounts in biofilm samples were quantified by a Bradford assay. Cell pellets were thawed on ice and 500 µL of H_2O were added to the samples. From the resuspensions, 100 µL were drawn off and added to a microcentrifuge tubes and spun at 9,000 g for 4 minutes. The supernatants were pipetted off of the pellets and discarded. To the pellets, 100 µL of RLT were added and samples were vortexed for 15 seconds. Samples were heated at 65˚C until complete lysis. 10 µL of lysed cells were added to 90 µL of 0.85% NaCl. 1 mL of room temperature Bradford reagent was added to each sample and allowed to incubate for 2 minutes at room temperature. Optical densities of the samples were measured at 595 nm. Standards were prepared from a stock solution of 2mg/ml bovine serum albumin (BSA). Stock solution was diluted into 0.85% NaCl for a total volume of 100 µL. 1 mL of room temperature Bradford reagent was added to each standard and allowed to incubate at room temperature for 2 minutes.

Total carbohydrates in biofilm samples were quantified by a phenol-sulfuric acid

assay[42]. Standards were made by diluting an 80 mg/mL stock solution of D-(+)-galactose (Sigma-Aldrich, St. Louis, MO) by 1,000. The resulting 80 ng/µL galactose solution was diluted to obtain proper standard concentrations. Samples were resuspended in 450 µL H_2O according to procedure. From each resuspension, 150 µL was transferred to new glass test tubes. Concentrated phenol was diluted 1:13 in H_2O to yield a 5% (w/v) phenol. To each tube, 150 µL of the 5% (w/v) phenol solution was added. Tubes were vortexed. To each tube, 750 µL of concentrated sulfuric acid was added rapidly. Tubes were incubated for 10 minutes at room temperature before vortexing. Tubes were then incubated for 30 minutes to develop color. Samples were read at 480 nm and 490 nm.

DNA was isolated from biofilm samples beginning with the procedure "Isolation of bacterial DNA from biological fluids" protocol from the QIAamp DNA Mini Handbook[43] using a QIAGEN Miniprep Kit (QIAGEN) . Samples were resuspended in 180 µL Buffer ATL by passaging the solution 3 times through a 23 gauge, 1 inch long, Precisionglide® needle. To each resuspension, 20 µL proteinase K was added. Samples were vortexed for 30 seconds and then incubated at 56˚C for 1.5 hours with periodic vortexing. Once incubation was complete, samples were briefly spun and 4 µL RNase A (100mg/ml) were added to each. Samples were vortexed for 15 seconds and incubated at room temperature for 2 minutes. After incubation, the samples were briefly spun and 200 µL Buffer AL were added and pulse-vortexed for 15 seconds. Samples were incubated for 10 minutes at 70˚C. Samples were then briefly spun and 200 µL of ethanol were added to each sample and pulse-vortexed for 15 seconds. Samples were briefly spun and the mixtures were added to the QIAamp Mini spin columns and spun for 1 minute at

6,000 g. Spin columns were then placed in clean elution tubes. QIAamp spin columns were then rinsed by adding 500 µL of Buffer AW1 and spinning the samples at 6,000 g for 1 minute. QIAMP Mini spin columns were then placed in clean elution tubes and 500 µL Buffer AW2 were added to each column and columns were spun at 13,000 g for 3 minutes. Columns were then spun for an additional minute to eliminate any residual Buffer AW2. The QIAamp Mini columns were placed in clean 1.5 mL microcentrifuge tubes. To each column, 200 µL H_2O were added and allowed to incubate on the column membrane for 2 minutes. Samples were then spun for 1 minute at 6,000 g. Eluent was reapplied and incubated on the column membrane for 2 minutes and spun for 1 minute at 6,000 g. Total DNA was quantified on the Nanodrop 1000 (Nanodrop Technologies, Wilmington, DE).

Preparation of RNA

A lysozyme mix was prepared by making a 1:20 dilution of lysozyme stock (0.1 g/mL) (Sigma Chemical Co., St. Louis, MO) into TE Buffer (pH 8). Each pellet was suspended in 100 µL of lysozyme mix (5 mg/mL) and vortexed. After incubating 3 minutes at room temperature, 650 µL of Tri-reagent from the Direct-zol™ RNA Miniprep (Zymo Research, Irvine, CA) was added to each lysozyme reaction. The sample was vortexed for 20 seconds and allowed to incubate at room temperature for 5 minutes. The lysed pellets were then placed in a Sorvall® Legend Micro 21R tabletop micro centrifuge (Thermo Scientific, Waltham, MA) and spun at 13,000 g for 4 minutes to pellet cell debris. Each supernatant, approximately 750 µL, was added to 750 µL of

molecular biology grade pure ethanol (Sigma-Aldrich, St. Louis, MO). The mixtures were vortexed. The ethanol/supernatant mixtures were then processed according to the Direct-zol™ RNA MiniPrep RNA Purification protocol beginning at step 2 using the RNA MiniPrep by Zymo Research. Total RNA was quantified on the Nanodrop 1000 (Nanodrop Technologies, Wilmington, DE). RNA aliquots were diluted to a concentration of approximately 200 ng/µL and the quality was verified on a Bioanlayzer 2100 Nanochip (Agilent, Santa Clara, CA).

Purified RNA was diluted to a concentration of 500 ng/µL for Turbo DNase treatments. Reactions were prepared by adding 29 µL of the diluted RNA to a nuclease-free 0.5 mL tube. One µL of 40 U/µL RNase inhibitor, RNasin® (Promega, Madison, WI), was added to each sample as well as 3.5 µL of 10x Turbo DNase Buffer. One µL of 2 U/µL Turbo DNase (Ambion®, Thermo Fisher Scientific, Waltham, MA) was added to each tube, mixed, and briefly spun-down. DNase reactions were incubated at 37˚C for 30 minutes. Tubes were removed briefly spun and an additional 1 µL of Turbo DNase was added to each. Reactions were incubated again for 30 minutes at 37˚C. Once the reactions had incubated, 8 µL of DNase inactivation reagent (Ambion®, Thermo Fisher Scientific, Waltham, MA) were added and mixed. Samples were incubated at room temperature for 3 minutes and mixed 2-3 times. Once they had incubated for 3 minutes, 5 µL of RNase free water was added and samples were mixed and then spun for 2 minutes at 13,000 g at 4˚C. The supernatants, approximately 35 µL, were transferred to fresh tubes.

One µL of Poly-A control RNA (Affymetrix, Santa Clara, CA) was diluted according to the manufacturer's specifications, and was added to approximately 8 µg of

purified RNA samples. One µL of random primers (Invitrogen, Thermo Fisher Scientific, Waltham, MA) at a concentration of 3 µg/µL and 1 µL of SUPERase-In™ RNase Inhibitor (Ambion®, Thermo Fisher Scientific, Waltham, MA) at 20 U/µL were added to the purified RNA for a total volume of approximately 11-13 µL. The reaction was mixed well, spun down and incubated for 10 minutes at 70˚C. Samples were then placed in a -20˚C freezer for 30 seconds and spun down. The first strand master mix was prepared by mixing 6 µL/sample 5x First Strand buffer (Invitrogen, Thermo Fisher Scientific, Waltham, MA), 3 µL/sample 0.1 M DTT (Invitrogen, Thermo Fisher Scientific, Waltham, MA), and 0.6 µL 100 mM dNTPs (Qiagen, Valencia, CA) for a total volume of 9.6 µL/sample. Master mix was added to each sample, mixed, and spun briefly. Samples were incubated at room temperature for 2 minutes before adding 3 µL of SuperScript® II Reverse Transcriptase (Invitrogen, Thermo Fisher Scientific, Waltham, MA) at a concentration of 200 U/µL. Reactions were mixed well and spun down. Reactions were incubated overnight at 42˚C. After the RNA was reverse transcribed overnight, the reactions were removed from the thermocycler and the RNA was hydrolyzed by adding 10 µL of 0.5 M EDTA (Ambion®, Thermo Fisher Scientific, Waltham, MA) and 10 µL of 1 N NaOH (Sigma, St. Louis, MO). Samples were mixed and incubated for 15 minutes at 70˚C. The pH was neutralized by adding 10 µL of 1 N HCl (Sigma, St. Louis, MO). To remove free amines and the degraded RNA templates, the cDNA reaction was cleaned using a Qiagen MinElute kit (Qiagen, Valencia, CA). To each cDNA sample, 10 µL 1 M NaOAc at pH 5.2 (Sigma, St. Louis, MO) and 350 µL PB buffer were added. Samples were transferred to MinElute columns and spun for 1 minute at 13,000 rpm. The effluent

of each sample was reapplied to its column and spun for another 1 minute at 13,000 rpm. The flow-through was discarded and each column was washed by adding 750 µL of PE buffer and spinning the sample for 1 minute at 13,000 rpm. The effluent was discarded and the wash step was repeated. To dry the columns, they were spun for 1 minute at 13,000 rpm. Cleaned cDNA was eluted by applying 15 µL EB buffer to the center of the filter. Each column was incubated for 2 minutes at room temperature and spun for 1 minute at 13,000 rpm. Eluents were reapplied to the column to improve yield. Quantity of cDNA was measured on the Nanodrop 1000 (Nanodrop Technologies, Wilmington, DE).

The buffer for the DNase I was prepared by combining 9 µL H_2O with 1 µL 10x One-Phor-All buffer (GE Healthcare) to make a 1x buffer. DNase I (Thermo Scientific, Waltham, MA) at a concentration of 1 U/µL was diluted to a concentration of 0.6 U/µL with the prepared 1x buffer. The reaction was prepared by combining 2 µL 10x One-Phor-All buffer, approximately 10 µL cDNA, and 1 µL of 0.6 U/µL DNase I for each µg cDNA. DNase I was added to the lid of the reaction to control the length of the digest. DEPC water was added to bring the volume to a total of 20 µL. Reactions were incubated for 2.5 minutes at 37˚C. The DNase was then inactivated by incubating samples at 70˚C for 10 minutes. The cDNA fragmentation was verified using the Bioanlayzer 2100 Nanochip (Agilent, Santa Clara, CA).

To the fragmented cDNA, 5 µL 5x reaction buffer (New England BioLabs® Inc., Ipswich, MA), 2 µL 7.5 mM GeneChip DNA labeling reagent (Affymetrix, Santa Clara, CA), and 2 µL terminal deoxynucleotidyl transferase at a concentration of 20 U/µL (New England BioLabs® Inc., Ipswich, MA) were added. The volume was brought to 50 µL

with water. Samples were mixed, spun, and incubated for 60 minutes at 37˚C. The reaction was stopped by the addition of 2 µL 0.5M EDTA (Ambion®, Thermo Fisher Scientific, Waltham, MA). Samples were stored at -20˚C.

Hybridization, Scanning, and Analysis (Kerry Williamson)

Labeled cDNA was hybridized to Affymetrix *Pseudomonas aeruginosa* microarrays (part 900640) for 16 hours at 50˚C with constant rotation. Microarrays were stained using a GCOS Fluidics Station 450 and scanned with an Affymetrix 7G scanner. Affymetrix GCOS v1.4 was used to generate CEL and CHP files. CEL files were imported into FlexArray v1.6.3 for quality control and data analysis[28].

Collection of Metabolic Data

Extracellular metabolite samples from biofilms were collected from DFR effluent lines in 15 mL Falcon Tubes (Corning Inc., Corning, NY). Collection lines were unclamped and allowed to drain for approximately 1 hour before biofilms were harvested. Samples were capped and placed in a -80˚C freezer. After biofilms were harvested, stock medium and ciprofloxacin-containing medium were collected in 50 mL Falcon Tubes and frozen at -80˚C. Extracellular metabolites from planktonic cultures were collected by decanting the supernatant from the pelleting process. Supernatants were placed in the -80˚C freezer for storage. Extracellular metabolite samples were thawed and 1 mL aliquots were dried. Derivatization of sample metabolites was carried out by re-suspending samples in 100 µL acetonitrile and 100 µL N-tert-

Butyldimethylsilyl-N-methyltrifluoroacetamide (MTBSTFA).

Intracellular metabolite samples were prepared by thawing bacterial cell pellets on ice. Pellets were suspended in 300 µL H_2O (Fisher Scientific, Waltham, MA) and transferred to a 2 mL Lysing Matrix B tube (MP Biomedicals LLC, Santa Ana, CA). Tubes were placed in a FastPrep™ FP120 (Thermo Electron Corporation, Thermo Fisher Scientific, Waltham, MA). The speed was set to 6 m/second and the FastPrep™ was run for 20 seconds and then samples were placed on ice for 1 minute. This procedure was repeated two additional times. To each sample, 300 µL of ice-cold methanol (Fisher Scientific, Waltham, MA) were added and allowed to incubate on ice for 3 minutes. The bead beating procedure was followed as before. The lysing matrix was allowed to settle and the top 300 µL of sample was added to 1.4 mL cold acetone (Fisher Scientific, Waltham, MA). Samples were placed in a -80˚C freezer overnight to precipitate cell debris and protein. Samples were then spun in a Sorvall® Legend Mach 1.6R centrifuge (Thermo Fisher Scientific, Waltham, MA) at 20,000 g for 5 minutes at 4˚C. The supernatant was collected and placed in fresh tubes. The precipitate was stored in a -80˚C freezer. The supernatants were placed into a Speed Vac® Plus SC110A (Thermo Fisher Scientific, Waltham, MA) and dried down under vacuum on the medium speed setting. Samples were re-suspended in 25 µL 50:50 H_2O: methanol.

Liquid Chromatography Mass Spectrometry (*Tim Hamerly*)

For reverse phase analysis, a Kinetex 1.7 µm C18 150 mm x 2.1 mm column (Phenomenex, Torrance, CA) kept at 50 °C was used for LC separation with a flow rate

of 600 μL min-1. Solvent A consisted of 0.1% formic acid in water, while solvent B was 0.1% formic acid in acetonitrile. The elution gradient consisted of 2% solvent B for 2 minutes (with the first two minutes going to waste to avoid contaminating the source with excess salt), to 95% solvent B over 24 minutes, held at 95% for 2 minutes, and then returned to 2% for 2 minutes, with a total run time of 30 minutes using an Agilent 1290 UPLC (Agilent, Santa Clara, CA) system connected to an Agilent 6538 Q-TOF Mass Spectrometer (Agilent, Santa Clara, CA).

Normal phase analysis used a Cogent Diamond Hydride HILIC 150 mm x 2.1 mm column (MicroSolv, Eatontown, NJ) was used for LC separation with a flow rate of 600 μL min-1. Solvent A consisted of 0.1% formic acid in water, while solvent B consisted of 0.1% formic acid in acetonitrile. The elution gradient consisted of 95% solvent B for 2 minutes (with the first minute going to waste to avoid contaminating the source with excess salt), to 50% solvent B over 24 minutes, held at 50% for 2 minutes, and then returned to 95% for 2 minutes, with a total run time of 30 minutes using an Agilent 1290 UPLC (Agilent, Santa Clara, CA) system connected to an Agilent 6538 Q-TOF Mass Spectrometer (Agilent, Santa Clara, CA).

Mass spectrometry analysis was conducted in positive ion mode, with a cone voltage of 3500V and a fragmentor voltage of 120V. Drying gas temperature was 350 °C with a flow of 12 L min-1 and the nebulizer was set to 60 psig. Spectra were collected at a rate of 2.52 per second with a mass range of 50 to 1000 m/z. The mass analyzer resolution was 18,000 and post calibration tests had a mass accuracy of approximately one ppm.

Data files from the LC-MS were converted to .MZxml format using the Masshunter Qualitative software provided with Agilent instruments (Agilent, Santa Clara, CA). Analysis of LC-MS data was done using the software package MZmine (version 2.14). Procedures, together with parameters used for the alignment of features and identification in MZmine, were as follows: LC-MS files were imported into MZmine, followed by data set filtering to remove the first minute of elution data for HILIC analysis, and the first two minutes of elution data for RP analysis. A minimum intensity cutoff of 5000 and a minimum elution time window of 0.1 minutes were used to create molecular feature lists. Lists included retention time (R/T) adjusted with a tolerance of 0.2 minutes or less. These R/T-adjusted lists were then aligned into one mass list, and then gap-filled to add missing peaks not detected in all runs with an m/z tolerance of 15.0 ppm. The m/z peak intensities were normalized by normalizing the total ion intensity of each run to the most intense total ion intensity. Significance was determined using a two-tailed T-test.

RESULTS AND DISCUSSION

Growth and Biomass of *P. aeruginosa* in Chronic Wound Medium

Typically, *P. aeruginosa* has a doubling time of approximately 1 to 1.5 hours in minimal media and 25 to 35 minutes in rich media[44]. Chronic wound medium supported a doubling time of 41.8 + 1.2 minutes for *P. aeruginosa*. Cells grew thick biofilms after 96 hours at 33˚C in chronic wound medium at a flow rate of 10 mL/h (Figure 1). $Log_{10}(CFU/cm^2)$ in biofilm samples were measured at 9.1 $\pm$ 0.2. The ciprofloxacin-treated biofilms demonstrated a significant decrease in CFU/cm^2, 7.2 $\pm$ 0.5 $P < 0.001$. These ciprofloxacin-treated biofilms were treated with 1 mg/L ciprofloxacin that was determined to be 16x the MIC as determined for planktonic cells in the chronic wound medium (Supplementary figure 2). There were no differences in protein levels or DNA between untreated and treated samples as determined by two-tailed T test (Figure 2a,b). Significantly higher amounts of hexose and pentose were observed in untreated biofilms ($P < 0.01$, $P < 0.05$) (Figure 2c,d).

Analysis of Expression Data

Microarray data was normalized by GC-RMA (Supplementary Figure 3). Samples from each of the growth conditions clustered with samples of the same group (Figure 3). Scatter plots of sample mean reveal a coefficient of multiple regression of 0.73 for the planktonic and biofilm microarray data and 0.80 for untreated biofilm and treated biofilm data.

Figure 1. *P. aeruginosa* Biofilm. Shown is a representative *P. aeruginosa* biofilm grown at 33°C for 96 hours in a DFR with 10 mL/h chronic wound medium. Arrow indicates point of medium entry.

Figure 2. Biofilm Biomass. Protein concentrations were determined by Bradford assay for biofilm ciprofloxacin-treated (gray) and untreated samples (green) (a). Average µg DNA/cm^2 was obtained for biofilm ciprofloxacin-treated and untreated samples (b). Carbohydrate concentrations were determined using a phenol-sulfuric acid colorimetric assay. Hexoses were measured at λ490 (c) and pentoses were measured at λ480 (d).

a.

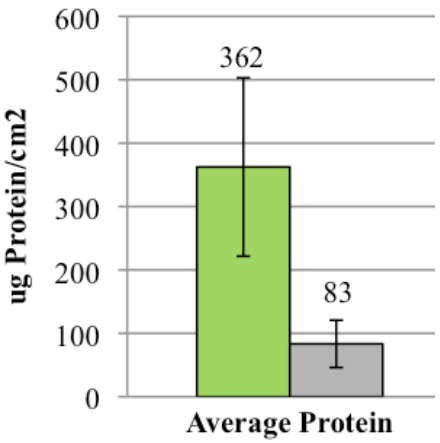

b.

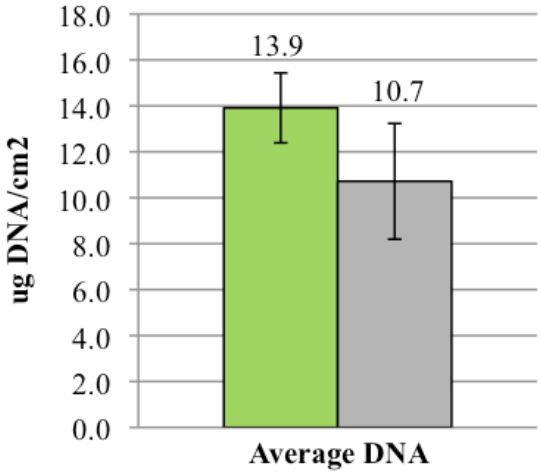

c.

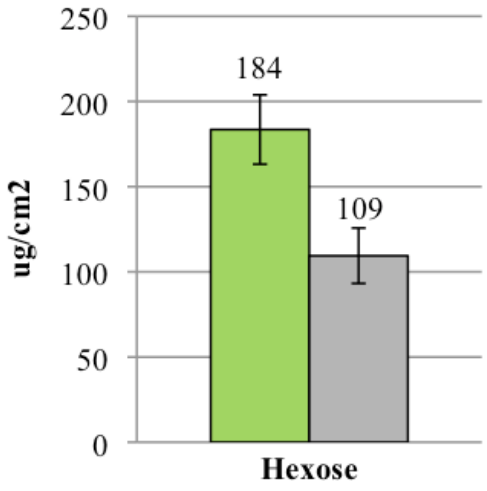

d.

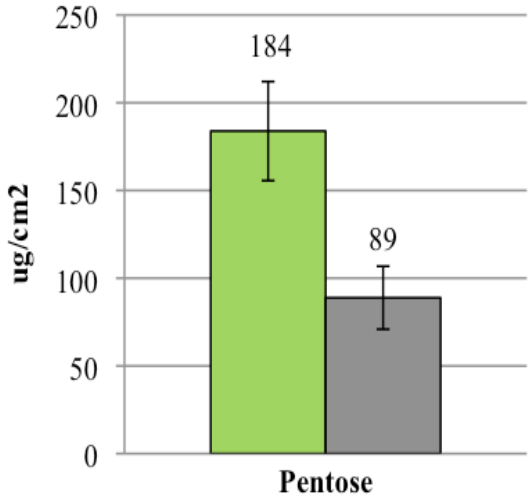

Figure 3. Principle Component Analysis of GC-RMA Normalized Data. Ciprofloxacin-treated biofilm samples and biofilm control samples cluster together based on component 1. Component 1 allows for the separation of planktonic samples from the two sets of biofilm samples. Treated and untreated biofilms separate along component 2.

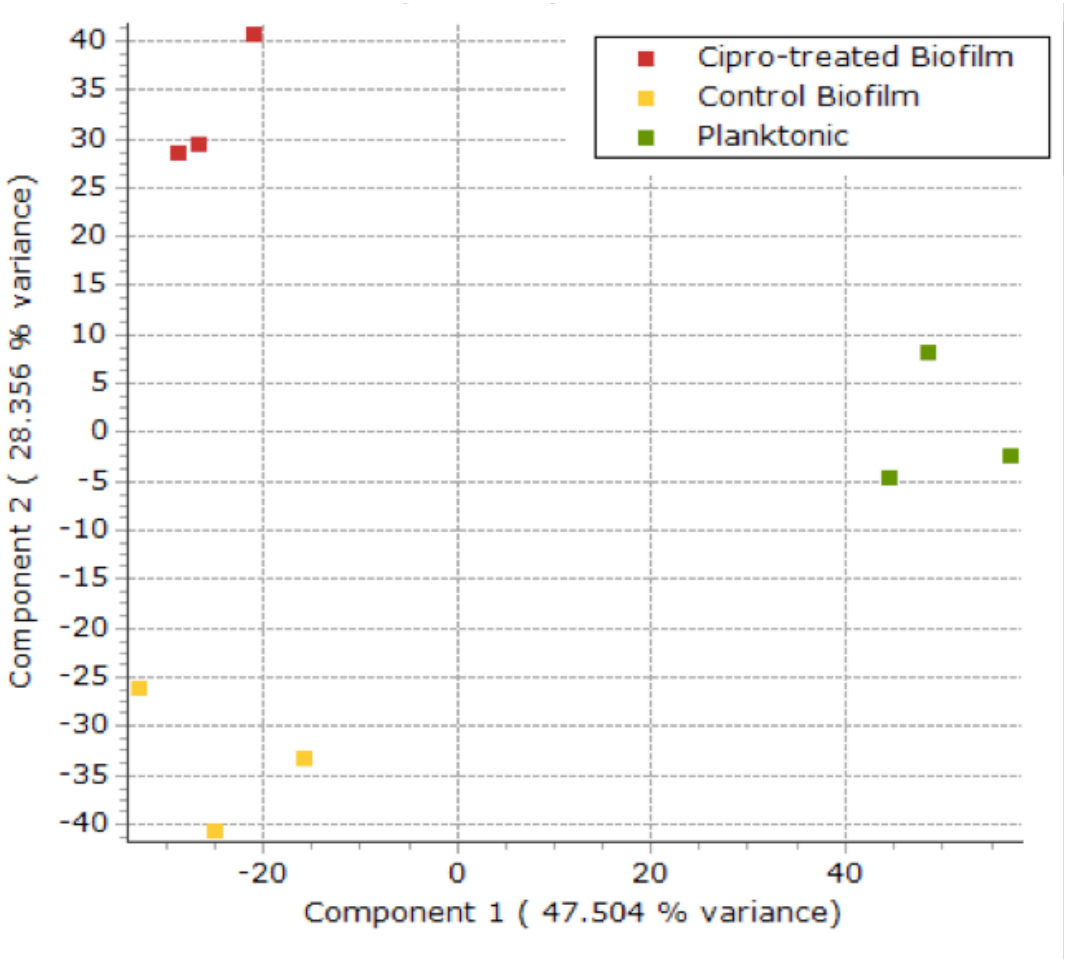

Differential Gene
Regulation upon Biofilm Growth

Based on a 2-fold difference in transcript abundance and an adjusted $P \leq 0.1$, *P. aeruginosa* grown in biofilms had 301 up-expressed genes and 462 down-expressed genes compared to mid-exponentially grown planktonic cells (Figure 4a). In order to recognize metabolic pathways that are differentially regulated between 96 hour biofilms

and planktonic cells grown to exponential phase, the adjusted gene lists were each submitted to analysis on the Database for Annotation, Visualization and Integrated Discovery (DAVID)[45,46]. The functional annotation clustering results of the DAVID analysis revealed the down-expression of a number of groups in biofilms including genes associated with translation, nitrogen compound biosynthetic processes, amino acid metabolism, as well as decreased expression of genes involved in central carbon metabolism (Table 1). These results correspond to a previous study in our lab examining the differences in expression of 72-hour biofilms grown in DFRs with exponential-phase planktonic cells. It is expected that the gene expression, as well as overall metabolic rate, is lower in biofilms due to oxygen and nutrient limitation. Since biofilm samples are homogenized, it is anticipated that, although the top layer of the biofilm may be active, genes associated with active metabolism will appear to be expressed at a lower abundance than planktonic cells.

It is important to note that although there is an overall decrease in gene expression in biofilm samples compared to planktonic samples, two gene ontology groups were up-expressed in the biofilm samples. Surprisingly, these two groups were different from what had previously been found[47]. Biofilm samples demonstrated a higher expression of siderophore biosynthesis genes as well as genes involved in the degradation of valine, leucine and isoleucine (Table 1).

Branched-chain Amino Acid Degradation

Up-expression of the genes in these pathways may provide insights into important survival mechanisms for *P. aeruginosa*. We observe increases in leucine dehydrogenase

Figure 4. Bubble Plot of Gene Expression. Genes with log2 fold change greater than 1 or less than -1 and an adjusted P < 0.1 were plotted. Circle diameter represents (1/adjusted P value). The larger the diameter, the more significant the P value. Genes up-expressed in biofilm samples are green and those down-expressed are red (a). Genes expressed differently upon ciprofloxacin treatment were plotted; green points indicate up-expression when treated with ciprofloxacin whereas red represents down-expressed genes (b). *oprD*, PA0958, had a much more significant adjusted P value (P = 2.7E-3) than other genes plotted. In order to visualize the other genes and compare relative P values, *oprD* was scaled down and marked with a black border and a patterned fill.

a.

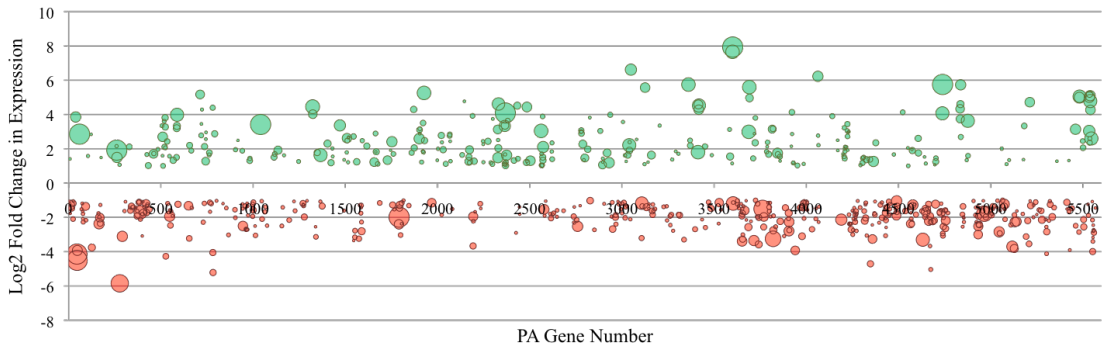

b.

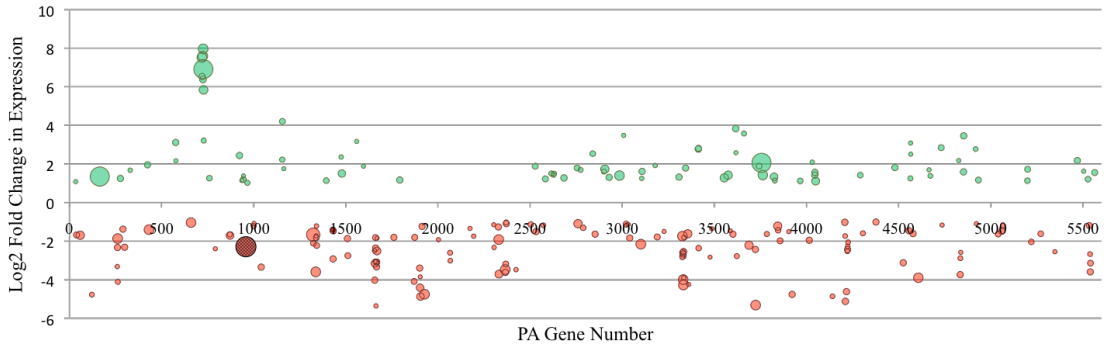

Table 1. Gene enrichment analysis of *P. aeruginosa* PAO1 biofilms compared to planktonically grown cells. DAVID analysis of functional annotation clustering was used, gene ontology groups with Enrichment Score > 1.30 and P values < 0.01 were selected.

Gene Ontology Term	Gene Count	P value
Down-Expressed in Biofilm		
Translation	50	6.36E-30
Nitrogen Compound Biosynthetic Processes	76	3.58E-22
Ligase	29	1.11E-21
Protein Biosynthesis	19	6.19E-18
Nucleotide-Binding	69	1.07E-17
Amino Acid Biosynthesis	23	2.37E-15
Carboxylic Acid Biosynthesis	43	2.84E-12
Purine Nucleotide Biosynthetic Process	21	4.96E-11
Metal-Binding	40	9.21E-11
Cell Inner Membrane	25	3.11E-08
Pyrimidine Metabolism	16	1.06E-07
Pyridoxine Biosynthesis	5	1.54E-06
Pentosyl-Transferase Activity	9	3.06E-06
Lipid Biosynthetic Processes	24	3.69E-06
Arginine Biosynthesis	6	1.83E-05
Water-Soluble Vitamin Biosynthetic Process	18	2.37E-05
GTP-Binding	8	3.25E-05
Glycolysis	6	6.54E-05
Cofactor Metabolic Processes	30	7.28E-05
Histidine Biosynthesis	5	2.61E-04
Glycine, Serine, and Threonine Metabolism	12	3.47E-04
Decarboxylase	6	4.64E-04
Alanine, Aspartate, and Glutamate Metabolism	10	5.76E-04
DNA Topoisomerase Activity	4	6.45E-04
Glutamine Family Amino Acid Biosynthetic Process	9	9.67E-04
Isoprene Biosynthesis	4	1.41E-03
Rotamase	6	1.73E-03
Fatty Acid Biosynthesis	7	3.56E-03
Tricarboxylic Acid Cycle	8	5.24E-03
Serine Family Amino Acid Metabolic Processes	8	6.27E-03
Up-Expressed in Biofilm		
Biosynthesis of Siderophore Group Nonribosomal Peptides	4	9.08E-05
Valine, Leucine, and Isoleucine Degradation	8	9.29E-05

transcripts (PA3418) in biofilms as well as all three components of the branched-chain keto acid dehydrogenase complex, Bkd (PA2247-9). Interestingly, for leucine catabolism there is no difference in the expression of genes that are responsible for the conversion of the product 3-methylcrotonyl-CoA to acetyl-CoA and acetoacetate (PA2011-4). Increases in expression of genes involved in valine degradation beyond the Bkd complex were observed. These genes include an enoyl-CoA hydratase (PA0745, E = 3.35e-66, $\log_2$ FC = 2.95, adjusted P < 0.1), a 3-hydroxyisobutyryl-CoA hydratase (PA0744, E = 1.22e-105, $\log_2$ FC = 2.56, adjusted P < 0.1), a 3-hydroxyisobutyrate dehydrogenase (PA0743, E = 4.55e-108, $\log_2$ FC = 1.28, adjusted P < 0.05), and a methylmalonate-semialdehyde dehydrogenase (PA0747, E = 0e+00, $\log_2$ FC = 1.71, P = 3.80E-02, adjusted P > 0.1) (Supplementary Table 1). Our data show that there are no differences in the regulation of the genes involved in the conversion of leucine degradation product methylcrotonyl-CoA to acetyl-CoA and acetoacetate, but there are increases in transcript abundance of genes involved in the conversion of valine to propionyl-CoA. The utilization of branched-chain amino acids is important in our wound model system, and may represent response to carbon starvation. Metabolite data was analyzed and valine was putatively identified. Decreased levels of valine were observed in biofilms compared to planktonic cells (FC = 21.98, P = 7E-03) (Supplementary Table 5). Although more repetitions are needed, the extracellular metabololite data is in agreement with these data. More valine, leucine, and isoleucine were consumed from the medium in samples that were growing in biofilms (Supplementary Figure 8). Work in the Carlson lab demonstrated that under carbon-limiting conditions isoleucine, leucine, and valine provided the highest energy yield to

production cost for biomass in *Geoarchaeum* str. OSPB[48]. The utilization of these amino acids may be preferential for generating energy and biomass in a limiting environment such as a biofilm. The use of this pathway and branched-chain amino acids could have large effects on central carbon metabolism as propionyl-CoA has been shown to inhibit pyruvate dehydrogenase, a key enzyme complex in central carbon metabolism, in *Rhodobacter sphaeroides*[49] and *Aspergillus nidulans*[50].

Regulation of the TCA Cycle and the Glyoxylate Bypass

Regulation of citrate synthase is important since it catalyzes the first limiting step of the cycle, the synthesis of the six carbon acid, citrate, from oxaloacetate and acetyl-CoA. It has been found that citrate synthases of Gram-negative bacteria are inhibited by the presence of NADH, where as those in Gram positive bacteria are not. In fact, citrate synthases in Gram-negative bacteria are larger than those of Gram-positive bacteria as well as eukaryotic organisms and only the large citrate synthases are allosterically inhibited by NADH[51]. These citrate synthases are categorized into two distinct groups, type I and type II, based on the size. Type I citrate synthases are the smaller of the two categories and form homodimers. Type I citrate synthases are found in eukaryotes, Gram-positive bacteria, and archaea[52]. The larger hexameric citrate synthase enzyme complexes, type II, are found only in Gram-negative bacteria[52]. Organisms that contain citrate synthases type II that are sensitive to NADH are also divided into two subclasses: those whose activity is restored by the presence of AMP and those whose inhibition is unaffected by AMP[53]. In this way, a high ratio of AMP to ATP or NAD^+ to NADH in the

cell provides the signal to begin energy production via the TCA cycle. Conversely, the accumulation of ATP and NADH allows the organism to down-regulate citrate synthase and transition to a lower metabolic state to conserve energy and carbon.

Regulation of the type II class is not limited only to the presence of ATP and NADH, within the type II class of citrate synthases, there are those that are sensitive to inhibition by 2-oxoglutarate and those that are not. Interestingly, Gram negative bacteria that are strict aerobes contain citrate synthases that are insensitive to inhibition by 2-oxoglutarate whereas those found in facultative anaerobes are sensitive[51,53]. The citrate synthase in *P. aeruginosa* is inhibited by NADH, but not by the TCA cycle intermediate 2-oxoglutarate[51]. 2-oxoglutarate accumulations may serve as an important adaptation for survival under starvation and oxidative stress, and thus, it may be important to note that citrate synthase is not inhibited by the increase in abundance of the metabolite. It is also important to note that the possibility of a second citrate synthase, a type I, in *P. aeruginosa* was realized in 1983 by Solomon and Weitzman[54]. That same year, Patton and colleagues made the same realization with *E. coli*[55]. Further work has identified a citrate synthase type I, a methyl-citrate synthase, in *E. coli*[56]. Mitchell identified that the citrate synthase type II (oppositely labeled as CSI) was more expressed during early exponential growth and then alternated with citrate synthase type I (CSII) during late exponential and stationary growth phases[57]. This observation aligns with our transcriptomic data. Up-expression of *gltA* (PA1580) is observed in planktonically grown samples ($\log_2$ FC = 1.28, adjusted P < 0.1) and *prpC* (PA0795) transcripts are observed at borderline higher levels in biofilm growth ($\log_2$ FC = 1.48, P = 8.82E-02, adjusted P >

0.1).

Once acetyl-CoA and oxaloacetate are condensed to citrate by citrate synthase, citrate can then be directed to citrate aconitase. The genome of *P. aeruginosa* harbors two genes that encode proteins with aconitate hydratase activity, *acnA* (PA1562) and *acnB* (PA1787). Another gene has been identified as possibly having this activity (PA0794). Our data indicate an up-expression of *acnA* ($\log_2$ FC = 1.24, adjusted P = 3.81E-02) in biofilm samples but no difference in *acnB* or PA0794. Aconitases are responsible for the interconversion of citrate, cis-aconitate, and isocitrate. In biofilm growth *acnA* was up-expressed as compared to its expression during planktonic growth. The up-expression of *acnA* is perplexing since it is the only TCA cycle gene to be up-expressed in biofilms. The reaction that its enzyme catalyzes produces a metabolite, isocitrate, which can have two fates as it progresses along the TCA cycle. Isocitrate can be shuttled into the glyoxylate shunt, or it can continue through the rest of the TCA cycle.

The utilization of the glyoxylate by-pass allows the cell to bypass 3 TCA cycle steps. The first bypassed step is the oxidation and decarboxylation of isocitrate to 2-oxoglutarate by isocitrate dehydrogenase, which reduces $NADP^+$ to NADPH and releases CO_2. This reaction rests at a branch point of central carbon metabolism. The next step is the conversion of 2-oxoglutarate into succinyl-CoA by 2-oxoglutarate dehydrogenase (PA1585-7), which produces NADH and CO_2. The last of these 3 steps is the conversion of succinyl-CoA by succinyl-CoA synthetase (PA1588-9) to succinate, GTP, and free CoA. It is interesting that there is a down regulation of transcripts for isocitrate dehydrogenase Idh (PA2624), 2-oxoglutarate dehydrogenase, and succinyl-CoA

synthetase in our data. This realization, in conjunction with up-expressed isocitrate lyase AceA (PA2634, $\log_2$ FC = 1.16, P = 3.38E-02, adjusted P > 0.1), identified before Benjamini-Hochberg, pointed to utilization of the glyoxylate bypass under biofilm conditions. Díaz-Pérez and colleagues identified AceA as a key enzyme involved in leucine catabolism[58]. It was perplexing that no up-expression was observed for malate synthase GltB (PA0482), the important second step of the glyoxylate bypass, which is responsible for the condensation of acetyl-CoA with glyoxylate to form malate. It has been found that isocitrate lyase provides precursors to hydrogen cyanide (HCN) production[59]. The role of AceA as a virulence factor has been demonstrated in an alfalfa infection model as well as a rat lung infection model[60]. Although *gltB* is not up-expressed, it may still be an active participant in metabolism.

The down-expression of isocitrate dehydrogenase and its possible posttranslational regulation could change the flux of isocitrate into the glyoxylate bypass. Differences in expression at this point of the TCA cycle are important for overall metabolism. Unlike most Gram-negative bacteria, *P. aeruginosa* contains two divergently transcribed genes each coding for an isocitrate dehydrogenase. These isozymes, Idh and Icd (PA2623), are, as most bacterial isocitrate dehydrogenases, $NADP^+$ - dependent but are functionally different. The Icd enzyme functions as a monomer and can reach a higher activity in planktonic stationary growth than Idh, which functions as a homodimer[61]. Their differences in activity lead to the natural assumption that these enzymes have different roles in *P. aeruginosa*. These isocitrate dehydrogenases are interesting targets for further study because of their pivotal position in determining the

fate of isocitrate in the TCA cycle. Due to their pivotal role in pathway determination isocitrate dehydrogenases are under strict regulation in the cell. The activity of isocitrate dehydrogenase is partially controlled by the bifunctional isocitrate dehydrogenase kinase/phosphatase AceK (PA1376). In *E. coli* the activity of the isocitrate dehydrogenase homodimer is abrogated upon phosphorylation by AceK[62]. The transcript levels of the succinate dehydrogenase enzyme complex, SdhABCD (PA1581-4), were unchanged between growth conditions as were the gene expression levels for the remaining steps of the TCA cycle (Figure 5).

Isoleucine, Valine,
Propionyl-CoA, and the TCA Cycle

Propionyl-CoA, a product of branched-chain amino acid degradation and β-oxidation of odd chain fatty acids, can be converted to succinate and pyruvate. This process can be executed by the 2-methylcitrate cycle. Although little research has explored the 2-methylcitrate cycle in *P. aeruginosa*, 2-methylcitrate synthase, *prpC*, has *prpC* and *gltA*. Citrate synthase is an important enzyme under complex regulation. PrpC is responsible for the condensation of oxaloacetate and propionyl-CoA to 2-methylcitrate. The conversion of 2-methylcitrate to 2-methyl-cis-aconitate is catalyzed by PrpD, a methyl-citrate dehydrogenase (PA0792). 2-methyl-cis-aconitate is then converted to methylisocitrate. This could be due to the involvement of *acnA* in the glyoxylate bypass, its involvement in the conversion of methyl-aconitate to methylisocitrate, or both. It is also peculiar that *acnA* is the only TCA cycle gene that is up-expressed in biofilm

Figure 5. TCA Cycle, Valine Degradation, and Connected Pathways. Genes that are up-expressed in biofilms are green, genes that are down-expressed are red. Genes listed by commas participate in a complex or work together. Those listed by semicolons share the same function, but do not rely on each other. Significantly regulated genes (FC > 2, adjusted P < 0.1) are listed in bold.

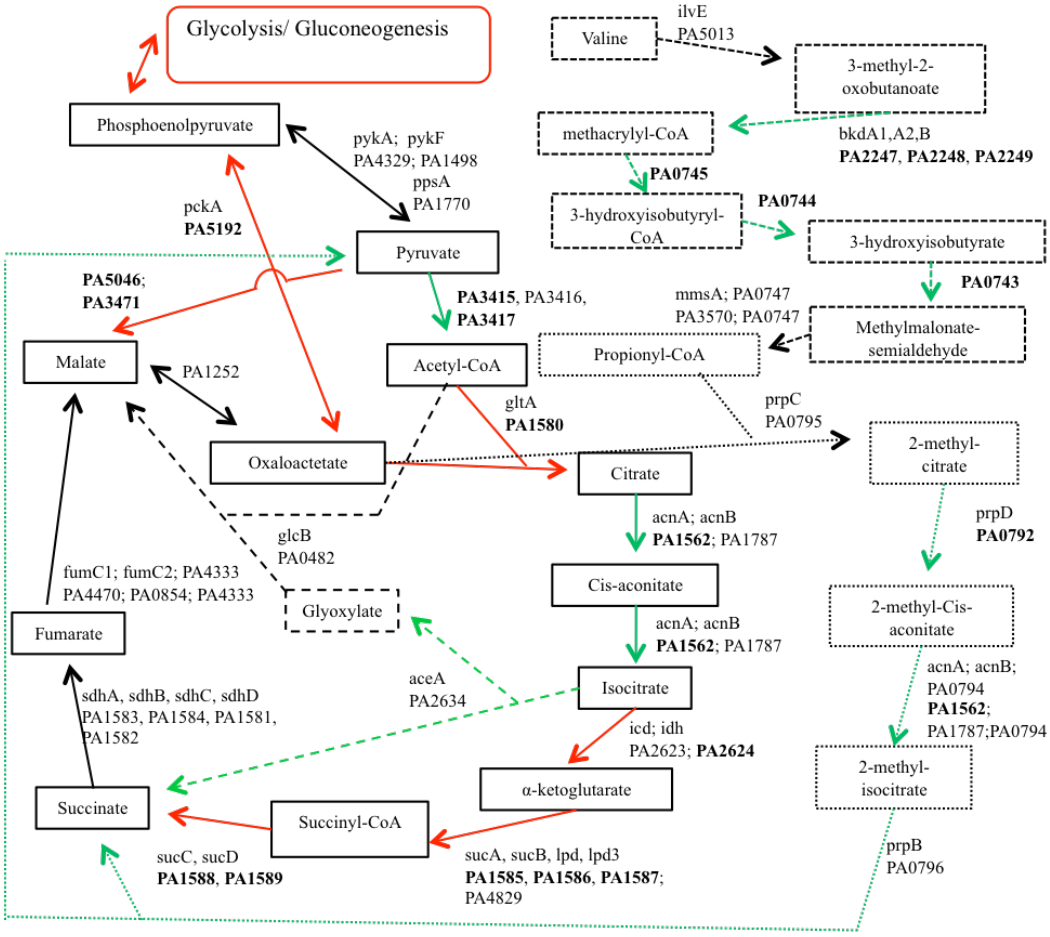

samples. Activity of aconitate hydratase on both aconitate and methyl-aconitate is not unheard of[64]. The resulting product, methylisocitrate, can be further split into succinate and pyruvate in a reaction catalyzed by PrpB, a methylisocitrate lyase (PA0796). The methylcitrate cycle rejoins the TCA cycle by producing succinate and pyruvate. Pyruvate can be decarboxylated and rejoin as acetyl-CoA. *prpB* is modestly up-expressed in

biofilm samples ($\log_2$ FC = 0.55, adjusted $P < 0.1$). TCA cycle enzymes and complexes show no significant difference in gene expression after the intersection of the 2-methylcitrate cycle. Textor and colleagues found that, in *E. coli*, the methylcitrate cycle was used to generate acetyl-CoA from propionate. *E. coli* also used the glyoxylate bypass to produce oxaloacetate[65]. The up-expression of genes from these two different, but interconnected, pathways is interesting. Wang et al. found that growth of *Ralsonia eutropha* on propionate was impaired by the deletion of *prpB* or either *aceA1* or *aceA2*, demonstrating the overlap of the methycitrate cycle and the glyoxylate bypass[66]. The methyl-citrate cycle feeds into the TCA cycle upon the production of succinate. 2-methylcitrate has been identified as an inhibitor of NADP-dependent isocitrate dehydrogenase in *Aspergillus nidulans*[67] so production of intracellular 2-methylcitrate could lead a downshift in isocitrate dehydrogenase activity, allowing isocitrate to be converted into succinate and glyoxylate via AceA. The identification of 2-methylcitrate as a possible inhibitor of isocitrate dehydrogenase by Brock could add another level of regulation to this important step and connects branched-chain amino acid degradation to regulation of the TCA cycle and the glyoxylate bypass. Interestingly, while trying to elucidate the role of AceA as a virulence factor, Lindsey et al. found that mutants in PA0794, a putative aconitate hydratase in the same operon as 2-methylcitrate synthase and 2-methylisocitrate lyase, demonstrated a decrease in elastase production and pyocyanin production as well as an increase in pyoverdine production[60]. Similarly, knockouts in the PQS operon demonstrated reduction in pyocyanin production as well[60].

Siderophore Biosynthesis in Biofilms

Chorismate can be metabolized in several different paths including the production of phenazines, pyochelin, and the Pseudomonas quorum signal (PQS). Interestingly in the biofilms, there is a down-expression of *phnAB* (PA1001-2, $\log_2$ FC > 1, adjusted P < 0.1) which are involved in the conversion of chorismate to anthranilate. In fact, other genes involved in the production of anthranilate *kynAB* are down-expressed in biofilms as well. As expected, we observed a decrease in abundance of kynurenine in biofilms (Supplementary Table 5). Downstream processing of anthranilate to the PQS by *pqsABCD* (PA0996-9) and *pqsH* (PA2587) is down-expressed in biofilms ($\log_2$ FC > 1, adjusted P < 0.1). DAVID analysis identified the pathway responsible for synthesis of pyochelin as up-expressed in biofilms. This pathway converts chorismate to pyochelin. The transcript abundance of the first enzyme of the pathway PchA (PA4231), involved in the conversion of chorismate to isochorismate, is up-expressed in biofilm samples ($\log_2$ FC = 2.99, adjusted P = 8.89E-02). No difference in the expression of *pchB* (PA4230), which catalyzes the conversion of isochorismate to salicylate, was observed; however, transcripts of three of the four genes involved in the conversion of salicylate to pyochelin, *pchEFG* (PA4226-24) were up-expressed in biofilm samples. Chorismate can also be processed to form phenazines. Phenazine biosynthesis was found to be up-expressed in biofilms (Table 2). These data indicate a shift from the use of chorismate in the production of anthranilate to its use in pyochelin and phenazine biosynthesis during growth in biofilms (Figure 6a). It has previously been found that production of PQS is associated with late stationary phase growth[68]. Although this may appear to be in conflict

with our data, this may be due to the prolonged growth of the biofilms. McKnight and colleagues observed a decrease in PQS abundance after 48 hours of growth[68]. Biofilms grown in these experiments are grown for 96 hours. Perhaps down-regulation of PQS biosynthesis is important for biofilm cells to ensure that precursors are shuttled into alternate pathways that are important in limiting conditions.

In a study by Kasper and colleagues, they found that when *P. aeruginosa* was treated with S-phenyl-L-cysteine sulfoxide which is structurally similar to kynurenine, the substrate of KynU (PA2580) a kynurenase, which catalyzes the formation of anthranilate, there is a decrease in gene expression of a number of groups including phenazine biosynthesis and two of the type VI secretion systems[69]. They observed an increase in transcripts whose products participate in pyochelin biosynthesis. Thus, the funneling-away of chorismate from anthranilate biosynthesis may play an important role in stress response and regulation of virulence factors such as the type VI secretion system (T6SS). The possible overlap of these systems will be discussed later.

Ciprofloxacin Treatment Alters the Transcriptome of Biofilms

Biofilms treated with ciprofloxacin demonstrated an up-regulation of 85 genes and a down-regulation of 137 genes (2-fold difference and adjusted $P \leq 0.1$) when compared to untreated biofilms (Figure 4b). Using the functional annotation clustering tool from DAVID, 4 enriched gene clusters were identified as being down-expressed upon treatment with ciprofloxacin. Significant decreases ($P < 0.01$) were observed in gene clusters associated with quorum sensing and signaling, non-ribosomal peptide

Table 2. Gene enrichment analysis of *P. aeruginosa* PAO1 biofilms compared to planktonically grown cells. P values calculated by overlap with gene ontology group.

Gene Ontology Group	Genes	Biofilm Down-expressed	P value	Biofilm Up-expressed	P value
HSL QS	72	10	7.33E-02	14	2.42E-05
Osmotic	56	0	1.00E+00	8	9.96E-03
c-di-GMP	38	1	9.64E-01	0	1.00E+00
Fe limit	61	3	8.94E-01	6	1.11E-01
O2 limit	159	10	8.64E-01	34	1.81E-12
O2 down	117	12	2.66E-01	23	4.58E-08
Virulence	195	8	9.94E-01	23	3.14E-04
Heat shock and chaperones	54	7	1.59E-01	1	9.52E-01
Mg limit	58	4	7.23E-01	2	8.31E-01
Peroxide stress	48	0	1.00E+00	7	1.40E-02
Stationary phase	250	7	1.00E+00	110	0.00E+00
Phenazine biosynthesis	17	0	1.00E+00	7	1.57E-05
Efflux pumps	39	3	6.42E-01	4	1.59E-01
Nitrosative stress	28	5	7.81E-02	4	6.22E-02
Biofilm consensus	83	8	3.87E-01	25	5.34E-13
Toxin-AT	4	0	1.00E+00	0	1.00E+00
TOB sensitivity	28	6	2.51E-02	2	4.54E-01
CIP sensitivity	35	5	1.62E-01	0	1.00E+00
CIP tolerance	82	8	3.74E-01	5	4.61E-01
Response to CIP in DFB - up	78	8	3.22E-01	0	1.00E+00
Response to CIP in DFB - down	15	2	3.59E-01	3	4.42E-02
Response to TOB in DFB - up	111	19	1.81E-03	5	7.28E-01
Response to TOB in DFB - down	70	3	9.39E-01	22	5.40E-12
SOS response	15	0	1.00E+00	1	5.67E-01
Type VI Secretion System	89	11	1.19E-01	18	9.00E-07

Figure 6. Chorismate Metabolism. Chorismate can have multiple fates. Biosynthesis of pyochelin and pyocyanin are up-expressed in biofilms compared to planktonic cells and, transcriptomically, show a shift away from anthranilate metabolism (a). Genes that are up-expressed in biofilms are green; genes that are down-expressed are red; bold text represents transcripts that are significantly regulated. Treatment of biofilms with ciprofloxacin causes a down-expression of genes involved in pyochelin and pyocyanin synthesis. Genes that are red are down-expressed with ciprofloxacin treatment, bold text represents transcripts that are significantly regulated. Genes listed by commas participate in a complex or work together. Those separated by semicolons share the same function, but do not rely on each other.

a.

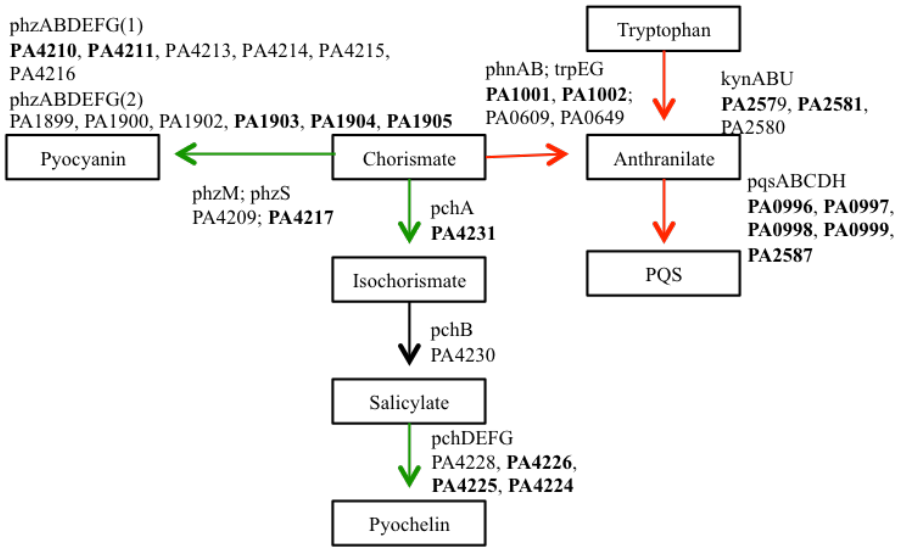

b.

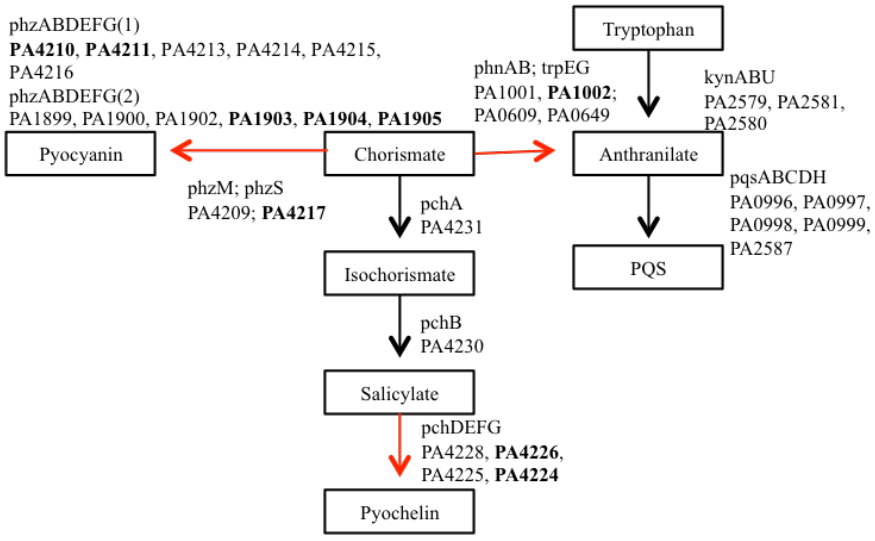

synthesis, and phenazine biosynthesis (Table 3). Visible differences in DFR effluent color was noted between the ciprofloxacin treated and control biofilms. Control biofilm effluent had a vibrant green color whereas the treated biofilms effluent appeared colorless. This color difference appears to correlate with the microarray data. Out of the 137 genes down-expressed in response to ciprofloxacin, 26 genes were not clustered by the functional annotation clustering tool. The only significant (enrichment score > 1.30, P < 0.01) non-clustered group was a bacterial secretion system (gene count = 10, P = 2.2E-07). Components of the secretion system have been consistently identified as up-regulated in *P. aeruginosa* biofilms and will be discussed in further detail.

Table 3. Gene enrichment analysis of *P. aeruginosa* PAO1 biofilms compared to ciprofloxacin-treated biofilm cells. DAVID analysis of functional annotation clustering was used, gene ontology groups with Enrichment Score > 1.30 and P value < 0.01 were selected.

Gene Ontology Term	Gene Count	P value
Down-Expressed in Biofilms Treated with Ciprofloxacin		
Signaling	10	3.60E-08
Condensation Domain	5	5.20E-05
Quorum Sensing	3	9.33E-04
Phenazine Biosynthesis	3	1.91E-03
Up-Expressed in Biofilms Treated with Ciprofloxacin		
SOS Response	4	6.50E-05
Purine Metabolism	6	1.44E-04
Purine Biosynthesis	3	1.64E-03
Nucleotide-Binding	12	1.66E-03
Helicase	4	3.94E-03
ATP-Binding	11	4.11E-03
DNA Replication	3	6.09E-03

DNA Repair, Prophage Genes, and Ciprofloxacin Treatment

Ciprofloxacin, a fluoroquinolone, is frequently used for treating *P. aeruginosa* infections[70]. Fluoroquinolones interact with complexes of DNA and either DNA gyrase and/or topoisomerase IV[71]. The enriched gene clusters in ciprofloxacin-treated biofilms include those associated with SOS response, purine metabolism, helicase activity, ATP-binding, and DNA replication (Table 3). The efflux pumps MexAB-OprM (PA0425-7), MexCD-OprJ (PA4597-9), MexEF-OprN (PA2493-5), and MexXY-OprM (PA2018-9, PA0427) are recognized as determinants of fluoroquinone resistance[70]; however, it has been demonstrated in this work and other previous studies that these efflux pumps are not responsible for the increased tolerance of biofilms. In fact, our data show no signs of up-regulation of efflux pumps as a group in biofilms compared to planktonic cultures ($P > 0.1$) or up-regulation in ciprofloxacin-treated biofilms ($P > 0.1$) (Table 2,4). Brazas and Hancock found that *P. aeruginosa* treated with sub-inhibitory ciprofloxacin demonstrated an up-regulation of the pyocin/phage region (PA0610-48)[72]. Cirz and colleagues also found that the phage region PA0610-48 was highly up-expressed in *P. aeruginosa* treated with ciprofloxacin[73]. Our data show all of the genes in this region are up-expressed in ciprofloxacin-treated biofilms ($\log_2 FC > 1.6$); however, all of the genes in this region have adjusted P values > 0.1 and were excluded from further analysis. Phage-related genes PA0719-20 and PA0724-9 are up-expressed in ciprofloxacin treatment.

Expression Upon Ciprofloxacin Treatment and Previous Work

There is a significant overlap between genes up-regulated in response to

Table 4. Gene enrichment analysis of *P. aeruginosa* PAO1 ciprofloxacin-treated biofilms compared to untreated biofilms. P values calculated by overlap with gene ontology group.

Gene Ontology Group	Genes	Up-expressed with Cipro.	P value	Down-expressed with Cipro.	P value
HSL QS	72	0	1.00E+00	25	0.00E+00
Osmotic	56	0	1.00E+00	3	1.60E-01
c-di-GMP	38	0	1.00E+00	0	1.00E+00
Fe limit	61	0	1.00E+00	5	1.68E-02
O2 limit	159	0	1.00E+00	12	5.07E-04
O2 down	117	1	8.39E-01	1	9.48E-01
Virulence	195	0	1.00E+00	21	8.11E-09
Heat shock and chaperones	54	2	2.00E-01	1	7.42E-01
Mg limit	58	3	5.86E-02	0	1.00E+00
Peroxide stress	48	3	3.66E-02	1	7.00E-01
Stationary phase	250	0	1.00E+00	51	0.00E+00
Phenazine biosynthesis	17	0	1.00E+00	7	7.59E-08
Efflux pumps	39	1	4.53E-01	2	2.50E-01
Nitrosative stress	28	0	1.00E+00	2	1.51E-01
Biofilm consensus	83	4	3.78E-02	10	3.17E-05
Toxin-AT	4	1	5.99E-02	0	1.00E+00
TOB sensitivity	28	4	7.93E-04	2	1.51E-01
CIP sensitivity	35	1	4.18E-01	1	5.84E-01
CIP tolerance	82	1	7.21E-01	2	6.06E-01
Response to CIP in DFB - up	78	13	9.85E-11	0	1.00E+00
Response to CIP in DFB - down	15	0	1.00E+00	4	3.93E-04
Response to TOB in DFB - up	111	21	0.00E+00	0	1.00E+00
Response to TOB in DFB - down	70	0	1.00E+00	10	6.80E-06
SOS response	15	5	1.99E-06	0	1.00E+00
Type VI Secretion System	89	2	3.97E-01	23	0.00E+00

ciprofloxacin between our dataset and 196 genes identified in the Cirz dataset (P = 2.53E-08); however, there is no significant overlap between genes down-expressed in our dataset and the 408 genes identified in the Cirz dataset[73]. The differences in the down-expression data may be accounted for by the fact that our *P. aeruginosa* samples were grown as biofilms instead of planktonic samples and treated with ciprofloxacin for 24 hours instead of 2 hours. Nonetheless, an interesting comparison is the overlap of genes identified as down-regulated in response to ciprofloxacin by Cirz and those identified in our data as down-regulated in the biofilm. This comparison can offer insight into biofilm down-regulated genes that may contribute to antibiotic resilience. There is a significant overlap between these (88 genes, P = 2.22E-18). When this overlap is analyzed using the functional annotation clustering tool in DAVID, clusters enriched in the overlap include those involved RNA binding and translation (enrichment score = 6.22, P < 1E-08), ATP synthesis and proton transport (enrichment score = 5.07, P < 1E-08), and fatty acid biosynthesis (enrichment score = 2.27, P < 1E-03).

Cirz et al. also investigated the regulon of LexA (PA3007), a repressor of phage mobilization and the SOS response, and discovered 15 genes under the control of LexA. In our biofilms, ciprofloxacin treatment led to significant increase in the SOS response as found by the functional annotation clustering tool in DAVID (Table 3) as well as was found by measuring the overlap of genes in our dataset compared with those identified by Cirz and colleagues. Overall, enrichment of transcripts involved in DNA metabolism was observed in treated biofilms. Down-regulated genes in treated biofilms appeared to be genes associated with cell-to-cell interactions such as signaling and quorum sensing. Due

to the overall nature of these genes, it appears that genes down-expressed by ciprofloxacin-treated planktonic cells are completely different than those down-expressed in treated biofilms. Our list of down-expressed genes was then compared to that of Stewart et al.[74]. Of the 15 genes they identified as down-expressed in ciprofloxacin-treated biofilms grown in a DFR, there was a 4 gene overlap with our dataset (P = 3.72E-04). These genes include *oprD* (PA0958), a gene containing an OmpA-like domain possibly involved with peptidoglycan interactions/T6SS (PA1041), *pilA* (PA4525), and a hypothetical gene that contains a domain of unknown function (DUF) 3015 (PA4607).

Phenazine Biosynthesis and Ciprofloxacin Treatment

The same 7 genes identified as up-expressed in biofilm, as compared to planktonic cells, were down-expressed in response to ciprofloxacin (Table 4). Down-expression in *phnB* is also observed in ciprofloxacin-treated biofilms; however there is no change in *phnA*. These genes are co-transcribed[75] and *phnB* is borderline significant (adjusted P = 9.57E-02), so gene expression of the anthranilate synthase complex may not decrease due to ciprofloxacin treatment. Down-expression of genes responsible for the biosynthesis of pyocyanin and pyochelin may allow chorismate to be shifted towards anthranilate production (Figure 6b). The switch of these pathways may indicate that cells have more access to electron acceptors or iron. Nonetheless, a reduction in pyocyanin and pyochelin production indicates a decrease in virulence. The shift in expression of the phenazine and pyochelin genes upon ciprofloxacin treatment returns the pathway to a state similar to that of planktonic cells.

The Type VI Secretion System is Differentially Expressed

DAVID analysis revealed down-expression of an unclustered group of genes in ciprofloxacin-treated samples. This group of genes was comprised of T6SS transcripts. T6SSs were identified as being up-expressed in biofilms compared to planktonic cells and down-expressed in biofilms treated with ciprofloxacin, much like the expression of phenazine biosynthesis genes (Table 2 & 4). This correlation may be relevant in understanding the role of these systems. Previously, up-expression of phenazine biosynthesis and both the H2- and H3-T6SS were identified in response to treatment with a competitive inhibitor of KynU[69]. KynU catalyzes the conversion of kynurenine, a product of tryptophan degradation, to anthranilate (Figure 6). The same T6SS loci, H2- and H3-, were up-expressed in biofilm samples compared to planktonic samples and down-expressed upon ciprofloxacin treatment in our data set (Table 5 & 6, Supplemental Figures 7 & 8).

The H2-T6SS is regulated by MvfR (PA1003) and the H3-T6SS is under the regulation of PqsE (PA1000), a regulatory protein which is coded between the *pqs* operon and the anthranilate synthase genes *phnAB*, as well as MvfR. Lesic and colleagues determined that an *mvfR* mutant showed reduced expression of the PQS biosynthesis genes and genes involved in the H2- and H3-T6SS[76]. They used anthranilate analogs to determine the transcriptional effect of inhibiting the production of PQS, a ligand for MvfR. The transcriptional response to these presumed inhibitors of MvfR was a drop in expression of H2- and H3-T6SS transcripts[76]. The regulation of phenazine and PQS

Table 5. Biofilm T6SS Gene Regulation. Regulation of the various type VI secretion system loci in biofilm samples.

Type VI Secretion System	Genes	Biofilm Down-expressed	P value	Biofilm Up-expressed	P value
H1-T6SS	35	11	7.82E-05	0	1.00E+00
H2-T6SS	32	0	1.00E+00	9	3.34E-05
H3-T6SS	20	0	1.00E+00	9	3.57E-07

Table 6. Ciprofloxacin-Treated Biofilm T6SS Gene Expression. Regulation of the various type VI secretion system loci in response to ciprofloxacin treatment.

Type VI Secretion System	Genes	Up-expressed with Cipro.	P value	Down-expressed with Cipro.	P value
H1-T6SS	35	2	9.97E-02	0	1.00E+00
H2-T6SS	32	0	1.00E+00	18	0.00E+00
H3-T6SS	20	0	1.00E+00	5	9.81E-05

biosynthesis is connected with the T6SS. The importance of the T6SS in reference to siderophore biosynthesis pathways is recent. Lin et al. found that a deletion of *icmF3* (*tssF3,* PA2361), an H3-T6SS gene, resulted in changes in pyocyanin production[77]. Podladchikova found a secreted T6SS protein, Hcp, was loaded with a novel siderophore, yersiniachelin, that contained bound iron in a strain of *Yersinia pestis*[78]. The up-expression of siderophore and phenazine biosynthesis genes may provide additional insight into the usefulness of the T6SS for maintaining adequate iron and redox balance.

The Roles of the T6SS Remain Elusive

The T6SS was first identified in *Vibrio cholerae* by Melakanos and coworkers in 2006[79]. Within the same year, this newly discovered secretion system was identified *in P.*

aeruginosa, specifically the H1-T6SS, and was determined to be upregulated in cystic fibrosis (CF) patients[80]. Even before its discovery as a novel secretion system, components of the T6SS had been identified as important factors in virulence. Approximately 8 years before its recognition as a new secretion system, a serine-threonine protein kinase (*ppkA*) gene in *P. aeruginosa* was discovered to be induced upon infection and necessary for virulence in a mouse model[81]. A gene cluster, *icmGCDJBF*, was also identified in *Legionella pneumophila* that was necessary for the killing of human macrophages[82,83]. Two years later, an *icmF* homologue was discovered in *V. cholerae* that was upregulated in a rabbit infection model[84]. During a survey of forkhead-associated (FHA) domains, domains that bind phospho-threonine peptides and mediate phosphorylation-dependent protein-protein interactions, *P. aeruginosa* was identified as harboring FHA domains in clusters that contain serine/threonine phosphatases and kinases as well as *icmF* gene homologues[85]. Related *icmF* gene clusters were described in *Salmonella enterica* and found to be useful in the invasion of eukaryotic cells[86]. The first detailed analysis of these virulence loci *in silico* was provided in 2003. Because of their previous discoveries of the importance of *icmF* in *V. cholerae*[84,87], the authors characterized the associated gene cluster in *V. cholerae* as well as homologous clusters in other Gram negative bacteria. Gene clusters were characterized by the *icmF* homologue, which at the time was associated with the T4SS. These clusters were dubbed IcmF-Associated Homologous Proteins (IAHP)[88]. Interestingly, many of the genes in the IAHP clusters showed no homology to T4SS genes. Because of the lack of homology of the genes in the cluster, despite *dotU* and *icmF* homologs in T4SSB[89], this analysis served as

a harbinger for the recognition of IAHP clusters as the sixth secretion system. In 2004, the Leung group used a proteomic approach to identify two novel virulence genes, *evpAB*, in the fish pathogen *Edwardisella tarda*. These genes belonged to a new virulence cluster[90]. A year later, Parsons and Heffron found that *sciS*, the *S. enterica* homolog of *icmF*, was necessary for long-term persistence in macrophages and belonged to a 9 gene IAHP locus. A deletion of the locus caused a host cell invasion defect in *S. enterica*.

After nearly a decade the virulence associated proteins of the IAHP clusters were recognized as part of a novel secretion system. This system, the T6SS, was finally recognized in 2006 by the Melakanos lab[79]. Following its discovery, the T6SS clusters were rapidly identified in a number of pathogenic Gram-negative bacteria. A majority of T6SSs identified to date are in Proteobacteria[91]. Although this system has been identified as a virulence factor in *P. aeruginosa*[80], *V. cholerae*[79], *Francisella novicida*[92], *S. enterica*[93], and *Burkholderia mallei*[94] it has been identified as present and functional in nonpathogenic bacteria[95]. In fact, *Rhizobium leguminosarum*, mutualistic bacteria that colonize legume roots, use an imp gene cluster (T6SS) to secrete proteins that block infection of colonized *Pisum sativum*[96]. It is important to recognize that this system, although it is a potent virulence factor in many organisms, may play important roles in ecology. Cell-to-cell interactions governed by these systems are not just limited to those between pathogen and host. Approximately 25% of sequenced Gram-negative bacteria contain at least one T6SS locus[97] and most of these bacteria contain more than one locus. Many of these organisms are not recognized as pathogens.

Typically, the T6SS loci contain approximately 13-15 conserved, core,

genes[97,91,98]. Bioinformatically, the 13-15 conserved genes can be classified into three categories. The first category includes genes that code for membrane-associated proteins. This includes integral membrane proteins TssL (IcmH) and TssM (IcmF) and lipoprotein TssJ. The second category consists of genes that have been shown to demonstrate homology to bacteriophage components. The homology of the encoded proteins is not apparent at the primary structure level, but rather at tertiary and quaternary level. These components include the TssD which will be referred to as Hcp, VgrG, TssB, TssC, and TssE proteins. The last category of genes in the typical conserved T6SS cluster is for those that no function has been inferred. These genes encode for the proteins TssA, TssF, TssG, and TssK[99].

TssL, TssM, and TssJ together form a membrane subcomplex that anchors the bacteriophage-related components to the membrane. SciN, a TssJ homolog in enteroaggregative *E. coli*, was identified as an outer membrane protein that interacts with the periplasmic space and was found to be necessary for the secretion of the TssD homolog SciD[100]. It has also been demonstrated that the inner membrane protein TssM directly interacts with TssJ[101]. Similarly, TssM and TssL proteins are membrane associated proteins and interact directly with each other to stabilize the T6SS complex. In the same study, $ImpK_L$, a TssL homolog, was found to possess an OmpA-like domain that interacts with peptidoglycan[102]. Another T6SS associated protein, TagL, also plays a role in stabilizing the membrane complex with the secretion machinery by interacting directly with TssL[99]. These proteins comprise the membrane subcomplex and anchors the rest of the secretion system to the membrane.

The second group of conserved T6SS genes shares homology with the secretion machinery of bacteriophage T4[103,104]. In fact, the syringe structure of the T6SS closely resembles an inverted phage tail. The "tail tube" of the T6SS machinery is composed of hexameric rings of hemolysin coregulated proteins, Hcps. These Hcps are secreted along with valine-glycine rich repeat proteins (VgrGs). The hexameric Hcps are structurally similar to g19 hexamers of the T4 bacteriophage tail. The Hcp hexamers stack to form a nanotube with an internal diameter of 40 Å and an external diameter of 85 Å[80,103]. The valine-glycine repeat G (VgrG) protein also shares homology with the gp5 and gp27 proteins of the same bacteriophage[103]. The VgrG proteins form a trimeric cap on the tail tube structure, forming a needle complex in a similar configuration that the gp5 and gp27 proteins in bacteriophage T4 do. The needle complex is used to puncture the cellular membrane of other cells. Some of the VgrG proteins are specialized and enzymatically active or can deliver effector proteins. Although they lack the lysozyme fold of gp-5, these specialized VgrG proteins interact with each other and have been found to have actin-remodeling activity[105]. The VgrG protein will be discussed in greater detail in regard to their interaction with effector proteins. It is interesting that the T6SS contains a gp25-like protein-encoding gene, *tssE* (*hsiF)*. In bacteriophage T4, the protein gp25 serves as an important baseplate. This protein is one of the most conserved proteins in all phages with contractile sheaths[103,106]. The presence of a gp25-like protein encoding gene in the T6SS locus, *tssE*, not only suggests a viral origin of the complex but its intracellular localization points to its function as a structural component in the secretion apparatus. In fact, TssE is also necessary for the secretion of Hcp and VgrG[106]. The last

two genes that show homology to phage proteins are the *tssB* and *tssC* genes, also commonly referred to as *vipA* and *vipB* in the literature. TssB and TssC form a heterodimer. The TssBC heterodimer has been found to form complexes that strongly resemble the contractile sheaths found in T4 bacteriophage. The TssBC tube structures are built from short segments and have a cogwheel-like structure consisting of 12 main cogs[107]. The entire assembled structure has a diameter of approximately 300 Å with an internal pore diameter of 100 Å, allowing for the internal accommodation of the 85 Å-diameter Hcp tube complex[107]. Basler and associates found that these sheaths can be assembled across the entire width of the cell at speeds of approximately 20 to 30 seconds per μm and that the contraction of the sheath occurs in about 5 milliseconds. The TssBC sheath can contract to nearly 50% of the extended sheath length[108]. This contraction is the driving force that expels the Hcp/VgrG tube from the cell. Although the mechanism powering contraction is yet to be elucidated, the interaction of TssB and TssC is critical to the formation of the sheath complex. TssB and TssC are represented by a 1:1 stoichiometry in the sheath complex. The TssBC complex also shares homology with the T4 bacteriophage sheath protein gp18. It is speculated that, like the attachment of the gp18 sheath to the gp25 baseplate in bacteriophage T4, the TssBC sheath connects with the highly conserved TssE[109]. The TssE co-purifies with the TssBC sheath as well as TssG and TssK, which suggests that these proteins may be important in sheath assembly[109]. The contractile sheath complex is different than that of bacteriophage in that it is recycled. So, unlike bacteriophage, bacteria need a means to disassemble the sheath complex so that it can be used again. This remodeling and disassembly of the TssBC

sheath is accomplished by the ClpV ATPase. The ClpV ATPases involved in T6SSs belong to the AAA+ (ATPases associated with various cellular activities) protein family and forms a ring complex[110]. These proteins co-localize with TssBC complexes with the assistance of the associated Fha protein[111,112]. Effective disassembly of the TssBC sheath by ClpV is accomplished when the sheath is in its contracted state[111,113]. ClpV is able to associate with the complex by interacting with the complexed TssC protein[110]. The absence of ClpV would prevent the cell from recycling the T6SS.

Hcp and VgrG are both important components of the secretion apparatus. Hcp has been found to aid in the delivery of effectors to targeted cells by the encapsulation of the effector inside a hexameric ring[114]. The VgrG proteins interact with effectors to deliver them into the target as well; however, *P. aeruginosa* contains an evolved VgrG, VgrG2b (PA0262), that possess enzymatic activity itself. VgrG2b interacts with the target cell's tubulin and actin causing a restructuring of the target's cytoskeleton[115]. The Hcp and VgrG proteins are necessary components of the T6SS, but the effectors that they deliver are important for survival. T6SS effectors are not necessary for secretion, but they can execute a number of different functions. Three main functions of these effectors have been elucidated. T6SS effectors can be classified as cell wall-degrading enzymes, membrane targeting proteins, and nucleases. An important aspect of this toxin system is the presence of antitoxins, or immunity proteins. The expression of immunity proteins allows for the detoxification of effectors in 'self' and related bacteria.

The first cell wall-degrading enzymes secreted by this system, type six effectors (Tse) were identified in P. aeruginosa and found to be delivered by the H1-T6SS, Tse1

(Tae1, PA1854) and Tse3(Tge1, PA3484)[116]. Both effectors target the cell wall; however, their modes of action are different.Tse1 is an amidase and cleaves the peptidoglycan peptide crosslink. Specifically, the enzyme targets the γ-D-glutamyl-L-meso-diaminopimelic acid bond in the donor peptide stem[117]. Based on its amidase activity it has received a new categorization as a type 6 secretion amidase effector (Tae). Tse3 functions as glycoside hydrolase and cleaves the β-1,4 bond between N-acetylmuramic acid and N-acetylglucosamine in the peptidoglycan backbone[117]. Also, because of its activity it has received new nomenclature as a type 6 secretion glycoside hydrolase effector (Tge). Tae1 and Tge1 are both effective at lysing competing bacteria when delivered to the periplasm of the targeted cell. Both tae1 and tge1 share an operon with a small immunity protein gene *tai1* (PA1845) and *tgi1* (PA3485) respectively. These immunity proteins inhibit their corresponding effector[117]. There are two other effectors that are targeted to the periplasm, Tse4(PA2774) and Tse5(PA2684)[114]. The direct mode of action of these enzymes has not yet been elucidated but localization of their immunity proteins, Tsi4 (PA2775) and Tsi5 (PA2685), to the periplasm provides immunity against the corresponding effector[114].

The T6SS also utilizes effectors that target the cellular membrane. These effectors have been categorized by their lipase activity as type 6 lipase effectors (Tle). The *tle* genes share operons with small genes coding for type 6 lipase immunity (Tli) proteins. Russell and colleagues found discovered 377 putative lipases that grouped into five divergent families. These families were widely and seemingly sporadically distributed within Gram-negative bacteria. They found that Tle1-4 families exhibit a motif that is

common in many lipases and esterases; however, these lipases fail to demonstrate any sequence homology to other lipases. Effectors of the Tle5 family harbor dual HxKxxxxD motifs that are commonly found in phospholipase D proteins[118]. The genome of *P. aeruginosa* str. PAO1 contains Tle1 (PA3290), Tle3 (PA0260), and Tle4 (PA1510) as well as two lipases from the Tle5 family, Tle5 (PldA, PA3487) and PldB (PA5089). PldA and PldB are secreted by H2-T6SS and H3-T6SS, respectively. These two genes, *pldA* and *pldB* show evidence of distinct lineages, demonstrating mammalian and plant homology respectively, and appear to be present in *P. aeruginosa* due to horizontal gene transfer[119]. Russel and colleagues determined that a PldA-self-intoxicating strain of *P. aeruginosa*, mutants of the PldA immunity gene (*tli5*), there was a major disturbance in the membrane phospholipid composition. These mutants demonstrated a 48-fold increase in phosphatidic acid and a similar decrease in phosphatidylethanolamine, a major constituent of bacterial membranes[118]. Although PldA and PldB do not demonstrate a strong toxic effect when expressed cytoplasmically, Jiang and colleagues found that when they are targeted to the periplasm of bacterial cells these toxins inhibited growth[120]. They also discovered that PldB had three corresponding immunity proteins (PA5088-86) which provide immunity to cell from PldB in a dose-dependent additive fashion[120]. Further work demonstrated that both PldA and PldB were important for cellular invasion of epithelial cells. Altogether, their work demonstrated the importance of these phospholipase D effectors in microbial antagonism and host interactions[120].

T6SS Loci are Regulated
Differently in *P. aeruginosa*

The T6SS is a major factor in bacterial virulence and has been demonstrated to be important in acute and chronic infection. *P. aeruginosa* contains not just one T6SS loci, but three. These different T6SS loci, H1-3, are phylogenetically distinct[121]. Not only do these loci have distinct heritage, but they also carry out different functions[122]. The function, regulation, and expression of each of these loci will be discussed as they pertain to physiology and the results of our experiments.

The H1-T6SS was the first of the T6SSs described in *P. aeruginosa*. As are other T6SSs, the H1 locus is under tight regulation. Its role as an important virulence factor has been well documented[80]. The H1-T6SS has been identified as a bacteria-targeting secretion system. This system secretes effectors, as described before, that target the peptidoglycan cell wall (Tae1 and Tge1) as well as effectors targeted to the periplasm (Tse4 and Tse5). At a post-transcriptional level, the H1-T6SS has been identified as being directly negatively regulated by RsmA (PA0905). RsmA itself is under positive regulation by RetS (PA4856). Goodman and associates demonstrated that a mutation in *retS* led to *P. aeruginosa* hyperadhesion to mammalian cells and resulted in a loss of toxicity[123]. Not only this but *retS* mutant displayed a phenotype that was similar to a type III secretion system (T3SS)-defective strain. In a reciprocal manner, genes involved in biofilm formation were activated as well as genes in and around the H1-T6SS, which was unidentified at the time of the study (PA0070-97)[123]. In fact, RetS is part of the GacS (PA0928)/GacA (PA2586)/RsmYZ (PA0527.1, PA3621.1) signaling network and has an opposite function to GacA. GacS/GacA (global activator of antibiotic and cyanide

synthesis) is a two component regulatory system involved the regulation of expression of virulence factors, stress response, and secondary metabolism, and periplasmic proteins[123]. GacS is a transmembrane sensor that interacts with GacA to transfer a phosphoryl group. Transcriptional regulator genes *lasR* (PA1430) and *rhlR* (PA3477) are positively regulated indirectly by GacA[124]. It should be noted that control of these systems is complex and LasR, although upregulated by GacA, has been demonstrated to repress the H1-T6SS[76]. Transcriptional regulator MvfR (PA1003) has also been shown to repress the H1-T6SS[76]. Activated MvfR may be responsible for the decreased expression of the H1-T6SS in our biofilm samples. LasR may also play an important role in the repression of this system in our model. Also part of this regulatory pathway is RsmZ and RsmY, untranslated small RNA. In fact, Brencic and colleagues found that the GacS/GacA signal transduction works exclusively through RsmY and RsmZ[125]. These small noncoding (nc) RNAs inactivate RsmA. In their study of the system in *P. aeruginosa*, the Lory group found that GacA directly regulates only RsmYZ. Using mutants, they were able to determine that expression of GacA and, in turn, RsmYZ positively regulate the expression of the H1-T6SS as well as seven genes involved in the H3-T6SS, whereas RetS negatively regulated the expression of the same genes[125]. The lost adherence sensor (LadS, PA3974) acts as a positive regulator of GacA/RsmYZ and, thus, indirectly the H1-T6SS. It should also be noted that the upregulation of the H1-T6SS by GacA and RsmYZ, as well as the production of cyclic-di-GMP (c-di-GMP) is opposite to the regulation of the type III secretion system (T3SS)[126]. Through this regulatory cascade the T3SS and the H1-T6SS are regulated in a reciprocal manner. It was found that artificial

changes in the c-di-GMP concentrations could be used to switch between H1-T6SS and T3SS[97,126]. Nonetheless, the regulation of the H1-T6SS system is complex and linked to quorum sensing.

Regulation of the H1-T6SS occurs post-translationally as well. Mougous and colleagues identified the TPP plays a role in post-translational control of the T6SS. As stated earlier, the ClpV protein interacts with Fha, which is an important component of the threonine phosphorylation pathway (TPP). In *P. aeruginosa* Pao1 the TPP is associated with only one T6SS locus, H1. Upon growth on a surface, the TPP has been found to be induced[127]. The genes involved in this pathway include *tagQ1*, *tagR1*, *tagS1*, *tagT1*, *ppkA* (*tagE1*), and *pppA* (*tagG1*) (PA0070-5), as well as *fha1* (PA0081). An appreciation of the TPP as a virulence factor can be traced back to 1998 when Wang and coworkers found that a serine/threonine protein phosphokinase was necessary for *P. aeruginosa* virulence in a mouse model[81]. In 2003, Bladergroen and associates identified protein phosphatases and kinases[96] in a locus that would later be identified as a T6SS by Mougous and colleagues[79]. After they identified the T6SS in 2006, Mougous and colleagues went on to describe the importance of a serine/threonine protein phosphatase (PppA, PA0075) and kinase (PpkA, PA0074) in *P. aeruginosa* PAO1[112]. In their work, they demonstrated that PpkA acts as a threonine protein kinase and is responsible for phosphorylating Fha1 that allows for the secretion of Hcp and VgrG proteins out of the cell[128]. PppA was found to work in an opposite manner. Increased expression of the threonine phosphatase decreased the secretion of the Hcp and VgrG proteins. Knockouts of *ppkA* and *pppA* did not affect the expression of Hcp1 and VgrG1, but they did affect

their export, and both proteins were found to interact directly with Fha1[129]. Casabona and colleagues demonstrated the function of TagT, TagS, and TagQ in the posttranslational control of the T6SS[130]. These T6SS associated proteins are involved in transmembrane signaling associated with the posttranslational regulation of the H1-T6SS. TagQST are necessary for TPP activation. TagQ is an outer membrane lipoprotein that aids in the localization of TagR, a positive regulator of the TPP. TagR facilitates the dimerization and activation of PpkA. TagT and TagS together form an ABC-transporter-like complex with ATPase activity. It may participate in the import or export of a H1-T6SS-related signal. Ultimately, this T6SS-associated set of genes participates in the TPP.

Our microarray data demonstrated that the H1-T6SS is at higher levels of expression in the planktonic samples than in our biofilm samples, P = 6.46E-05. While this seems counterintuitive, given that the H1-T6SS has been associated with chronic lung infections where *P. aeruginosa* would be living in biofilms, this does not mean it is primarily expressed planktonically. Perhaps the expression of the H1 locus occurs early in biofilm development and is significantly reduced as the biofilm matures in a similar fashion to PQS synthesis. Although there is no direct evidence of this, the Sauer group noted that LasR, a repressor of the H1-T6SS, is upregulated during stage II of biofilm development[131]. Early regulation of this system may be useful in securing a niche and outcompeting competitors, since this system is antibacterial in nature. This then raises the question as to why the Hcp associated with this locus is observed in the chronically infected cystic fibrosis (CF) lung. It is likely that the abundance of Hcp1 observed in the CF lung is due to, at least in part, its regulatory relationship with LasR. It has been

observed that LasR mutants are frequently isolated from infected CF patients[132]. The H1-T6SS, a virulence factor that is repressed by quorum sensing, may play an important role in LasR mutants in chronic CF infections.

The H2-T6SS has been determined to be involved in the internalization of *P. aeruginosa* into host cells. Work by Sana and colleagues demonstrated the importance of the H2-T6SS locus in the invasion of not only HeLa cells, but also into lung epithelial cells[122]. They went on to demonstrate that the H2-T6SS is important in *P. aeruginosa* virulence in a *Caenorhabditis elegans* model; however, the H2-T6SS is associated with internalization of *P. aeruginosa* not necessarily with cytotoxicity[120]. Its relevance to virulence is not limited to interactions with eukaryotic organisms, but also includes interactions between bacteria. The H2-T6SS is used to deliver the phospholipase PldA to neighboring cells. As described above, PldA acts on phosphatidylethanolamine which is present in the bacterial membrane[118]. While PldA acts as an antibacterial effector, it also contributes to virulence in a rat lung model[119]. Regulation of the H2-T6SS has been found to be regulated by iron and quorum sensing. The Sauer group identified the H2-T6SS associated Hcp (Hcp2, PA0263) as upregulated during the stage II biofilm maturation[131].

Expression of the H2-T6SS appears to be directly controlled by the Las and Rhl quorum sensing systems. Sana and coworkers noticed that levels of expression decreased more in a *lasR* mutant than in an *rhlI* mutant. Nonetheless, a promoter region for quorum sensing regulated genes, the Las-Rhl box, was identified upstream of the H2-T6SS[133]. It has also been demonstrated that a deletion in *mvfR* causes a downregulation of almost all

H2-T6SS genes[76]. The H2-T6SS is also repressed by a number of factors. RpoN (PA4462) has been identified in some bacteria as a T6SS activator, and in others as a repressor[134]. The H2-T6SS locus in PAO1 contains an RpoN binding box and the *sfa2* gene, a sigma factor activator. Surprisingly, Sana and coworkers found that the H2-T6SS is negatively regulated in some manner by RpoN and Sfa2 contributes to the repression. They found that expression of the H2-T6SS in an RpoN mutant was 4.5 fold higher than the wild type[135]. RpoN is not the only negative regulator of the H2 locus. The transcriptional regulator PsrA (PA3006) and the H-NS-like protein, MvaT (PA4315) also regulate expression of the H2 locus via repression[136].

Post-translational regulation of the H2-T6SS could occur via a TPP. Although this pathway is not well studied in regard to the H2 locus, it does contain a serine/threonine protein kinase (Stk2, PA1671), a serine/threonine protein phosphatase (Stp2, PA1670), and an FHA protein (Fha2, PA1665). The regulation of the H2-T6SS is complex and interconnected with many pathways in the cell.

Unlike the H1-, the H2-T6SS has been identified as an important virulence factor utilized in not only bacterial interactions but also eukaryotic ones. An increase in the expression of the H2 locus has been noted during the transition between exponential and stationary growth phases[135] and Hcp2 has been identified as an expressed protein in mature biofilms[131]. Our biofilm samples exhibit sharp upregulation of this T6SS locus as compared to planktonic cells and ciprofloxacin-treated biofilms, p-values of 2.92E-05 and 1.29E-21 respectively. This raises the question as to why the H2-T6SS is so heavily upregulated in the control biofilm as compared to the other sample groups. These cells

are growing in monoculture biofilms with no eukaryotic hosts present, so what benefit is it to upregulate these genes? The H2 locus is upregulated by quorum sensing, so this upregulation could be due largely to an increase in the presence of LasR, which increased by a $\log_2$ FC of 2.02 in biofilms and decreased by $\log_2$ FC of 3.47 during ciprofloxacin treatment (adjusted P = 7.42E-02 and P = 9.10E-02, respectively). The decrease in expression of this system in ciprofloxacin-treated biofilms is interesting. Lin and colleagues determined that a non-functional H3-T6SS actually increased resistance to aminoglycosides. Although ciprofloxacin susceptibility was unaffected, the detection of antibiotic stress may reduce the expression of these T6SS loci[77].

The H3-T6SS locus consists of two divergently transcribed, and oppositely regulated, operons. Knowledge of the H3-T6SS is much more limited than that of the other two T6SSs in *P. aeruginosa*. These operons are commonly identified as left (PA2359-64) and right (PA2365-72). Lesic and colleagues determined that both the H2- and H3-T6SS are important *P. aeruginosa* virulence factors for plant infection and lung and burn infection in mice[76]. Not only are they both important, but they appear to compensate for one another in the event that one of the loci is non-functional. So, much like the H2-T6SS, the H3-T6SS is important for interactions with eukaryotic organisms as well as prokaryotic competitors. The H3 locus differs from the H2 in that it contains two bidirectional operons. These operons are commonly identified as left and right.

The H3-T6SS right has been demonstrated to be under positive control of the transcription factor MvfR as well as LasR[76]. Unlike the H2 locus, several genes in the H3 locus are positively regulated by a quinolone response protein, PqsE (PA1000). These

genes include *tssL3* (PA2362) of the left operon and *tssB3* (PA2365), *tssC3* (PA2366), *hcp3* (PA2367), and *tssE3* (PA2368) of the right operon. Sana and colleagues found that the region between the start of the left operon, *tssA3* (PA2364), and the start of the right operon, *tssB3*, contains two RpoS binding sites upstream of each operon[135]. They also discovered that the two operons are regulated by RpoN in an opposite manner. RpoN promotes the transcription of the left operon, but in an unknown way represses the right. So, RpoN acts indirectly as a repressor of the H2- and right H3-T6SS. Like the H2 locus, the H3 locus does contain a sigma factor activator gene (*sfa3*, PA2659); however, its role has not yet been elucidated and does not appear to play a role in the regulation of the H3-T6SS or the H2-T6SS[135].

The H3-T6SS is an important virulence factor. We have noted that the H3-T6SS locus is upregulated in our control biofilm samples as compared to planktonic and ciprofloxacin-treated biofilm samples (P = 3.36E-07 and P = 9.22E-05, respectively). More specifically, we note an up-expression of the right operon. This operon contains the bacteriophage-like components such as: contractile sheath genes *tssB3* and *tssC3*, baseplate gene *tssE3*, secreted protein gene *hcp3*. *tssM3* is not changed between samples. Lin and colleagues found that deletion of *tssM3* resulted in an increase in pyocyanin production[77]. As described above, a typical T6SS locus contains 13-15 conserved genes. The entire range of genes involved in the H2-T6SS is up-expressed in biofilm samples and down expressed upon ciprofloxacin treatment. Interestingly, only half of the H3-T6SS is ever differentially regulated in these samples. The genes are those involved in the phage-like components and secreted proteins. This strange regulation of the system

could be because the H3-T6SS phage-like complex uses the H2-T6SS intermembrane complex in our system. Similar regulation has been observed by others[69,76,77,135]. Due to the evidence that tssM3 has a negative impact on pyocyanin production, *P. aeruginosa* may use the integral membrane components of the H2-T6SS when it is growing under electron acceptor-limiting conditions. Nonetheless, the T6SS is an important virulence factor of *P. aeruginosa* and may play a central role in establishing chronic infections.

Possible Gene Targets for Resensitizing Biofilms to Ciprofloxacin

Several gene targets have been identified for future experiments, including those associated with the glyoxylate bypass, branched-chain amino acid degradation, chorismate metabolism, as well as some involved in the T6SS. As described earlier in this thesis, the change in gene expression of TCA cycle is interesting. We noticed an up-expression of *aceA* before Benjamini-Hochberg correction, and identified *aceA* as a gene of interest. Genes bypassed by the glyoxylate shunt were all down-expressed (adjusted $P < 0.1$) in the biofilm samples corroborating the noticed increase in expression of *aceA*. Lindsey and colleagues identified AceA as an important virulence factor for successful mammalian infection[60]. In fact, AceA mutants were impaired in their ability to establish and maintain infections in rat lungs. We hypothesized that disruption of AceA could affect the ability of *P. aeruginosa* to form biofilms and may render it susceptible to ciprofloxacin treatment. Surprisingly, in a screen by a member of the Montana State University Medical Biofilms Lab, Laura Boegli, the *aceA* mutant demonstrated an increased resistance to ciprofloxacin ($P = 1.35E-02$). This observation may help explain

the increase in Idh gene expression (P = 2.85E-02) after ciprofloxacin treatment. Since AceA and the isocitrate dehydrogenases Icd and Idh compete for isocitrate, an up-expression of *idh* may allow the flow of more isocitrate into the rest of the TCA cycle. In fact, Idh catalyzes the reaction of isocitrate to 2-oxoglutarate. 2-oxoglutarate can be used to combat oxidative stress[137]. It would be of interest to disrupt the cell's ability to pool 2-oxoglutarate by constitutively expressing AceA to compete for substrate, hypothetically reducing the ciprofloxacin resistance. The other alternative is the use of an *icd* and *idh* double mutant[138] to force isocitrate into the glyoxylate bypass. We would expect to see a decrease in ciprofloxacin resistance based on the *aceA* knockout results.

Disruption of branched-chain amino acid catabolism may cause a decrease in the robustness of the biofilm. The branched-chain amino acids provide an efficient carbon source under starvation conditions[48]. The catabolism of isoleucine and valine results in the generation of acetyl-CoA and propionyl-CoA, providing intermediates for the TCA cycle. Interference of valine degradation may greatly affect the overall carbon-flow of the cells. Disruption of the branched keto-acid dehydrogenase complex, either BkdA1 or BkdA2, could offer valuable insight in to the role of branched-chain amino acids in the biofilm. An alternative to knocking out bkdA1 or bkdA2 would be to remove the branched-chain amino acids from the medium.

The interruption of the T6SS may also affect antibiotic resistance. Lin and colleagues realized that TssM3, an integral membrane component of the H3-T6SS locus can actually cause an increase in antibiotic susceptibility[77]. Although this gene is not differentially expressed in our data, we do observe a sharp down-expression of the T6SS

loci. This seems to correspond well with its down regulation in the ciprofloxacin-treated biofilm as compared to the control. As described previously, the gene products of the right H3-T6SS locus may use the TssM protein from the H2-T6SS locus. Knockouts in the *tssm2* may prevent the secretion of proteins encoded on the right H3-T6SS operon as well as H2-T6SS secreted proteins. The inability to use the T6SS may impact antibiotic tolerance of biofilms. Biofilms are known for their antibiotic tolerance, but the upregulation of a system that increases susceptibility seems counterintuitive. This system may provide a different kind of defense to the bacteria.

The H2- and H3-T6SS may be involved in modulating immune system interactions in the body. Work by our lab has demonstrated unusual interactions between neutrophils and *P. aeruginosa* str. PAO1 biofilms[139]. In their work, biofilms were grown on glass slides in the same drip flow reactors that were used in this study. Neutrophils were added to biofilms that were grown for 72 hours. The neutrophil-biofilm interactions were observed using scanning and transmission electron microscopy. Our lab found that neutrophils interacting with the slide exhibited the "fried egg" morphology that is associated with tight adherence and frustrated phagocytosis; however, those interacting with the biofilms did not demonstrate any polarization or irregular morphology. In fact, they retained their round shape. Bacteria were observed inside the neutrophils, but it could not be determined if the neutrophils were involved in phagocytosis. The authors speculated that the inability of neutrophils to polarize their actin may be due to the production of exotoxins by *P. aeruginosa*. It has been since demonstrated that components of the H2-T6SS are upregulated in the *P. aeruginosa* biofilms[131] and that the

H2-T6SS secretes an evolved VgrG protein, VgrG2b (PA0262), that is involved in disrupting cytoskeletal structure and polarization in eukaryotic cells[133]. The up-expression of the H2- and right H3-T6SS loci may provide biofilms with an inherent defense against predation by the immune system. By knocking out *clpV2*, *clpV3*, and both *clpV2* and *V3* we could elucidate the role, if any, of these T6SSs in immune system interactions. Further work may even include the effects of antibiotics on these interactions.

REFERENCES CITED

1. Nickel, J. C. *et al.* Antibiotic resistance ofPseudomonas aeruginosa colonizing a urinary catheter in vitro. *Eur. J. Clin. Microbiol.* **4,** 213–218 (1985).

2. Borriello, G., Richards, L., Ehrlich, G. D. & Stewart, P. S. Arginine or Nitrate Enhances Antibiotic Susceptibility of Pseudomonas aeruginosa in Biofilms. *Antimicrob. Agents Chemother.* **50,** 382–384 (2006).

3. Anderson, G. G., Moreau-Marquis, S., Stanton, B. A. & O'Toole, G. A. In Vitro Analysis of Tobramycin-Treated Pseudomonas aeruginosa Biofilms on Cystic Fibrosis-Derived Airway Epithelial Cells. *Infect. Immun.* **76,** 1423–1433 (2008).

4. Mah, T.-F. *et al.* A genetic basis for Pseudomonas aeruginosa biofilm antibiotic resistance. *Nature* **426,** 306–310 (2003).

5. Field, T. R., White, A., Elborn, J. S. & Tunney, M. M. Effect of oxygen limitation on the in vitro antimicrobial susceptibility of clinical isolates of Pseudomonas aeruginosa grown planktonically and as biofilms. *Eur. J. Clin. Microbiol. Infect. Dis.* **24,** 677–687 (2005).

6. Evans, D. J., Allison, D. G., Brown, M. R. W. & Gilbert, P. Susceptibility of *Pseudomonas aeruginosa* and *Escherichia coli* biofilms towards ciprofloxacin: effect of specific growth rate. *J. Antimicrob. Chemother.* **27,** 177–184 (1991).

7. Zhang, L. & Mah, T.-F. Involvement of a Novel Efflux System in Biofilm-Specific Resistance to Antibiotics. *J. Bacteriol.* **190,** 4447–4452 (2008).

8. Pamp, S. J., Gjermansen, M., Johansen, H. K. & Tolker-Nielsen, T. Tolerance to the antimicrobial peptide colistin in Pseudomonas aeruginosa biofilms is linked to metabolically active cells, and depends on the pmr and mexAB-oprM genes. *Mol. Microbiol.* **68,** 223–240 (2008).

9. Tré-Hardy, M., Vanderbist, F. & Traore, H. In vitro activity of antibiotic combinations against Pseudomonas aeruginosa biofilm and planktonic cultures. *Int. J.* (2008). at http://www.sciencedirect.com/science/article/pii/S0924857908000137

10. Garo, E. *et al.* Asiatic Acid and Corosolic Acid Enhance the Susceptibility of Pseudomonas aeruginosa Biofilms to Tobramycin. *Antimicrob. Agents Chemother.* **51,** 1813–1817 (2007).

11. Hill, D. *et al.* Antibiotic Susceptibilities of Pseudomonas aeruginosa Isolates Derived from Patients with Cystic Fibrosis under Aerobic, Anaerobic, and Biofilm Conditions. *J. Clin. Microbiol.* **43,** 5085–5090 (2005).

12. Bjarnsholt, T. *et al.* Pseudomonas aeruginosa tolerance to tobramycin, hydrogen

peroxide and polymorphonuclear leukocytes is quorum-sensing dependent. *Microbiology* **151,** 373–383 (2005).

13. Brooun, A., Liu, S. & Lewis, K. A dose-response study of antibiotic resistance inPseudomonas aeruginosa biofilms. *Antimicrob. agents* (2000). at http://aac.asm.org/content/44/3/640.short

14. Folsom, J. P. *et al.* Physiology of Pseudomonas aeruginosa in biofilms as revealed by transcriptome analysis. *BMC Microbiol.* **10,** 294 (2010).

15. Stewart, P. S. Theoretical aspects of antibiotic diffusion into microbial biofilms. *Antimicrob. Agents Chemother.* **40,** 2517–22 (1996).

16. Stewart, P. S. & William Costerton, J. Antibiotic resistance of bacteria in biofilms. *Lancet* **358,** 135–138 (2001).

17. Stewart, P. S., Davison, W. M. & Steenbergen, J. N. Daptomycin Rapidly Penetrates a Staphylococcus epidermidis Biofilm. *Antimicrob. Agents Chemother.* **53,** 3505–3507 (2009).

18. Suci, P. A., Mittelman, M. W., Yu, F. P. & Geesey, G. G. Investigation of ciprofloxacin penetration into Pseudomonas aeruginosa biofilms. *Antimicrob. Agents Chemother.* **38,** 2125–2133 (1994).

19. Shigeta, M. *et al.* Permeation of Antimicrobial Agents through Pseudomonas aeruginosa Biofilms: A Simple Method. *Chemotherapy* **43,** 340–345 (1997).

20. Walters, M. C., Roe, F., Bugnicourt, A., Franklin, M. J. & Stewart, P. S. Contributions of Antibiotic Penetration, Oxygen Limitation, and Low Metabolic Activity to Tolerance of Pseudomonas aeruginosa Biofilms to Ciprofloxacin and Tobramycin. *Antimicrob. Agents Chemother.* **47,** 317–323 (2003).

21. Stewart, P. S. Mechanisms of antibiotic resistance in bacterial biofilms. *Int. J. Med. Microbiol.* **292,** 107–113 (2002).

22. Tseng, B. S. *et al.* The extracellular matrix protects *Pseudomonas aeruginosa* biofilms by limiting the penetration of tobramycin. *Environ. Microbiol.* n/a-n/a (2013). doi:10.1111/1462-2920.12155

23. Borriello, G. *et al.* Oxygen Limitation Contributes to Antibiotic Tolerance of Pseudomonas aeruginosa in Biofilms. *Antimicrob. Agents Chemother.* **48,** 2659–2664 (2004).

24. Xu, K. D., Stewart, P. S., Xia, F., Huang, C. T. & McFeters, G. A. Spatial physiological heterogeneity in Pseudomonas aeruginosa biofilm is determined by oxygen availability. *Appl. Environ. Microbiol.* **64,** 4035–9 (1998).

25. Rani, S. A. *et al.* Spatial Patterns of DNA Replication, Protein Synthesis, and Oxygen Concentration within Bacterial Biofilms Reveal Diverse Physiological States. *J. Bacteriol.* **189,** 4223–4233 (2007).

26. Werner, E. *et al.* Stratified Growth in Pseudomonas aeruginosa Biofilms. *Appl. Environ. Microbiol.* **70,** 6188–6196 (2004).

27. Lenz, A. P., Williamson, K. S., Pitts, B., Stewart, P. S. & Franklin, M. J. Localized Gene Expression in Pseudomonas aeruginosa Biofilms. *Appl. Environ. Microbiol.* **74,** 4463–4471 (2008).

28. Williamson, K. S. *et al.* Heterogeneity in Pseudomonas aeruginosa Biofilms Includes Expression of Ribosome Hibernation Factors in the Antibiotic-Tolerant Subpopulation and Hypoxia-Induced Stress Response in the Metabolically Active Population. *J. Bacteriol.* **194,** 2062–2073 (2012).

29. Perez-Osorio, A. C., Williamson, K. S. & Franklin, M. J. Heterogeneous rpoS and rhlR mRNA Levels and 16S rRNA/rDNA (rRNA Gene) Ratios within Pseudomonas aeruginosa Biofilms, Sampled by Laser Capture Microdissection. *J. Bacteriol.* **192,** 2991–3000 (2010).

30. De Kievit, T. R. *et al.* Multidrug Efflux Pumps: Expression Patterns and Contribution to Antibiotic Resistance in Pseudomonas aeruginosa Biofilms. *Antimicrob. Agents Chemother.* **45,** 1761–1770 (2001).

31. Zhang, L., Hinz, A. J., Nadeau, J.-P. & Mah, T.-F. Pseudomonas aeruginosa tssC1 Links Type VI Secretion and Biofilm-Specific Antibiotic Resistance. *J. Bacteriol.* **193,** 5510–5513 (2011).

32. Colvin, K. M. *et al.* The Pel Polysaccharide Can Serve a Structural and Protective Role in the Biofilm Matrix of Pseudomonas aeruginosa. *PLoS Pathog.* **7,** e1001264 (2011).

33. Brem, H. *et al.* Molecular markers in patients with chronic wounds to guide surgical debridement. *Mol. Med.* **13,** 30–9 (2007).

34. James, G. A. *et al.* Biofilms in chronic wounds. *Wound Repair Regen.* **16,** 37–44

35. Zhao, G. *et al.* Time course study of delayed wound healing in a biofilm-challenged diabetic mouse model. *Wound Repair Regen.* **20,** 342–352 (2012).

36. Zhao, G. *et al.* Delayed wound healing in diabetic (db/db) mice with Pseudomonas aeruginosa biofilm challenge: a model for the study of chronic wounds. *Wound Repair Regen.* **18,** 467–77

37. Kirker, K. R. *et al.* Loss of viability and induction of apoptosis in human

keratinocytes exposed to Staphylococcus aureus biofilms in vitro. *Wound Repair Regen.* **17,** 690–9

38. Secor, P. R. *et al.* Staphylococcus aureus Biofilm and Planktonic cultures differentially impact gene expression, mapk phosphorylation, and cytokine production in human keratinocytes. *BMC Microbiol.* **11,** 143 (2011).

39. James, T. J., Hughes, M. A., Cherry, G. W. & Taylor, R. P. Simple biochemical markers to assess chronic wounds. *Wound Repair Regen.* **8,** 264–269 (2000).

40. Trengove, N. J., Langton, S. R. & Stacey, M. C. Biochemical analysis of wound fluid from nonhealing and healing chronic leg ulcers. *Wound Repair Regen.* **4,** 234–239 (1996).

41. Debats, I. B. J. G. *et al.* Infected Chronic Wounds Show Different Local and Systemic Arginine Conversion Compared With Acute Wounds. *J. Surg. Res.* **134,** 205–214 (2006).

42. Manzi, A. E. in *Current Protocols in Molecular Biology* (eds. Ausubel, F. et al.) 1–17 (1993).

43. Qiagen. *DNA Mini and Blood Mini Handbook*. (2012).

44. LaBauve, A. E. & Wargo, M. J. Growth and laboratory maintenance of Pseudomonas aeruginosa. *Curr. Protoc. Microbiol.* **Chapter 6,** Unit 6E.1. (2012).

45. Huang, D. W., Sherman, B. T. & Lempicki, R. A. Bioinformatics enrichment tools: paths toward the comprehensive functional analysis of large gene lists. *Nucleic Acids Res.* **37,** 1–13 (2009).

46. Huang, D. W., Sherman, B. T. & Lempicki, R. A. Systematic and integrative analysis of large gene lists using DAVID bioinformatics resources. *Nat. Protoc.* **4,** 44–57 (2009).

47. Stewart, P. S. *et al.* Contribution of Stress Responses to Antibiotic Tolerance in Pseudomonas aeruginosa Biofilms. *Antimicrob. Agents Chemother.* **59,** 3838–47 (2015).

48. Hunt, K. A., deM. Jennings, R., Inskeep, W. P. & Carlson, R. P. Stoichiometric modeling of assimilatory and dissimilatory biomass utilization in a microbial community. *Environ. Microbiol.* (2016). doi:10.1111/1462-2920.13444

49. Brock, M. & Buckel, W. On the mechanism of action of the antifungal agent propionate. *Eur. J. Biochem.* **271,** 3227–3241 (2004).

50. Maerker, C., Rohde, M., Brakhage, A. A. & Brock, M. Methylcitrate synthase

from Aspergillus fumigatus. Propionyl-CoA affects polyketide synthesis, growth and morphology of conidia. *FEBS J.* **272,** 3615–3630 (2005).

51. Weitzman, P. D. J. & Dunmore, P. Regulation of citrate synthase activity by α-ketoglutarate. Metabolic and taxonomic significance. *FEBS Lett.* **3,** 265–267 (1969).

52. Nham T. Nguyen, § *et al.* Comparative Analysis of Folding and Substrate Binding Sites between Regulated Hexameric Type II Citrate Synthases and Unregulated Dimeric Type I Enzymes†,‡. (2001).

53. Weitzman, P. & Danson, M. in *Current Topics in Cellular Regulation* (eds. Horecker, B. L. & Stadtman, E. R.) 161–200 (Academic Press, 1976).

54. Solomon, M. & Weitzman, P. D. J. Occurrence of two distinct citrate synthases in a mutant of *Pseudomonas aeruginosa* and their growth-dependent variation. *FEBS Lett.* **155,** 157–160 (1983).

55. PATTON, A. J., HOUGH, D. W., TOWNER, P. & DANSON, M. J. Does Escherichia coli possess a second citrate synthase gene? *Eur. J. Biochem.* **214,** 75–81 (1993).

56. Gerike, U., Hough, D. W., Russell, N. J., Dyall-Smith, M. L. & Danson, M. J. Citrate synthase and 2-methylcitrate synthase: structural, functional and evolutionary relationships. *Microbiology* **144,** 929–935 (1998).

57. Mitchell, C. G. Identification of a multienzyme complex of the tricarboxylic acid cycle enzymes containing citrate synthase isoenzymes from Pseudomonas aeruginosa. *Biochem. J* **313,** 769–774 (1996).

58. Díaz-Pérez, A. L. *et al.* Identification of the aceA gene encoding isocitrate lyase required for the growth of Pseudomonas aeruginosa on acetate, acyclic terpenes and leucine. *FEMS Microbiol. Lett.* **269,** 309–16 (2007).

59. Hagins, J. M., Locy, R. & Silo-Suh, L. Isocitrate Lyase Supplies Precursors for Hydrogen Cyanide Production in a Cystic Fibrosis Isolate of Pseudomonas aeruginosa. *J. Bacteriol.* **191,** 6335–6339 (2009).

60. Lindsey, T. L., Hagins, J. M., Sokol, P. A. & Silo-Suh, L. A. Virulence determinants from a cystic fibrosis isolate of Pseudomonas aeruginosa include isocitrate lyase. *Microbiology* **154,** 1616–1627 (2008).

61. Eichner, A. *et al.* Marker genes for the metabolic adaptation of Pseudomonas aeruginosa to the hypoxic cystic fibrosis lung environment. *Int. J. Med. Microbiol.* **304,** 1050–1061 (2014).

62. LaPorte, D. C., Thorsness, P. E. & Koshland, D. E. Compensatory phosphorylation of isocitrate dehydrogenase. A mechanism for adaptation to the intracellular environment. *J. Biol. Chem.* **260,** 10563–8 (1985).

63. Watson, D., Lindel, D. & Fall, R. Pseudomonas aeruginosa contains an inducible methylcitrate synthase. *Curr. Microbiol.* (1983). at http://link.springer.com/article/10.1007/BF01567308

64. Horswill, A. R. & Escalante-Semerena, J. C. In Vitro Conversion of Propionate to Pyruvate by *Salmonella enterica* Enzymes: 2-Methylcitrate Dehydratase (PrpD) and Aconitase Enzymes Catalyze the Conversion of 2-Methylcitrate to 2-Methylisocitrate †. *Biochemistry* **40,** 4703–4713 (2001).

65. Textor, S. *et al.* Propionate oxidation in Escherichia coli: evidence for operation of a methylcitrate cycle in bacteria. *Arch. Microbiol.* **168,** 428–36 (1997).

66. Wang, Z.-X. *et al.* The glyoxylate bypass of Ralstonia eutropha. *FEMS Microbiol. Lett.* **228,** 63–71 (2003).

67. Brock, M. Generation and phenotypic characterization of Aspergillus nidulans methylisocitrate lyase deletion mutants: methylisocitrate inhibits growth and conidiation. *Appl. Environ. Microbiol.* **71,** 5465–75 (2005).

68. McKnight, S. L., Iglewski, B. H. & Pesci, E. C. The Pseudomonas Quinolone Signal Regulates rhl Quorum Sensing in Pseudomonas aeruginosa. *J. Bacteriol.* **182,** 2702–2708 (2000).

69. Kasper, S. H., Bonocora, R. P., Wade, J. T., Musah, R. A. & Cady, N. C. Chemical Inhibition of Kynureninase Reduces *Pseudomonas aeruginosa* Quorum Sensing and Virulence Factor Expression. *ACS Chem. Biol.* **11,** 1106–1117 (2016).

70. Poole, K. Multidrug efflux pumps and antimicrobial resistance in Pseudomonas aeruginosa and related organisms. *J. Mol. Microbiol. Biotechnol.* (2001). at http://www.horizonpress.com/jmmb/v/v3/v3n2/17.pdf

71. Morita, Y., Tomida, J. & Kawamura, Y. Responses of Pseudomonas aeruginosa to antimicrobials. *Front. Microbiol.* **4,** 422 (2014).

72. Brazas, M. D. & Hancock, R. E. W. Ciprofloxacin Induction of a Susceptibility Determinant in Pseudomonas aeruginosa. *Antimicrob. Agents Chemother.* **49,** 3222–3227 (2005).

73. Cirz, R. T., O'Neill, B. M., Hammond, J. A., Head, S. R. & Romesberg, F. E. Defining the Pseudomonas aeruginosa SOS Response and Its Role in the Global Response to the Antibiotic Ciprofloxacin. *J. Bacteriol.* **188,** 7101–7110 (2006).

74. Stewart, P. S. *et al.* Contribution of stress responses to antibiotic tolerance in Pseudomonas aeruginosa biofilms. *Antimicrob. Agents Chemother.* **59,** 3838–47 (2015).

75. Essar, D. W., Eberly, L., Hadero, A. & Crawford, I. P. Identification and characterization of genes for a second anthranilate synthase in Pseudomonas aeruginosa: interchangeability of the two anthranilate synthases and evolutionary implications. *J. Bacteriol.* **172,** 884–900 (1990).

76. Lesic, B., Starkey, M., He, J., Hazan, R. & Rahme, L. G. Quorum sensing differentially regulates Pseudomonas aeruginosa type VI secretion locus I and homologous loci II and III, which are required for pathogenesis. *Microbiology* **155,** 2845–2855 (2009).

77. Lin, J. *et al.* The icmF3 locus is involved in multiple adaptation- and virulence-related characteristics in Pseudomonas aeruginosa PAO1. *Front. Cell. Infect. Microbiol.* **5,** 70 (2015).

78. Rakin, A., Schneider, L. & Podladchikova, O. Hunger for iron: the alternative siderophore iron scavenging systems in highly virulent Yersinia. *Front. Cell. Infect. Microbiol.* **2,** 151 (2012).

79. Pukatzki, S. *et al.* Identification of a conserved bacterial protein secretion system in Vibrio cholerae using the Dictyostelium host model system. *Proc. Natl. Acad. Sci. U. S. A.* **103,** 1528–33 (2006).

80. Mougous, J. D. *et al.* A virulence locus of Pseudomonas aeruginosa encodes a protein secretion apparatus. *Science* **312,** 1526–30 (2006).

81. Wang, J., Li, C., Yang, H., Mushegian, A. & Jin, S. A novel serine/threonine protein kinase homologue of Pseudomonas aeruginosa is specifically inducible within the host infection site and is required for full virulence in neutropenic mice. *J. Bacteriol.* **180,** 6764–8 (1998).

82. Segal, G., Purcell, M. & Shuman, H. A. Host cell killing and bacterial conjugation require overlapping sets of genes within a 22-kb region of the Legionella pneumophila genome. *Proc. Natl. Acad. Sci. U. S. A.* **95,** 1669–74 (1998).

83. Purcell, M. & Shuman, H. A. The Legionella pneumophila icmGCDJBF genes are required for killing of human macrophages. *Infect. Immun.* **66,** 2245–55 (1998).

84. Das, S. *et al.* Comparison of global transcription responses allows identification of Vibrio cholerae genes differentially expressed following infection. *FEMS Microbiol. Lett.* **190,** 87–91 (2000).

85. Pallen, M., Chaudhuri, R. & Khan, A. Bacterial FHA domains: neglected players

in the phospho-threonine signalling game? *Trends Microbiol.* **10,** 556–563 (2002).

86. Folkesson, A., Löfdahl, S. & Normark, S. The Salmonella enterica subspecies I specific centisome 7 genomic island encodes novel protein families present in bacteria living in close contact with eukaryotic cells. *Res. Microbiol.* **153,** 537–545 (2002).

87. Das, S., Chakrabortty, A., Banerjee, R. & Chaudhuri, K. Involvement of in vivo induced icmF gene of Vibrio cholerae in motility, adherence to epithelial cells, and conjugation frequency. *Biochem. Biophys. Res. Commun.* **295,** 922–928 (2002).

88. Das, S. & Chaudhuri, K. Identification of a unique IAHP (IcmF associated homologous proteins) cluster in Vibrio cholerae and other proteobacteria through in silico analysis. *In Silico Biol.* **3,** (2003).

89. Sexton, J. A. & Vogel, J. P. Type IVB Secretion by Intracellular Pathogens. *Traffic* **3,** 178–185 (2002).

90. Srinivasa Rao, P. S., Yamada, Y., Tan, Y. P. & Leung, K. Y. Use of proteomics to identify novel virulence determinants that are required for Edwardsiella tarda pathogenesis. *Mol. Microbiol.* **53,** 573–586 (2004).

91. Boyer, F., Fichant, G., Berthod, J., Vandenbrouck, Y. & Attree, I. Dissecting the bacterial type VI secretion system by a genome wide in silico analysis: what can be learned from available microbial genomic resources? *BMC Genomics* **10,** 104 (2009).

92. de Bruin, O. M., Ludu, J. S. & Nano, F. E. The Francisella pathogenicity island protein IglA localizes to the bacterial cytoplasm and is needed for intracellular growth. *BMC Microbiol.* **7,** 1 (2007).

93. Parsons, D. A. & Heffron, F. sciS, an icmF homolog in Salmonella enterica serovar Typhimurium, limits intracellular replication and decreases virulence. *Infect. Immun.* **73,** 4338–45 (2005).

94. Schell, M. A. *et al.* Type VI secretion is a major virulence determinant in *Burkholderia mallei*. *Mol. Microbiol.* **64,** 1466–1485 (2007).

95. Jani, A. J. & Cotter, P. A. Type VI Secretion: Not Just for Pathogenesis Anymore. *Cell Host Microbe* **8,** 2–6 (2010).

96. Bladergroen, M. R., Badelt, K. & Spaink, H. P. Infection-blocking genes of a symbiotic Rhizobium leguminosarum strain that are involved in temperature-dependent protein secretion. *Mol. Plant Microbe Interact.* **16,** 53–64 (2003).

97. Chen, L., Zou, Y., She, P. & Wu, Y. Composition, function, and regulation of T6SS in Pseudomonas aeruginosa. *Microbiol. Res.* **172,** 19–25 (2015).

98. Hachani, A. *et al.* Type VI Secretion System in Pseudomonas aeruginosa: SECRETION AND MULTIMERIZATION OF VgrG PROTEINS. *J. Biol. Chem.* **286,** 12317–12327 (2011).99. Silverman, J. M., Brunet, Y. R., Cascales, E. & Mougous, J. D. Structure and regulation of the type VI secretion system. *Annu. Rev. Microbiol.* **66,** 453–72 (2012).

100. Aschtgen, M.-S., Bernard, C. S., De Bentzmann, S., Lloubès, R. & Cascales, E. SciN is an outer membrane lipoprotein required for type VI secretion in enteroaggregative Escherichia coli. *J. Bacteriol.* **190,** 7523–31 (2008).

101. Felisberto-Rodrigues, C. *et al.* Towards a structural comprehension of bacterial type VI secretion systems: characterization of the TssJ-TssM complex of an Escherichia coli pathovar. *PLoS Pathog.* **7,** e1002386 (2011).

102. Ma, L.-S., Lin, J.-S. & Lai, E.-M. An IcmF Family Protein, ImpLM, Is an Integral Inner Membrane Protein Interacting with ImpKL, and Its Walker A Motif Is Required for Type VI Secretion System-Mediated Hcp Secretion in Agrobacterium tumefaciens. *J. Bacteriol.* **191,** 4316–4329 (2009).

103. Leiman, P. G. *et al.* Type VI secretion apparatus and phage tail-associated protein complexes share a common evolutionary origin. *Proc. Natl. Acad. Sci.* **106,** 4154–4159 (2009).

104. Kanamaru, S. Structural similarity of tailed phages and pathogenic bacterial secretion systems. *Proc. Natl. Acad. Sci.* **106,** 4067–4068 (2009).

105. Pukatzki, S., Ma, A. T., Revel, A. T., Sturtevant, D. & Mekalanos, J. J. Type VI secretion system translocates a phage tail spike-like protein into target cells where it cross-links actin. *Proc. Natl. Acad. Sci.* **104,** 15508–15513 (2007).

106. Lossi, N. S., Dajani, R., Freemont, P. & Filloux, A. Structure-function analysis of HsiF, a gp25-like component of the type VI secretion system, in Pseudomonas aeruginosa. *Microbiology* **157,** 3292–3305 (2011).

107. Bönemann, G. *et al.* Remodelling of VipA/VipB tubules by ClpV-mediated threading is crucial for type VI protein secretion. *EMBO J.* **28,** 315–325 (2009).

108. Basler, M., Pilhofer, M., Henderson, G. P., Jensen, G. J. & Mekalanos, J. J. Type VI secretion requires a dynamic contractile phage tail-like structure. *Nature* **483,** 182–6 (2012).

109. Kudryashev, M. *et al.* Structure of the type VI secretion system contractile sheath. *Cell* **160,** 952–62 (2015).

110. Pietrosiuk, A. *et al.* Molecular Basis for the Unique Role of the AAA+ Chaperone ClpV in Type VI Protein Secretion. *J. Biol. Chem.* **286,** 30010–30021 (2011).

111. Kapitein, N. *et al.* ClpV recycles VipA/VipB tubules and prevents non-productive tubule formation to ensure efficient type VI protein secretion. *Mol. Microbiol.* **87,** 1013–1028 (2013).

112. Mougous, J. D., Gifford, C. A., Ramsdell, T. L. & Mekalanos, J. J. Threonine phosphorylation post-translationally regulates protein secretion in Pseudomonas aeruginosa. *Nat. Cell Biol.* **9,** 797–803 (2007).

113. Basler, M. & Mekalanos, J. J. Type 6 secretion dynamics within and between bacterial cells. *Science* **337,** 815 (2012).

114. Whitney, J. C. *et al.* Genetically distinct pathways guide effector export through the type VI secretion system. *Mol. Microbiol.* **92,** 529–42 (2014).

115. Sana, T. G. *et al.* Internalization of *Pseudomonas aeruginosa* Strain PAO1 into Epithelial Cells Is Promoted by Interaction of a T6SS Effector with the Microtubule Network. *MBio* **6,** e00712-15 (2015).

116. Hood, R. D. *et al.* A type VI secretion system of Pseudomonas aeruginosa targets a toxin to bacteria. *Cell Host Microbe* **7,** 25–37 (2010).

117. Russell, A. B. *et al.* Type VI secretion delivers bacteriolytic effectors to target cells. *Nature* **475,** 343–347 (2011).

118. Russell, A. B. *et al.* Diverse type VI secretion phospholipases are functionally plastic antibacterial effectors. *Nature* **496,** 508–12 (2013).

119. Wilderman, P. J., Vasil, A. I., Johnson, Z. & Vasil, M. L. Genetic and biochemical analyses of a eukaryotic-like phospholipase D of Pseudomonas aeruginosa suggest horizontal acquisition and a role for persistence in a chronic pulmonary infection model. *Mol. Microbiol.* **39,** 291–304 (2001).

120. Jiang, F., Waterfield, N. R., Yang, J., Yang, G. & Jin, Q. A Pseudomonas aeruginosa Type VI Secretion Phospholipase D Effector Targets Both Prokaryotic and Eukaryotic Cells. *Cell Host Microbe* **15,** 600–610 (2014).

121. Bingle, L. E., Bailey, C. M. & Pallen, M. J. Type VI secretion: a beginner's guide. *Curr. Opin. Microbiol.* **11,** 3–8 (2008).

122. Sana, T. G. *et al.* The Second Type VI Secretion System of Pseudomonas aeruginosa Strain PAO1 Is Regulated by Quorum Sensing and Fur and Modulates Internalization in Epithelial Cells. *J. Biol. Chem.* **287,** 27095–27105 (2012).

123. Goodman, A. L. *et al.* A Signaling Network Reciprocally Regulates Genes Associated with Acute Infection and Chronic Persistence in Pseudomonas aeruginosa. *Dev. Cell* **7,** 745–754 (2004).

124. Pessi, G. *et al.* Dual control of hydrogen cyanide biosynthesis by the global activator GacA in Pseudomonas aeruginosa PAO1. *FEMS Microbiol. Lett.* **200,** 73–8 (2001).

125. Brencic, A. *et al.* The GacS/GacA signal transduction system of *Pseudomonas aeruginosa* acts exclusively through its control over the transcription of the RsmY and RsmZ regulatory small RNAs. *Mol. Microbiol.* **73,** 434–445 (2009).

126. Moscoso, J., Mikkelsen, H. & Heeb, S. The Pseudomonas aeruginosa sensor RetS switches Type III and Type VI secretion via c-di-GMP signalling. *Environmental* (2011). at http://onlinelibrary.wiley.com/doi/10.1111/j.1462-2920.2011.02595.x/full

127. Silverman, J. M. *et al.* Separate inputs modulate phosphorylation-dependent and -independent type VI secretion activation. *Mol. Microbiol.* **82,** 1277–1290 (2011).

128. Lin, J.-S. *et al.* Fha Interaction with Phosphothreonine of TssL Activates Type VI Secretion in Agrobacterium tumefaciens. *PLoS Pathog.* **10,** e1003991 (2014).

129. Mougous, J. D., Gifford, C. A., Ramsdell, T. L. & Mekalanos, J. J. Threonine phosphorylation post-translationally regulates protein secretion in Pseudomonas aeruginosa. *Nat. Cell Biol.* **9,** 797–803 (2007).

130. Casabona, M. G. *et al.* An ABC transporter and an outer membrane lipoprotein participate in posttranslational activation of type VI secretion in Pseudomonas aeruginosa. *Environ. Microbiol.* **15,** 471–86 (2013).

131. Southey-Pillig, C. J., Davies, D. G. & Sauer, K. Characterization of Temporal Protein Production in Pseudomonas aeruginosa Biofilms. *J. Bacteriol.* **187,** 8114–8126 (2005).

132. Hoffman, L. R. *et al.* Pseudomonas aeruginosa lasR mutants are associated with cystic fibrosis lung disease progression. *J. Cyst. Fibros.* **8,** 66–70 (2009).

133. Sana, T. G. *et al.* Internalization of *Pseudomonas aeruginosa* Strain PAO1 into Epithelial Cells Is Promoted by Interaction of a T6SS Effector with the Microtubule Network. *MBio* **6,** e00712-15 (2015).

134. Bernard, C. S., Brunet, Y. R., Gueguen, E. & Cascales, E. Nooks and crannies in type VI secretion regulation. *J. Bacteriol.* **192,** 3850–60 (2010).

135. Sana, T. G. *et al.* Divergent Control of Two Type VI Secretion Systems by RpoN

in Pseudomonas aeruginosa. *PLoS One* **8,** e76030 (2013).

136. Castang, S., McManus, H. R., Turner, K. H. & Dove, S. L. H-NS family members function coordinately in an opportunistic pathogen. *Proc. Natl. Acad. Sci.* **105,** 18947–18952 (2008).

137. Lemire, J. *et al.* Histidine is a source of the antioxidant, alpha-ketoglutarate, in Pseudomonas fluorescens challenged by oxidative stress. *FEMS Microbiol. Lett.* **309,** 170–7 (2010).

138. Chung, J. C. S., Rzhepishevska, O., Ramstedt, M. & Welch, M. Type III secretion system expression in oxygen-limited Pseudomonas aeruginosa cultures is stimulated by isocitrate lyase activity. *Open Biol.* **3,** 120131 (2013).

139. Jesaitis, A. J. *et al.* Compromised host defense on Pseudomonas aeruginosa biofilms: characterization of neutrophil and biofilm interactions. *J. Immunol.* **171,** 4329–39 (2003).

APPENDICES

APPENDIX A

SUPPLEMENTARY TABLES

Supplementary Table 1. Genes up-expressed in biofilm samples (log2(FC) > 1, adjusted P value < 0.1).

Gene	log2(Fold change)	P value	Adjusted P value
PA0007	1.41	1.52E-02	8.79E-02
PA0038	3.86	2.69E-04	2.40E-02
PA0059	2.85	1.88E-05	1.23E-02
PA0105	1.58	1.10E-02	7.64E-02
PA0122	2.84	1.76E-02	9.47E-02
PA0176	1.49	1.94E-02	9.89E-02
PA0260	2.15	1.06E-02	7.51E-02
PA0261	1.92	1.82E-05	1.23E-02
PA0262	1.49	2.32E-04	2.40E-02
PA0276	1.07	9.60E-03	7.25E-02
PA0329	2.11	2.49E-03	4.37E-02
PA0424	1.67	6.45E-03	6.25E-02
PA0432	1.02	1.98E-03	4.08E-02
PA0460	1.71	5.17E-04	2.84E-02
PA0462	1.72	5.04E-03	5.62E-02
PA0484	1.97	7.09E-03	6.40E-02
PA0506	3.34	7.12E-03	6.40E-02
PA0509	1.60	1.53E-02	8.82E-02
PA0510	2.70	3.97E-04	2.58E-02
PA0512	1.00	3.75E-03	5.13E-02
PA0518	3.60	6.63E-03	6.28E-02
PA0520	2.11	2.71E-03	4.58E-02
PA0523	3.81	1.36E-03	3.89E-02
PA0524	3.27	1.56E-03	3.94E-02
PA0525	2.06	6.42E-03	6.24E-02
PA0534	2.43	2.59E-03	4.49E-02
PA0547	1.57	7.71E-03	6.63E-02
PA0567	1.33	1.48E-03	3.93E-02
PA0585	1.50	2.24E-03	4.32E-02
PA0586	3.20	1.06E-03	3.56E-02
PA0587	3.33	1.02E-03	3.51E-02
PA0588	3.98	7.90E-05	1.89E-02
PA0656	2.20	1.88E-03	4.08E-02
PA0665	1.90	3.34E-03	4.93E-02
PA0713	5.17	5.65E-04	2.85E-02
PA0719	2.78	4.04E-03	5.16E-02
PA0720	3.45	1.45E-02	8.61E-02
PA0723	4.29	1.15E-02	7.79E-02

Supplementary Table 1 - CONTINUED

PA0737	2.13	1.72E-03	4.00E-02
PA0743	1.28	8.34E-04	3.21E-02
PA0744	2.56	1.41E-02	8.51E-02
PA0745	2.95	1.46E-02	8.66E-02
PA0762	1.64	6.08E-03	6.14E-02
PA0763	1.78	2.47E-03	4.37E-02
PA0781	4.39	2.98E-03	4.76E-02
PA0792	2.87	1.70E-03	3.99E-02
PA0905	1.95	5.40E-03	5.82E-02
PA0918	2.49	1.87E-02	9.69E-02
PA0942	1.89	4.32E-03	5.25E-02
PA0982	1.31	2.47E-03	4.37E-02
PA0983	1.44	5.08E-03	5.64E-02
PA1041	3.42	1.50E-05	1.23E-02
PA1114	1.51	2.12E-03	4.22E-02
PA1118	1.70	4.04E-03	5.16E-02
PA1135	1.92	6.82E-04	3.04E-02
PA1168	1.62	1.21E-02	7.96E-02
PA1247	1.26	6.68E-03	6.29E-02
PA1323	4.45	4.24E-05	1.79E-02
PA1324	4.02	5.65E-04	2.85E-02
PA1348	1.78	1.47E-03	3.93E-02
PA1366	1.63	1.15E-04	1.89E-02
PA1404	2.30	9.68E-04	3.46E-02
PA1423	1.19	1.51E-03	3.93E-02
PA1430	2.02	1.02E-02	7.42E-02
PA1432	1.55	1.29E-02	8.24E-02
PA1471	3.36	1.57E-04	2.21E-02
PA1494	1.35	1.49E-02	8.72E-02
PA1508	1.79	9.24E-03	7.17E-02
PA1509	2.62	4.27E-04	2.63E-02
PA1511	2.48	3.73E-03	5.13E-02
PA1515	1.22	1.05E-02	7.48E-02
PA1517	2.64	1.78E-02	9.49E-02
PA1518	2.68	1.80E-02	9.53E-02
PA1545	2.72	2.68E-03	4.56E-02
PA1562	1.24	1.23E-03	3.81E-02
PA1592	2.47	5.50E-03	5.83E-02
PA1617	2.16	1.78E-03	4.01E-02
PA1657	1.23	5.16E-04	2.84E-02

Supplementary Table 1 - CONTINUED

PA1664	2.89	3.90E-03	5.16E-02
PA1666	1.82	1.98E-02	9.96E-02
PA1668	1.83	1.72E-03	4.00E-02
PA1676	1.12	4.67E-03	5.42E-02
PA1729	1.34	6.03E-04	2.87E-02
PA1746	1.92	1.98E-02	9.96E-02
PA1753	2.41	2.77E-04	2.40E-02
PA1761	1.70	4.34E-03	5.26E-02
PA1860	1.77	2.93E-03	4.76E-02
PA1871	4.29	1.30E-03	3.88E-02
PA1874	2.05	1.42E-03	3.92E-02
PA1901	2.59	2.60E-04	2.40E-02
PA1903	3.10	2.40E-03	4.36E-02
PA1904	2.89	1.32E-02	8.28E-02
PA1905	3.17	6.19E-03	6.18E-02
PA1914	1.22	5.93E-03	6.09E-02
PA1921	1.86	8.74E-03	7.05E-02
PA1922	3.50	2.58E-03	4.48E-02
PA1924	1.80	7.33E-03	6.46E-02
PA1927	5.26	6.12E-05	1.83E-02
PA1930	2.48	1.66E-03	3.96E-02
PA1999	1.33	1.51E-02	8.77E-02
PA2003	2.00	9.75E-03	7.32E-02
PA2021	2.78	1.59E-03	3.94E-02
PA2024	2.38	1.11E-02	7.64E-02
PA2031	1.95	1.59E-03	3.94E-02
PA2045	1.12	3.20E-03	4.89E-02
PA2066	2.76	3.66E-03	5.11E-02
PA2067	2.84	4.41E-03	5.29E-02
PA2069	2.44	1.57E-02	8.92E-02
PA2071	1.28	8.42E-03	6.93E-02
PA2134	1.64	3.99E-03	5.16E-02
PA2146	4.77	1.57E-02	8.93E-02
PA2170	1.26	8.23E-04	3.21E-02
PA2171	1.52	1.94E-03	4.08E-02
PA2173	1.19	5.97E-03	6.10E-02
PA2174	1.94	7.22E-04	3.09E-02
PA2190	3.92	3.90E-03	5.16E-02
PA2199	1.27	1.42E-03	3.92E-02
PA2247	2.44	1.01E-02	7.40E-02

Supplementary Table 1 - CONTINUED

PA2248	2.26	1.49E-02	8.74E-02
PA2249	1.22	1.11E-02	7.64E-02
PA2274	2.44	1.49E-03	3.93E-02
PA2290	1.19	7.47E-03	6.51E-02
PA2298	1.11	4.19E-03	5.22E-02
PA2300	3.74	1.34E-02	8.33E-02
PA2327	3.13	5.18E-04	2.84E-02
PA2328	1.48	2.45E-04	2.40E-02
PA2329	2.51	1.00E-02	7.39E-02
PA2330	2.04	9.60E-04	3.46E-02
PA2331	4.61	1.28E-04	1.98E-02
PA2364	1.14	3.53E-03	5.08E-02
PA2365	3.33	1.65E-04	2.21E-02
PA2366	3.36	8.59E-04	3.27E-02
PA2367	1.67	1.05E-02	7.48E-02
PA2368	4.09	1.02E-05	1.23E-02
PA2369	1.02	1.29E-03	3.87E-02
PA2370	1.05	8.94E-03	7.09E-02
PA2371	1.23	4.14E-03	5.22E-02
PA2375	1.63	2.40E-04	2.40E-02
PA2381	3.64	4.09E-03	5.21E-02
PA2415	1.32	2.49E-03	4.37E-02
PA2433	4.51	1.03E-03	3.51E-02
PA2436	1.42	3.24E-03	4.91E-02
PA2483	1.20	1.46E-03	3.93E-02
PA2485	4.44	3.58E-04	2.55E-02
PA2486	1.26	1.97E-02	9.93E-02
PA2504	1.30	4.03E-04	2.58E-02
PA2562	3.04	6.62E-05	1.83E-02
PA2564	1.04	4.49E-03	5.35E-02
PA2565	1.71	7.57E-03	6.57E-02
PA2566	1.01	5.23E-03	5.75E-02
PA2569	1.05	5.61E-03	5.85E-02
PA2570	3.89	4.50E-03	5.35E-02
PA2571	1.51	1.80E-03	4.03E-02
PA2572	1.33	1.60E-03	3.94E-02
PA2573	2.10	1.54E-04	2.21E-02
PA2620	1.84	8.40E-03	6.93E-02
PA2621	2.34	5.86E-03	6.03E-02
PA2622	1.39	3.59E-03	5.09E-02

Supplementary Table 1 - CONTINUED

PA2779	3.00	6.58E-03	6.28E-02
PA2780	3.07	2.73E-03	4.60E-02
PA2781	2.90	2.26E-03	4.32E-02
PA2788	2.27	7.59E-04	3.12E-02
PA2794	1.35	1.37E-02	8.40E-02
PA2799	1.46	7.58E-04	3.12E-02
PA2815	1.97	1.24E-03	3.81E-02
PA2826	3.82	1.36E-02	8.37E-02
PA2883	3.04	3.25E-03	4.91E-02
PA2895	1.06	7.62E-04	3.12E-02
PA2896	1.23	1.87E-02	9.69E-02
PA2897	1.43	1.21E-02	7.96E-02
PA2920	1.77	7.85E-04	3.15E-02
PA2931	1.19	2.48E-04	2.40E-02
PA2937	3.98	3.04E-03	4.81E-02
PA3006	3.57	1.04E-02	7.48E-02
PA3017	1.62	8.68E-03	7.02E-02
PA3023	1.26	1.86E-02	9.66E-02
PA3032	1.63	1.67E-03	3.98E-02
PA3040	2.21	9.85E-05	1.89E-02
PA3041	1.91	1.16E-03	3.73E-02
PA3042	2.39	9.88E-03	7.35E-02
PA3049	6.61	1.63E-04	2.21E-02
PA3080	2.55	1.76E-02	9.47E-02
PA3123	1.10	1.01E-02	7.40E-02
PA3126	5.57	3.91E-04	2.58E-02
PA3142	1.22	1.79E-02	9.49E-02
PA3160	1.63	7.43E-04	3.12E-02
PA3205	3.35	1.08E-02	7.56E-02
PA3273	1.38	1.03E-02	7.45E-02
PA3292	1.85	1.37E-02	8.40E-02
PA3307	1.71	1.10E-02	7.64E-02
PA3361	5.75	6.04E-05	1.83E-02
PA3370	2.49	4.11E-03	5.21E-02
PA3371	2.18	2.24E-03	4.32E-02
PA3413	1.80	5.11E-05	1.83E-02
PA3415	4.59	4.85E-04	2.78E-02
PA3417	4.28	3.99E-04	2.58E-02
PA3418	4.52	1.09E-04	1.89E-02
PA3451	2.13	2.65E-03	4.54E-02

Supplementary Table 1 - CONTINUED

PA3488	1.63	1.07E-02	7.54E-02
PA3584	3.13	6.62E-03	6.28E-02
PA3587	1.55	9.71E-04	3.46E-02
PA3598	1.15	1.39E-02	8.44E-02
PA3600	7.65	5.44E-05	1.83E-02
PA3601	7.93	9.39E-06	1.23E-02
PA3688	2.99	7.12E-05	1.83E-02
PA3691	5.60	6.93E-05	1.83E-02
PA3692	4.96	-4.96E+00	3.21E-02
PA3712	1.44	2.95E-03	4.76E-02
PA3719	2.88	1.60E-02	8.98E-02
PA3723	2.35	1.51E-03	3.93E-02
PA3724	3.80	4.27E-03	5.25E-02
PA3785	1.84	5.01E-03	5.60E-02
PA3788	2.12	1.44E-02	8.60E-02
PA3790	2.38	4.61E-03	5.41E-02
PA3796	1.68	1.97E-03	4.08E-02
PA3815	3.15	7.67E-04	3.12E-02
PA3819	3.16	2.41E-03	4.36E-02
PA3844	1.75	3.23E-04	2.48E-02
PA3846	1.68	2.83E-03	4.71E-02
PA3857	1.54	3.39E-03	4.98E-02
PA3858	1.29	1.64E-02	9.12E-02
PA3919	2.14	1.70E-02	9.30E-02
PA3922	4.13	2.47E-03	4.37E-02
PA3923	2.86	1.06E-02	7.52E-02
PA3929	1.20	1.48E-02	8.70E-02
PA3930	1.17	6.00E-03	6.10E-02
PA3952	1.03	3.84E-03	5.13E-02
PA3986	1.12	1.05E-02	7.48E-02
PA4063	6.22	2.03E-04	2.40E-02
PA4064	2.76	8.89E-03	7.09E-02
PA4066	2.21	8.98E-03	7.11E-02
PA4141	3.90	3.30E-03	4.93E-02
PA4170	2.50	1.65E-02	9.14E-02
PA4171	1.91	1.55E-02	8.88E-02
PA4199	1.69	1.67E-02	9.19E-02
PA4205	1.56	4.68E-03	5.42E-02
PA4206	3.23	5.17E-03	5.69E-02
PA4207	2.00	1.39E-02	8.44E-02

Supplementary Table 1 - CONTINUED

PA4208	1.44	2.97E-03	4.76E-02
PA4210	1.84	6.62E-03	6.28E-02
PA4211	2.11	9.43E-03	7.21E-02
PA4217	2.10	1.05E-02	7.48E-02
PA4222	3.05	5.32E-03	5.79E-02
PA4223	3.44	2.82E-03	4.71E-02
PA4224	2.72	4.29E-03	5.25E-02
PA4225	1.92	1.65E-02	9.14E-02
PA4226	2.95	1.42E-02	8.52E-02
PA4231	2.99	1.55E-02	8.89E-02
PA4294	1.05	9.61E-03	7.25E-02
PA4305	1.18	2.87E-03	4.74E-02
PA4306	1.46	5.60E-03	5.85E-02
PA4311	1.50	5.26E-03	5.75E-02
PA4326	1.37	1.62E-03	3.94E-02
PA4345	1.38	2.37E-03	4.36E-02
PA4364	1.26	2.61E-04	2.40E-02
PA4377	2.35	1.98E-03	4.08E-02
PA4475	1.67	8.89E-03	7.09E-02
PA4523	4.13	3.65E-03	5.11E-02
PA4551	2.05	1.37E-02	8.40E-02
PA4553	1.00	7.92E-03	6.69E-02
PA4573	1.95	1.95E-02	9.92E-02
PA4575	1.90	1.78E-03	4.01E-02
PA4607	2.61	1.50E-03	3.93E-02
PA4608	1.76	1.61E-03	3.94E-02
PA4641	1.53	1.71E-02	9.32E-02
PA4648	1.14	1.10E-02	7.64E-02
PA4697	1.07	1.98E-02	9.94E-02
PA4702	1.25	1.84E-03	4.08E-02
PA4703	1.46	4.72E-03	5.42E-02
PA4738	4.07	8.99E-05	1.89E-02
PA4739	5.75	1.18E-05	1.23E-02
PA4834	4.33	6.08E-04	2.87E-02
PA4835	3.74	6.79E-04	3.04E-02
PA4836	4.60	9.64E-04	3.46E-02
PA4837	5.73	2.95E-04	2.40E-02
PA4838	2.69	3.06E-03	4.83E-02
PA4870	1.34	1.05E-02	7.48E-02
PA4876	3.63	8.66E-05	1.89E-02

Supplementary Table 1 - CONTINUED

PA4877	1.59	4.19E-03	5.22E-02
PA5060	2.01	9.01E-03	7.12E-02
PA5086	1.11	1.15E-02	7.77E-02
PA5100	1.34	1.23E-02	8.04E-02
PA5178	1.37	1.69E-02	9.28E-02
PA5182	3.33	2.46E-03	4.37E-02
PA5212	4.72	3.98E-04	2.58E-02
PA5359	1.28	1.59E-02	8.95E-02
PA5424	1.32	1.95E-02	9.92E-02
PA5460	3.14	3.01E-04	2.40E-02
PA5481	5.00	2.78E-04	2.40E-02
PA5482	5.05	1.07E-04	1.89E-02
PA5499	2.45	4.02E-03	5.16E-02
PA5501	2.06	2.48E-03	4.37E-02
PA5534	3.04	1.44E-04	2.18E-02
PA5535	5.00	1.89E-04	2.37E-02
PA5536	5.18	1.33E-03	3.88E-02
PA5537	2.35	3.00E-03	4.77E-02
PA5538	2.60	5.94E-03	6.09E-02
PA5539	5.10	3.02E-04	2.40E-02
PA5540	4.78	1.12E-04	1.89E-02
PA5541	4.27	3.95E-04	2.58E-02
PA5546	2.60	9.75E-05	1.89E-02

Supplementary Table 2. Genes down-expressed in biofilms (log2(FC) > 1, adjusted P value < 0.1).

Gene	log2(Fold change)	P value	Adjusted P value
PA0003	1.20	8.95E-03	7.09E-02
PA0004	1.29	2.62E-04	2.40E-02
PA0008	1.76	1.55E-02	8.89E-02
PA0016	1.46	1.69E-03	3.99E-02
PA0022	1.18	1.09E-03	3.62E-02
PA0024	2.10	4.25E-03	5.25E-02
PA0025	1.04	1.60E-02	9.00E-02
PA0045	4.14	1.78E-05	1.23E-02
PA0046	4.50	7.32E-06	1.23E-02
PA0047	3.93	3.21E-04	2.48E-02
PA0070	1.52	1.21E-02	7.96E-02
PA0074	1.19	1.33E-02	8.28E-02
PA0076	1.64	1.80E-02	9.52E-02
PA0077	2.08	1.48E-02	8.70E-02
PA0078	1.79	8.28E-03	6.88E-02
PA0079	2.27	5.80E-03	5.99E-02
PA0092	1.36	7.51E-04	3.12E-02
PA0094	2.17	7.87E-03	6.68E-02
PA0126	3.76	1.03E-03	3.51E-02
PA0162	1.76	9.50E-03	7.21E-02
PA0165	2.37	3.01E-04	2.40E-02
PA0167	1.99	7.85E-03	6.68E-02
PA0169	2.01	5.35E-04	2.84E-02
PA0171	2.35	2.13E-03	4.22E-02
PA0172	1.27	1.14E-02	7.74E-02
PA0277	5.84	2.51E-05	1.43E-02
PA0291	3.11	2.30E-04	2.40E-02
PA0303	1.63	1.00E-02	7.39E-02
PA0308	1.09	1.50E-02	8.74E-02
PA0331	1.43	1.75E-02	9.44E-02
PA0335	1.60	2.29E-03	4.34E-02
PA0341	1.35	1.38E-03	3.89E-02
PA0350	1.41	5.14E-03	5.68E-02
PA0363	1.41	1.23E-02	8.05E-02
PA0371	1.92	1.98E-03	4.08E-02
PA0372	1.63	8.63E-03	7.01E-02
PA0381	1.11	5.53E-03	5.84E-02
PA0382	1.12	1.80E-03	4.03E-02

Supplementary Table 2 – CONTINUED

PA0389	2.11	5.61E-03	5.85E-02
PA0390	1.70	9.94E-05	1.89E-02
PA0399	3.08	1.88E-02	9.75E-02
PA0401	1.81	7.89E-03	6.68E-02
PA0402	1.09	1.52E-02	8.80E-02
PA0403	1.71	1.31E-03	3.88E-02
PA0410	1.39	1.17E-02	7.90E-02
PA0420	1.19	8.31E-04	3.21E-02
PA0422	1.72	1.25E-03	3.81E-02
PA0426	1.33	9.04E-03	7.13E-02
PA0427	1.24	9.09E-03	7.14E-02
PA0437	1.54	1.92E-03	4.08E-02
PA0527	4.27	2.15E-03	4.22E-02
PA0537	1.19	5.77E-03	5.98E-02
PA0548	1.93	2.16E-04	2.40E-02
PA0549	1.58	1.22E-02	7.98E-02
PA0552	2.46	2.37E-03	4.36E-02
PA0555	1.64	7.16E-03	6.40E-02
PA0563	1.91	1.65E-02	9.13E-02
PA0593	1.24	1.49E-03	3.93E-02
PA0650	1.32	5.47E-04	2.85E-02
PA0654	3.23	2.30E-03	4.34E-02
PA0668	1.44	9.21E-03	7.17E-02
PA0730	2.28	5.25E-03	5.75E-02
PA0736	1.18	5.09E-03	5.64E-02
PA0766	1.13	3.19E-03	4.89E-02
PA0767	1.67	1.13E-02	7.70E-02
PA0773	1.19	4.55E-03	5.40E-02
PA0782	4.05	1.45E-03	3.93E-02
PA0783	5.21	1.45E-03	3.93E-02
PA0802	1.03	1.35E-02	8.33E-02
PA0837	1.20	1.82E-02	9.55E-02
PA0855	1.45	7.84E-03	6.68E-02
PA0867	3.02	7.21E-03	6.41E-02
PA0902	1.55	4.69E-03	5.42E-02
PA0904	2.02	7.54E-03	6.56E-02
PA0943	1.21	1.90E-02	9.79E-02
PA0944	1.49	1.01E-02	7.40E-02
PA0945	2.50	4.15E-04	2.61E-02
PA0956	1.31	6.04E-03	6.13E-02

Supplementary Table 2 – CONTINUED

PA0958	1.35	3.61E-03	5.10E-02
PA0963	2.70	4.56E-03	5.40E-02
PA0964	2.70	8.56E-03	6.99E-02
PA0968	1.19	1.45E-02	8.62E-02
PA0969	2.71	9.08E-03	7.14E-02
PA0970	1.35	1.37E-02	8.40E-02
PA0973	1.88	1.11E-02	7.64E-02
PA0996	1.66	1.49E-02	8.74E-02
PA0997	1.23	5.63E-03	5.86E-02
PA0998	1.94	5.48E-03	5.82E-02
PA0999	1.44	1.70E-02	9.30E-02
PA1001	1.58	1.70E-03	3.99E-02
PA1002	1.12	3.82E-03	5.13E-02
PA1011	2.50	1.62E-02	9.05E-02
PA1013	3.05	4.74E-03	5.43E-02
PA1047	1.05	8.63E-03	7.01E-02
PA1049	2.10	3.64E-03	5.11E-02
PA1064	1.68	5.45E-03	5.82E-02
PA1068	1.39	7.14E-03	6.40E-02
PA1076	2.48	9.14E-03	7.16E-02
PA1156	2.50	6.79E-03	6.33E-02
PA1161	1.41	8.48E-03	6.96E-02
PA1196	2.16	3.95E-03	5.16E-02
PA1222	1.07	1.56E-02	8.92E-02
PA1228	1.62	6.21E-03	6.18E-02
PA1271	1.19	1.89E-03	4.08E-02
PA1272	1.24	1.81E-02	9.53E-02
PA1274	1.32	6.31E-03	6.19E-02
PA1278	1.98	1.78E-03	4.01E-02
PA1293	1.03	1.73E-02	9.39E-02
PA1339	2.55	1.76E-02	9.47E-02
PA1341	3.13	4.25E-03	5.25E-02
PA1365	1.08	1.11E-02	7.64E-02
PA1375	1.34	1.93E-03	4.08E-02
PA1493	1.61	1.21E-02	7.96E-02
PA1546	3.35	1.81E-02	9.53E-02
PA1552	3.16	4.58E-03	5.40E-02
PA1553	2.77	4.04E-03	5.16E-02
PA1574	3.24	2.66E-03	4.55E-02
PA1580	1.28	9.44E-03	7.21E-02

Supplementary Table 2 – CONTINUED

PA1585	1.75	6.30E-03	6.19E-02
PA1586	1.30	4.42E-03	5.29E-02
PA1587	1.43	1.84E-02	9.62E-02
PA1588	2.27	6.17E-03	6.18E-02
PA1589	2.81	9.75E-04	3.46E-02
PA1687	1.16	4.15E-03	5.22E-02
PA1757	1.27	1.96E-03	4.08E-02
PA1766	1.53	1.08E-02	7.57E-02
PA1791	2.41	4.32E-04	2.63E-02
PA1792	1.98	4.75E-06	1.23E-02
PA1794	1.46	1.49E-03	3.93E-02
PA1795	1.27	1.01E-03	3.51E-02
PA1800	3.03	4.28E-03	5.25E-02
PA1805	2.37	1.71E-02	9.34E-02
PA1806	1.16	3.33E-03	4.93E-02
PA1816	1.01	1.08E-02	7.59E-02
PA1845	1.31	4.97E-03	5.56E-02
PA1969	1.15	6.07E-04	2.87E-02
PA2023	1.86	8.58E-03	6.99E-02
PA2080	1.51	9.84E-03	7.35E-02
PA2193	3.67	1.55E-03	3.94E-02
PA2194	1.95	4.50E-04	2.70E-02
PA2195	2.22	6.74E-03	6.30E-02
PA2204	1.68	1.47E-02	8.70E-02
PA2232	1.21	3.72E-03	5.13E-02
PA2235	1.48	1.76E-02	9.47E-02
PA2426	2.90	1.37E-02	8.40E-02
PA2445	1.40	1.78E-02	9.49E-02
PA2446	1.81	1.54E-02	8.82E-02
PA2579	1.53	3.87E-04	2.58E-02
PA2581	1.91	1.23E-02	8.05E-02
PA2587	1.05	1.73E-02	9.41E-02
PA2612	1.80	9.84E-03	7.35E-02
PA2616	2.05	2.87E-03	4.74E-02
PA2624	1.83	9.47E-03	7.21E-02
PA2630	1.75	5.12E-03	5.67E-02
PA2648	1.96	1.14E-02	7.76E-02
PA2649	1.59	8.15E-03	6.79E-02
PA2684	1.61	7.70E-03	6.63E-02
PA2739	1.95	2.74E-03	4.60E-02

Supplementary Table 2 – CONTINUED

PA2741	2.30	9.29E-03	7.19E-02
PA2742	1.39	1.71E-02	9.33E-02
PA2755	2.15	3.83E-03	5.13E-02
PA2760	2.52	2.23E-04	2.40E-02
PA2774	1.32	1.96E-02	9.92E-02
PA2828	1.02	1.16E-03	3.73E-02
PA2851	2.73	7.60E-03	6.58E-02
PA2904	1.21	1.31E-02	8.28E-02
PA2945	1.95	9.53E-03	7.21E-02
PA2948	1.13	6.93E-03	6.38E-02
PA2950	2.68	1.15E-03	3.73E-02
PA2965	1.99	1.38E-03	3.89E-02
PA2967	1.85	3.57E-03	5.09E-02
PA2968	2.40	5.58E-03	5.85E-02
PA2979	1.07	1.97E-02	9.94E-02
PA2987	1.22	4.37E-03	5.28E-02
PA2995	1.52	8.75E-03	7.05E-02
PA3000	1.19	7.90E-03	6.68E-02
PA3001	1.76	1.09E-02	7.62E-02
PA3011	1.14	3.15E-03	4.88E-02
PA3018	2.03	4.11E-03	5.21E-02
PA3021	1.40	6.30E-03	6.19E-02
PA3029	1.34	1.25E-02	8.08E-02
PA3046	2.11	9.93E-03	7.37E-02
PA3107	3.20	3.06E-03	4.83E-02
PA3108	1.17	1.26E-04	1.98E-02
PA3111	1.35	3.30E-03	4.93E-02
PA3134	1.41	1.03E-03	3.51E-02
PA3146	1.49	1.94E-02	9.90E-02
PA3147	1.21	1.93E-02	9.87E-02
PA3165	1.62	1.96E-03	4.08E-02
PA3167	1.85	2.54E-03	4.44E-02
PA3168	1.25	8.06E-03	6.74E-02
PA3172	1.62	8.56E-03	6.99E-02
PA3179	1.51	6.82E-03	6.34E-02
PA3227	1.38	7.27E-03	6.44E-02
PA3243	1.35	9.49E-03	7.21E-02
PA3245	2.18	9.93E-03	7.37E-02
PA3262	1.92	4.94E-03	5.56E-02
PA3263	2.45	8.31E-03	6.88E-02

Supplementary Table 2 – CONTINUED

PA3268	1.85	3.30E-03	4.93E-02
PA3278	2.78	1.07E-02	7.56E-02
PA3308	1.84	3.50E-03	5.06E-02
PA3313	1.87	1.94E-03	4.08E-02
PA3337	3.30	3.84E-03	5.13E-02
PA3397	2.69	3.16E-03	4.88E-02
PA3435	2.12	1.32E-02	8.28E-02
PA3453	2.59	5.65E-03	5.87E-02
PA3470	1.11	4.77E-03	5.45E-02
PA3471	1.29	1.79E-02	9.50E-02
PA3484	1.48	1.49E-03	3.93E-02
PA3525	2.36	1.32E-02	8.28E-02
PA3528	1.14	6.39E-04	2.98E-02
PA3537	1.56	1.42E-02	8.53E-02
PA3603	1.19	5.47E-05	1.83E-02
PA3604	1.13	7.98E-03	6.70E-02
PA3625	1.23	1.06E-02	7.52E-02
PA3627	1.02	5.98E-03	6.10E-02
PA3632	1.34	1.62E-02	9.06E-02
PA3635	1.47	9.53E-03	7.21E-02
PA3647	1.21	1.51E-02	8.79E-02
PA3650	1.74	1.72E-02	9.35E-02
PA3651	1.92	1.91E-03	4.08E-02
PA3652	3.39	3.55E-04	2.55E-02
PA3653	1.77	1.62E-03	3.94E-02
PA3654	1.49	1.33E-02	8.28E-02
PA3655	3.27	1.62E-03	3.94E-02
PA3656	3.01	7.46E-03	6.51E-02
PA3659	1.35	1.11E-02	7.64E-02
PA3666	1.59	5.69E-04	2.85E-02
PA3674	1.03	1.97E-02	9.94E-02
PA3675	2.15	1.67E-02	9.19E-02
PA3686	2.57	9.17E-04	3.42E-02
PA3700	2.23	1.47E-02	8.69E-02
PA3716	3.35	2.19E-04	2.40E-02
PA3725	1.00	4.86E-03	5.52E-02
PA3735	1.96	5.55E-03	5.84E-02
PA3736	1.21	4.13E-03	5.22E-02
PA3742	3.57	9.97E-04	3.51E-02
PA3743	2.01	1.89E-03	4.08E-02

Supplementary Table 2 – CONTINUED

PA3763	1.50	2.67E-05	1.43E-02
PA3769	2.56	1.88E-03	4.08E-02
PA3770	1.97	6.05E-04	2.87E-02
PA3794	1.15	1.25E-02	8.09E-02
PA3799	1.40	3.66E-03	5.11E-02
PA3800	1.65	5.66E-03	5.87E-02
PA3803	1.15	9.46E-03	7.21E-02
PA3807	1.95	1.21E-02	7.96E-02
PA3820	3.25	3.50E-05	1.59E-02
PA3821	2.75	9.64E-04	3.46E-02
PA3822	1.91	6.36E-03	6.22E-02
PA3834	2.54	6.25E-03	6.18E-02
PA3859	2.23	1.19E-03	3.76E-02
PA3880	3.09	1.03E-02	7.45E-02
PA3887	1.44	1.63E-03	3.94E-02
PA3904	2.07	6.05E-03	6.13E-02
PA3905	1.74	9.44E-04	3.46E-02
PA3906	2.79	3.33E-04	2.52E-02
PA3907	2.26	3.52E-04	2.55E-02
PA3908	2.75	3.09E-03	4.84E-02
PA3940	3.92	6.01E-04	2.87E-02
PA3967	1.43	2.01E-03	4.13E-02
PA3976	1.35	1.06E-02	7.52E-02
PA3977	3.10	1.11E-03	3.65E-02
PA3981	1.53	9.29E-03	7.19E-02
PA3984	1.17	2.04E-03	4.13E-02
PA3988	2.06	6.58E-03	6.28E-02
PA3989	1.09	4.69E-03	5.42E-02
PA3996	1.50	8.30E-03	6.88E-02
PA3997	1.41	6.38E-03	6.23E-02
PA3999	1.13	3.14E-03	4.88E-02
PA4004	1.14	1.41E-02	8.51E-02
PA4006	1.56	1.30E-02	8.24E-02
PA4031	2.69	2.65E-03	4.54E-02
PA4052	2.08	6.40E-03	6.24E-02
PA4053	1.48	1.38E-02	8.40E-02
PA4067	2.27	1.36E-02	8.37E-02
PA4069	1.38	1.22E-02	7.99E-02
PA4190	2.13	1.62E-04	2.21E-02
PA4232	1.84	7.84E-03	6.68E-02

Supplementary Table 2 – CONTINUED

PA4235	2.38	5.95E-03	6.09E-02
PA4237	2.38	1.11E-02	7.64E-02
PA4239	2.35	1.78E-02	9.49E-02
PA4243	2.71	1.78E-03	4.01E-02
PA4244	2.37	1.20E-02	7.96E-02
PA4250	1.61	1.52E-02	8.79E-02
PA4252	3.00	6.73E-03	6.30E-02
PA4255	2.74	8.46E-03	6.95E-02
PA4256	2.09	1.18E-02	7.94E-02
PA4258	1.68	1.80E-02	9.53E-02
PA4260	1.44	1.41E-02	8.52E-02
PA4261	1.86	1.29E-02	8.24E-02
PA4265	2.26	2.96E-03	4.76E-02
PA4266	2.14	1.81E-02	9.53E-02
PA4268	2.01	1.48E-02	8.70E-02
PA4270	1.64	4.31E-03	5.25E-02
PA4271	1.87	1.19E-02	7.95E-02
PA4272	2.79	8.24E-03	6.85E-02
PA4274	1.78	1.33E-02	8.28E-02
PA4279	1.04	1.30E-02	8.24E-02
PA4292	1.42	7.45E-03	6.51E-02
PA4314	1.63	3.95E-03	5.16E-02
PA4317	2.20	1.05E-03	3.55E-02
PA4321	1.25	1.44E-02	8.60E-02
PA4322	2.03	1.70E-03	3.99E-02
PA4323	1.15	7.08E-03	6.40E-02
PA4328	3.06	9.64E-03	7.27E-02
PA4348	4.71	1.56E-03	3.94E-02
PA4358	2.44	1.90E-02	9.82E-02
PA4359	3.26	5.70E-04	2.85E-02
PA4370	1.77	7.96E-03	6.70E-02
PA4372	1.84	3.71E-03	5.13E-02
PA4373	1.08	1.28E-02	8.22E-02
PA4395	2.31	1.25E-02	8.11E-02
PA4402	1.27	3.92E-03	5.16E-02
PA4410	1.13	9.13E-03	7.16E-02
PA4411	2.02	2.47E-03	4.37E-02
PA4428	2.05	1.01E-02	7.40E-02
PA4429	1.73	1.59E-03	3.94E-02
PA4430	3.07	6.65E-03	6.29E-02

Supplementary Table 2 – CONTINUED

PA4431	1.41	4.79E-03	5.47E-02
PA4432	2.17	3.08E-03	4.84E-02
PA4433	2.59	1.92E-02	9.86E-02
PA4438	1.39	3.18E-03	4.88E-02
PA4448	1.09	2.89E-03	4.75E-02
PA4449	1.89	7.23E-03	6.42E-02
PA4452	1.52	6.53E-03	6.28E-02
PA4453	1.82	1.12E-02	7.66E-02
PA4455	1.22	7.66E-03	6.62E-02
PA4484	1.68	1.74E-02	9.42E-02
PA4487	1.49	6.40E-03	6.24E-02
PA4489	1.90	5.22E-04	2.84E-02
PA4490	1.03	3.00E-04	2.40E-02
PA4491	1.70	3.91E-03	5.16E-02
PA4493	1.34	2.04E-03	4.13E-02
PA4538	1.62	2.30E-03	4.34E-02
PA4559	1.44	7.19E-03	6.41E-02
PA4565	2.37	6.58E-04	3.03E-02
PA4568	1.74	1.92E-02	9.84E-02
PA4569	2.08	7.15E-03	6.40E-02
PA4572	2.39	2.34E-03	4.36E-02
PA4576	1.30	1.66E-03	3.96E-02
PA4578	1.27	2.35E-04	2.40E-02
PA4588	1.24	1.28E-02	8.21E-02
PA4595	1.84	2.97E-03	4.76E-02
PA4628	1.63	3.54E-03	5.08E-02
PA4632	3.30	1.12E-04	1.89E-02
PA4645	1.97	2.70E-03	4.57E-02
PA4646	1.47	1.75E-03	4.01E-02
PA4647	1.69	5.29E-04	2.84E-02
PA4661	1.50	3.47E-03	5.03E-02
PA4663	1.23	2.05E-03	4.13E-02
PA4664	2.22	5.65E-04	2.85E-02
PA4665	1.66	7.31E-03	6.46E-02
PA4671	3.67	8.64E-03	7.01E-02
PA4672	1.92	1.09E-03	3.62E-02
PA4673	2.28	4.42E-03	5.29E-02
PA4675	5.04	6.13E-03	6.17E-02
PA4686	2.24	1.23E-03	3.81E-02
PA4694	2.19	1.41E-03	3.91E-02

Supplementary Table 2 – CONTINUED

PA4701	1.23	7.16E-04	3.09E-02
PA4723	1.71	3.21E-03	4.89E-02
PA4730	1.59	1.68E-02	9.24E-02
PA4731	1.72	6.99E-04	3.06E-02
PA4732	1.20	8.94E-03	7.09E-02
PA4740	2.94	3.95E-03	5.16E-02
PA4741	3.07	3.40E-03	4.98E-02
PA4742	1.78	6.81E-03	6.33E-02
PA4743	2.53	1.53E-03	3.94E-02
PA4744	2.02	7.47E-03	6.51E-02
PA4754	1.58	3.36E-03	4.95E-02
PA4755	2.65	1.27E-03	3.87E-02
PA4756	2.18	4.78E-04	2.78E-02
PA4757	1.59	9.22E-03	7.17E-02
PA4768	1.74	7.55E-03	6.56E-02
PA4847	1.83	3.96E-03	5.16E-02
PA4848	2.54	1.29E-02	8.24E-02
PA4850	1.36	2.38E-03	4.36E-02
PA4853	1.98	1.78E-02	9.49E-02
PA4854	2.02	1.31E-02	8.28E-02
PA4855	2.27	1.05E-02	7.48E-02
PA4907	1.04	1.02E-02	7.42E-02
PA4919	1.87	5.51E-03	5.84E-02
PA4920	1.42	1.03E-02	7.45E-02
PA4923	2.27	1.18E-02	7.90E-02
PA4931	1.39	1.37E-02	8.40E-02
PA4932	3.00	5.25E-04	2.84E-02
PA4933	2.51	4.58E-04	2.70E-02
PA4934	1.93	1.64E-03	3.94E-02
PA4935	2.44	3.76E-03	5.13E-02
PA4938	2.42	1.16E-03	3.73E-02
PA4942	1.48	9.31E-03	7.19E-02
PA4957	1.63	4.58E-03	5.40E-02
PA4960	1.04	1.62E-02	9.06E-02
PA4966	1.78	3.39E-05	1.59E-02
PA4967	1.68	2.57E-04	2.40E-02
PA4974	1.97	2.40E-03	4.36E-02
PA5001	1.59	1.54E-02	8.82E-02
PA5004	1.86	2.06E-03	4.14E-02
PA5007	1.79	8.97E-03	7.11E-02

Supplementary Table 2 – CONTINUED

PA5008	1.48	1.85E-02	9.65E-02
PA5011	1.49	6.95E-03	6.38E-02
PA5012	1.35	2.63E-03	4.54E-02
PA5035	1.43	1.71E-02	9.33E-02
PA5037	1.03	8.11E-03	6.77E-02
PA5046	2.84	2.60E-04	2.40E-02
PA5049	2.92	2.97E-03	4.76E-02
PA5051	1.60	1.42E-02	8.54E-02
PA5065	1.00	4.89E-03	5.54E-02
PA5074	1.23	3.21E-04	2.48E-02
PA5075	1.35	1.86E-03	4.08E-02
PA5076	1.52	9.40E-03	7.21E-02
PA5078	2.11	4.73E-03	5.42E-02
PA5110	2.44	4.91E-03	5.55E-02
PA5117	3.70	1.71E-04	2.24E-02
PA5128	3.81	6.91E-04	3.04E-02
PA5129	1.86	4.37E-03	5.28E-02
PA5131	2.27	3.99E-04	2.58E-02
PA5140	2.24	4.32E-04	2.63E-02
PA5142	1.63	1.86E-02	9.65E-02
PA5174	1.80	8.40E-03	6.93E-02
PA5192	3.12	2.35E-03	4.36E-02
PA5201	2.19	1.73E-03	4.01E-02
PA5208	3.54	2.24E-03	4.32E-02
PA5214	1.04	1.83E-02	9.57E-02
PA5217	1.31	1.34E-03	3.88E-02
PA5232	1.99	1.15E-02	7.77E-02
PA5233	1.28	1.32E-02	8.28E-02
PA5244	1.11	3.98E-03	5.16E-02
PA5250	1.83	1.95E-02	9.92E-02
PA5263	1.56	5.37E-03	5.82E-02
PA5274	1.62	2.31E-03	4.34E-02
PA5278	2.13	8.95E-04	3.38E-02
PA5298	2.12	1.27E-02	8.21E-02
PA5302	2.55	1.00E-02	7.39E-02
PA5303	4.12	6.61E-03	6.28E-02
PA5304	2.84	1.32E-03	3.88E-02
PA5316	2.19	8.42E-03	6.93E-02
PA5321	1.06	9.39E-03	7.21E-02
PA5323	1.25	2.04E-03	4.13E-02

Supplementary Table 2 – CONTINUED

PA5334	1.97	1.11E-03	3.65E-02
PA5344	1.43	3.96E-03	5.16E-02
PA5413	1.12	1.58E-03	3.94E-02
PA5414	1.51	1.91E-02	9.83E-02
PA5425	1.67	7.12E-03	6.40E-02
PA5426	1.48	1.01E-02	7.40E-02
PA5429	3.90	1.32E-02	8.28E-02
PA5441	1.47	3.23E-03	4.91E-02
PA5461	2.49	3.78E-03	5.13E-02
PA5479	2.85	4.63E-03	5.42E-02
PA5504	2.12	1.85E-03	4.08E-02
PA5505	2.55	1.60E-03	3.94E-02
PA5528	1.24	1.75E-02	9.44E-02
PA5530	1.88	5.47E-03	5.82E-02
PA5551	1.08	1.82E-02	9.56E-02
PA5552	2.15	7.10E-03	6.40E-02
PA5553	3.99	1.78E-03	4.01E-02
PA5554	3.40	7.48E-03	6.51E-02
PA5555	3.17	1.92E-02	9.84E-02
PA5556	2.45	1.65E-02	9.14E-02
PA5557	2.79	1.10E-02	7.64E-02
PA5559	2.74	8.81E-03	7.08E-02
PA5560	2.89	2.69E-03	4.57E-02
PA5568	1.45	1.85E-02	9.63E-02

Supplementary Table 3. Genes down-expressed with ciprofloxacin treatment (log2(FC) > 1, adjusted P value < 0.1).

Gene	log2(Fold change)	P value	Adjusted P value
PA0039	5.36	1.52E-03	6.64E-02
PA0059	5.32	2.85E-04	4.87E-02
PA0122	5.12	3.32E-03	8.29E-02
PA0260	4.87	4.08E-03	9.12E-02
PA0261	4.86	8.02E-04	6.41E-02
PA0262	4.77	1.15E-04	4.16E-02
PA0263	4.76	2.96E-03	7.94E-02
PA0291	4.75	7.90E-04	6.41E-02
PA0300	4.62	9.44E-04	6.41E-02
PA0432	4.42	1.57E-04	4.16E-02
PA0660	4.27	1.84E-04	4.24E-02
PA0792	4.25	4.52E-03	9.52E-02
PA0871	4.11	2.74E-03	7.93E-02
PA0872	4.09	4.22E-04	5.33E-02
PA0958	4.03	4.62E-07	2.73E-03
PA1000	3.99	2.79E-03	7.94E-02
PA1002	3.90	4.89E-03	9.57E-02
PA1041	3.90	7.79E-04	6.41E-02
PA1323	3.85	3.11E-05	3.06E-02
PA1324	3.74	2.19E-03	7.15E-02
PA1337	3.71	1.62E-04	4.16E-02
PA1339	3.62	5.30E-03	9.85E-02
PA1340	3.60	2.02E-03	7.03E-02
PA1341	3.59	3.84E-03	8.98E-02
PA1342	3.48	1.91E-03	6.90E-02
PA1430	3.47	4.01E-03	9.10E-02
PA1431	3.40	1.05E-03	6.41E-02
PA1432	3.35	1.16E-03	6.42E-02
PA1509	3.33	1.25E-03	6.43E-02
PA1511	3.32	1.86E-03	6.90E-02
PA1656	3.19	4.17E-03	9.16E-02
PA1657	3.16	1.25E-03	6.43E-02
PA1658	3.14	4.71E-04	5.41E-02
PA1659	3.12	4.39E-03	9.34E-02
PA1661	3.09	1.86E-03	6.90E-02
PA1662	3.07	1.27E-03	6.43E-02
PA1664	3.04	4.29E-03	9.16E-02
PA1666	3.01	3.04E-03	7.99E-02

Supplementary Table 3 – CONTINUED

PA1667	2.92	9.91E-04	6.41E-02
PA1668	2.89	1.37E-03	6.49E-02
PA1669	2.83	3.85E-04	5.16E-02
PA1670	2.82	5.21E-03	9.78E-02
PA1761	2.78	1.36E-03	6.48E-02
PA1871	2.78	1.73E-03	6.81E-02
PA1874	2.75	1.55E-03	6.64E-02
PA1901	2.67	1.09E-03	6.42E-02
PA1903	2.67	4.68E-04	5.41E-02
PA1904	2.60	5.52E-03	9.98E-02
PA1905	2.59	4.77E-04	5.41E-02
PA1914	2.58	8.35E-04	6.41E-02
PA1927	2.55	1.19E-04	4.16E-02
PA2003	2.54	4.70E-03	9.57E-02
PA2066	2.53	3.03E-03	7.99E-02
PA2067	2.51	3.44E-03	8.44E-02
PA2174	2.50	4.55E-03	9.55E-02
PA2194	2.44	4.07E-03	9.12E-02
PA2303	2.43	5.32E-03	9.85E-02
PA2305	2.40	3.92E-03	9.00E-02
PA2328	2.36	7.16E-04	6.37E-02
PA2330	2.36	1.50E-04	4.16E-02
PA2331	2.33	3.75E-04	5.16E-02
PA2365	2.33	1.04E-04	4.16E-02
PA2366	2.32	1.05E-03	6.41E-02
PA2368	2.29	1.93E-03	6.90E-02
PA2370	2.27	2.85E-03	7.94E-02
PA2371	2.22	7.97E-04	6.41E-02
PA2424	2.21	4.03E-03	9.10E-02
PA2504	2.16	2.18E-03	7.14E-02
PA2532	2.11	1.40E-03	6.51E-02
PA2572	2.06	3.39E-03	8.44E-02
PA2760	2.04	2.77E-04	4.87E-02
PA2788	1.98	2.24E-03	7.18E-02
PA2853	1.95	1.27E-03	6.43E-02
PA3021	1.93	1.76E-03	6.81E-02
PA3032	1.92	4.82E-03	9.57E-02
PA3041	1.87	1.19E-03	6.43E-02
PA3101	1.87	1.59E-04	4.16E-02
PA3190	1.85	1.42E-03	6.55E-02

Supplementary Table 3 – CONTINUED

PA3227	1.84	5.06E-03	9.66E-02
PA3326	1.83	3.01E-03	7.99E-02
PA3327	1.82	1.34E-04	4.16E-02
PA3328	1.81	1.58E-03	6.70E-02
PA3329	1.81	9.71E-04	6.41E-02
PA3330	1.81	1.07E-03	6.41E-02
PA3331	1.78	8.54E-05	4.16E-02
PA3332	1.74	8.95E-05	4.16E-02
PA3333	1.74	1.04E-03	6.41E-02
PA3334	1.74	4.22E-03	9.16E-02
PA3335	1.73	3.75E-03	8.84E-02
PA3356	1.71	3.30E-04	4.93E-02
PA3361	1.70	5.48E-03	9.98E-02
PA3415	1.68	2.10E-03	7.12E-02
PA3477	1.67	5.45E-03	9.95E-02
PA3486	1.65	5.14E-03	9.72E-02
PA3587	1.64	5.50E-03	9.98E-02
PA3601	1.64	1.39E-03	6.49E-02
PA3622	1.64	2.90E-03	7.94E-02
PA3688	1.63	2.89E-04	4.87E-02
PA3723	1.62	1.05E-03	6.41E-02
PA3724	1.62	1.06E-04	4.16E-02
PA3785	1.61	2.62E-03	7.83E-02
PA3844	1.60	3.20E-04	4.93E-02
PA3846	1.51	2.34E-03	7.22E-02
PA3857	1.51	1.62E-03	6.72E-02
PA3904	1.50	4.89E-03	9.57E-02
PA3922	1.49	7.35E-04	6.37E-02
PA4015	1.47	7.34E-04	6.37E-02
PA4141	1.46	3.45E-03	8.44E-02
PA4208	1.46	5.91E-04	6.20E-02
PA4210	1.44	3.49E-03	8.44E-02
PA4211	1.41	6.20E-04	6.20E-02
PA4217	1.41	7.05E-04	6.37E-02
PA4222	1.38	3.42E-03	8.44E-02
PA4223	1.36	1.27E-03	6.43E-02
PA4224	1.34	3.62E-03	8.65E-02
PA4226	1.31	3.49E-03	8.44E-02
PA4306	1.27	2.95E-03	7.94E-02
PA4377	1.24	1.33E-03	6.45E-02

Supplementary Table 3 – CONTINUED

PA4525	1.22	1.12E-03	6.42E-02
PA4556	1.22	1.15E-03	6.42E-02
PA4578	1.22	1.08E-03	6.41E-02
PA4607	1.19	1.97E-04	4.24E-02
PA4736	1.18	4.72E-03	9.57E-02
PA4834	1.18	9.18E-04	6.41E-02
PA4835	1.17	3.23E-03	8.21E-02
PA4837	1.15	5.04E-03	9.66E-02
PA4922	1.14	4.89E-03	9.57E-02
PA5040	1.13	1.93E-03	6.90E-02
PA5060	1.12	1.15E-03	6.42E-02
PA5066	1.10	2.59E-03	7.78E-02
PA5220	1.10	2.26E-03	7.18E-02
PA5271	1.09	2.07E-03	7.09E-02
PA5348	1.08	4.68E-03	9.57E-02
PA5534	1.04	1.74E-03	6.81E-02
PA5539	1.03	3.24E-03	8.21E-02
PA5540	1.02	1.07E-03	6.41E-02
PA5541	1.01	1.89E-03	6.90E-02

Supplementary Table 4. Genes up-expressed with ciprofloxacin treatment (log2(FC) > 1, adjusted P value < 0.1).

Gene	log2(Fold change)	P value	Adjusted P value
PA0034	1.09	5.03E-03	9.66E-02
PA0165	1.35	1.62E-05	2.12E-02
PA0277	1.25	8.35E-04	6.41E-02
PA0330	1.67	3.92E-03	9.00E-02
PA0424	1.95	1.20E-03	6.43E-02
PA0577	3.11	8.17E-04	6.41E-02
PA0578	2.16	4.62E-03	9.57E-02
PA0719	7.52	8.75E-05	4.16E-02
PA0720	6.53	1.29E-03	6.43E-02
PA0724	7.59	1.25E-04	4.16E-02
PA0725	6.38	5.35E-04	5.95E-02
PA0726	7.96	1.01E-04	4.16E-02
PA0727	6.91	1.40E-05	2.12E-02
PA0728	5.84	2.38E-04	4.68E-02
PA0729	3.21	2.92E-03	7.94E-02
PA0760	1.26	2.31E-03	7.18E-02
PA0923	2.44	8.75E-04	6.41E-02
PA0936	1.14	4.58E-03	9.57E-02
PA0944	1.19	2.00E-03	7.03E-02
PA0945	1.38	5.43E-03	9.95E-02
PA0966	1.02	2.96E-03	7.94E-02
PA1155	2.22	2.53E-03	7.69E-02
PA1156	4.20	1.79E-03	6.81E-02
PA1164	1.75	5.41E-03	9.95E-02
PA1394	1.14	2.11E-03	7.12E-02
PA1475	2.36	3.87E-03	9.00E-02
PA1479	1.50	4.63E-04	5.41E-02
PA1559	3.16	4.91E-03	9.57E-02
PA1596	1.89	5.17E-03	9.74E-02
PA1793	1.17	9.64E-04	6.41E-02
PA2528	1.88	1.63E-03	6.72E-02
PA2583	1.22	1.70E-03	6.81E-02
PA2616	1.51	2.69E-03	7.91E-02
PA2627	1.42	3.78E-03	8.90E-02
PA2630	1.49	2.77E-03	7.94E-02
PA2684	1.28	6.09E-04	6.20E-02
PA2755	1.79	1.77E-03	6.81E-02
PA2774	1.69	2.71E-03	7.91E-02

Supplementary Table 4 – CONTINUED

PA2840	2.53	2.13E-03	7.12E-02
PA2901	1.60	3.17E-03	8.10E-02
PA2906	1.73	3.30E-04	4.93E-02
PA2929	1.30	9.53E-04	6.41E-02
PA2985	1.40	1.84E-04	4.24E-02
PA3008	3.48	4.46E-03	9.44E-02
PA3106	1.25	4.07E-03	9.12E-02
PA3108	1.61	8.14E-04	6.41E-02
PA3179	1.92	4.24E-03	9.16E-02
PA3308	1.32	1.33E-03	6.45E-02
PA3344	1.79	1.22E-03	6.43E-02
PA3413	2.77	5.78E-04	6.20E-02
PA3414	2.81	1.54E-03	6.64E-02
PA3554	1.28	2.89E-04	4.87E-02
PA3575	1.42	2.78E-04	4.87E-02
PA3616	3.83	6.03E-04	6.20E-02
PA3617	2.58	5.27E-03	9.85E-02
PA3661	3.57	3.16E-03	8.10E-02
PA3743	1.89	2.15E-03	7.12E-02
PA3756	2.06	1.80E-05	2.12E-02
PA3763	1.42	2.01E-04	4.24E-02
PA3824	1.33	4.08E-04	5.33E-02
PA3828	1.14	3.17E-03	8.10E-02
PA3966	1.12	2.30E-03	7.18E-02
PA4031	2.09	3.94E-03	9.00E-02
PA4045	1.42	9.94E-04	6.41E-02
PA4046	1.56	8.61E-04	6.41E-02
PA4050	1.11	3.75E-04	5.16E-02
PA4292	1.42	2.13E-03	7.12E-02
PA4480	1.81	1.05E-03	6.41E-02
PA4564	1.25	2.93E-03	7.94E-02
PA4565	3.08	5.14E-03	9.72E-02
PA4566	2.50	5.32E-03	9.85E-02
PA4665	1.70	4.77E-03	9.57E-02
PA4672	1.38	3.31E-03	8.29E-02
PA4731	2.84	1.61E-03	6.72E-02
PA4826	2.18	4.74E-03	9.57E-02
PA4852	1.59	8.40E-04	6.41E-02
PA4853	3.45	9.99E-04	6.41E-02
PA4918	2.77	3.48E-03	8.44E-02

Supplementary Table 4 – CONTINUED

PA4933	1.17	1.87E-03	6.90E-02
PA5199	1.13	2.29E-03	7.18E-02
PA5200	1.72	1.80E-03	6.81E-02
PA5470	2.18	1.44E-03	6.55E-02
PA5504	1.62	4.64E-03	9.57E-02
PA5528	1.21	2.28E-03	7.18E-02
PA5564	1.55	1.62E-03	6.72E-02

Supplementary Table 5. Combined list of putatively identified intracellular metabolites. Lists were assembled from Biocyc.

Name	Plank/ Biofilm	P value	Cipro./ Biofilm	P value
(+)-7-iso-jasmonate	4.20	2.21E-01	1.03	9.16E-01
(12Z,15Z)-9,10-dihydroxyoctadeca-12,15-dienoate	-1.53	2.69E-01	1.48	3.54E-01
(12Z,15Z)-9,10-epoxyoctadeca-12,15-dienoate	2.32	6.11E-01	-1.15	2.34E-01
(2R,4S)-2-methyl-2,4-dihydroxydihydrofuran-3-one	1.04	9.11E-01	-2.59	1.36E-01
(2S)-2-amino-3-oxo-4-phosphonooxybutanoate	12.45	9.77E-03	-1.16	6.10E-01
(2S,4S)-2-methyl-2,4-dihydroxydihydrofuran-3-one	1.04	9.11E-01	-2.59	1.36E-01
(2S,4S)-4-hydroxy-2,3,4,5-tetrahydrodipicolinate	4.00	8.35E-02	-1.09	7.63E-01
(2Z)-2-aminobut-2-enoate	38.78	6.15E-02	-1.57	3.70E-01
(2Z,4Z)-2-hydroxyhexa-2,4-dienoate	3.56	8.92E-02	-1.20	2.63E-01
(3E,5Z)-tetradecadienoate	3.58	8.79E-02	-1.24	5.49E-01
(4S,5S)-4,5-dihydroxy-2,6-dioxohexanoate	-1.15	5.54E-01	-1.45	6.65E-02
(9Z)-12,13-dihydroxyoctadeca-9-enoate	3.12	1.47E-02	1.73	3.11E-01
(9Z,12Z)-15,16-dihydroxyoctadeca-9,12-dienoate	-1.53	2.69E-01	1.48	3.54E-01
(9Z,12Z)-15,16-epoxyoctadeca-9,12-dienoate	2.32	6.11E-01	-1.15	2.34E-01
(9Z,15Z)-12,13-dihydroxyoctadeca-9,15-dienoate	-1.53	2.69E-01	1.48	3.54E-01
(9Z,15Z)-12,13-epoxyoctadeca-9,15-dienoate	2.32	6.11E-01	-1.15	2.34E-01
(R)-1-amino-2-propanol O-2-phosphate	4.78	2.13E-01	1.13	1.60E-01
(R)-2,3-dihydroxy-3-methylbutanoate	-1.81	2.94E-01	-1.21	6.06E-01
(R)-2,3-dihydroxy-3-methylpentanoate	1.16	8.52E-01	-1.15	8.30E-01
(R)-acetoin	1.89	3.94E-01	-1.51	2.73E-01
(R)-pantoate	1.16	8.52E-01	-1.15	8.30E-01
(R)-pantothenate	142.30	1.51E-01	-1.01	9.36E-01
(R,R)-2,3-butanediol	4.21	2.11E-01	1.09	2.85E-01
(S)-2,3,4,5-tetrahydrodipicolinate	1.01	9.86E-01	-1.32	3.52E-01

Supplementary Table 5 – CONTINUED

(S)-2-aceto-2-hydroxybutanoate	20.08	4.92E-02	-1.18	7.63E-01
(S)-2-acetolactate	1.04	9.11E-01	-2.59	1.36E-01
(S)-3-amino-2-methylpropanoate	7.13	1.74E-01	-1.61	2.84E-01
(S)-3-methyl-2-oxopentanoate	2.52	2.52E-01	-1.44	9.10E-02
(S)-4,5-dihydroxypentan-2,3-dione	1.04	9.11E-01	-2.59	1.36E-01
(S)-4-hydroxy-2-oxohexanoate	20.08	4.92E-02	-1.18	7.63E-01
(S)-acetoin	1.89	3.94E-01	-1.51	2.73E-01
(S)-nicotine	17.74	4.15E-02	2.11	5.63E-01
(S,S)-2,3-butanediol	4.21	2.11E-01	1.09	2.85E-01
1-(β-D ribofuranosyl)nicotinamide	6.99	1.10E-01	1.07	4.11E-01
1,6-anhydro-N-acetyl-β-muramate	44.88	2.27E-02	-1.38	5.44E-01
13(S)-HPOTE	3.23	6.59E-02	1.79	3.73E-02
1-aminocyclopropane-1-carboxylate	38.78	6.15E-02	-1.57	3.70E-01
1-butanesulfonate	-1.18	5.54E-01	-1.42	1.47E-01
1-deoxy-D-xylulose 5-phosphate	-7.19	2.28E-01	-4.59	2.59E-01
1-hydroxy-2-methyl-2-(E)-butenyl 4-diphosphate	16.53	7.61E-02	1.16	2.87E-01
1-oleoyl-2-lyso-glycerone phosphate	3.38	3.80E-02	1.06	4.11E-01
1-oleyl-2-lyso-phosphatidate	9.54	3.62E-02	1.45	3.17E-01
1-palmitoylglycerol 3-phosphate	3.58	4.64E-02	1.16	5.45E-01
1-pyrroline	97.39	4.11E-04	1.05	8.89E-01
2-(2-carboxy-4-methylthiazol-5-yl)ethyl phosphate	13.21	1.86E-01	-1.12	6.59E-01
2,6-diamino-4-hydroxy-5-(N-methyl)formamidopyrimidine	16.07	1.75E-01	2.11	1.09E-01
2-[(2R,5Z)-(2-carboxy-4-methylthiazol-5(2H)-ylidene]ethyl phosphate	13.21	1.86E-01	-1.12	6.59E-01
2-C-methyl-D-erythritol 4-phosphate	7.32	2.41E-02	-1.10	7.12E-01
2-deoxy-D-ribose 5-phosphate	-7.19	2.28E-01	-4.59	2.59E-01
2'-deoxyguanosine	5.84	5.07E-02	1.14	4.68E-01
2'-deoxyinosine	13.05	7.90E-02	1.08	3.81E-01
2'-deoxyribose	-1.81	2.94E-01	-1.21	6.06E-01
2-deoxy-α-D-ribose 1-phosphate	-7.19	2.28E-01	-4.59	2.59E-01
2-deydropantoate	20.08	4.92E-02	-1.18	7.63E-01
2-iminobutanoate	38.78	6.15E-02	-1.57	3.70E-01
2-isopropylmaleate	-2.80	3.40E-01	-1.88	2.62E-01
2-keto-4-hydroxypimelate	3.65	1.27E-03	1.32	2.83E-01
2-keto-6-aminocaproate	1.72	5.38E-01	-2.54	1.20E-01
2-keto-D-gluconate	2.97	1.78E-02	1.38	4.16E-01
2-keto-L-gulonate	2.97	1.78E-02	1.38	4.16E-01

Supplementary Table 5 – CONTINUED

2-oleoylglycerol	-1.55	6.52E-01	-1.65	6.61E-01
2-oxo-3-hydroxy-4-phosphobutanoate	-3.77	4.41E-01	-1.97	6.11E-01
2-oxo-3-phenylpropanoate	52.41	1.55E-01	1.01	9.17E-01
2-oxo-4-hydroxy-4-carboxy-5-ureidoimidazoline	15.11	1.76E-01	1.16	1.69E-01
2-oxo-4-methylthiobutanoate	1.98	1.14E-01	1.04	8.03E-01
2-oxoglutarate	2.19	1.54E-01	-2.26	1.01E-01
2-phenylethanol	21.71	1.17E-03	-1.31	3.10E-01
3-(N-morpholino)propanal	17.92	1.38E-01	1.15	4.77E-01
3,4-dihydroxy-9,10-secoandrosta-1,3,5(10)-triene-9,17-dione	-3.41	1.26E-02	-3.75	1.54E-03
3-[(3aS,4S,5R,7aS)-5-hydroxy-7a-methyl-1-oxo-octahydro-1H-indene-4-carboxylate	26.63	5.98E-02	1.08	3.69E-01
3-[(3aS,4S,7aS)-7a-methyl-1,5-dioxo-octahydro-1H-inden-4-yl]propanoate	17.23	3.40E-02	1.11	5.87E-01
3-acetylamino-4-hydroxybenzoate	25.80	3.26E-02	-1.07	5.63E-01
3-amino-4-hydroxybenzaldehyde	29.72	8.43E-02	1.09	2.89E-02
3-amino-4-hydroxybenzoate	13.07	6.64E-02	-1.04	6.66E-01
3-dehydroquinate	3.65	1.27E-03	1.32	2.83E-01
3-deoxy-D-manno-octulosonate	-3.40	4.14E-02	-1.93	3.46E-02
3-hydroxy-9,10-secoandrosta-1,3,5(10)-triene-9,17-dione	5.26	6.90E-02	1.89	3.59E-01
3-hydroxyanthranilate	13.07	6.64E-02	-1.04	6.66E-01
3-hydroxy-L-kynurenine	3.57	3.00E-01	-1.22	4.81E-01
3-methoxy-4-hydroxyphenylglycol	9.50	2.57E-02	1.88	9.42E-02
3-methyladenine	1.01	9.86E-01	-1.32	3.52E-01
3-oxo-dodecanoate	-2.76	2.72E-02	-2.03	2.78E-02
3-oxohexanoate	2.52	2.52E-01	-1.44	9.10E-02
3-oxooctanoate	23.61	1.06E-01	1.07	3.34E-01
3-phospho-hydroxypyruvate	3.52	3.11E-03	1.07	3.92E-01
3-phospho-L-serine	10.70	9.91E-02	-1.04	8.12E-01
4-acetamidobutanal	2.09	4.52E-01	-1.23	6.75E-01
4-acetamidobutanoate	1.72	5.38E-01	-2.54	1.20E-01
4-amino-2-methyl-5-phosphomethylpyrimidine	17.03	3.05E-01	1.30	8.82E-02
4-aminobenzoate	5.54	1.62E-01	26.37	1.98E-02
4-aminobutanoate	7.13	1.74E-01	-1.61	2.84E-01
4-deoxy-β-L-threo-hex-4-enopyranuronose	-1.15	5.54E-01	-1.45	6.65E-02
4-dimethylaminophenylazobenzene	13.98	1.85E-01	1.15	4.74E-01

Supplementary Table 5 – CONTINUED

4-guanidinobutyramide	2.97	2.85E-01	1.16	9.37E-03
4-guanidinobutyrate	1.72	5.38E-01	-2.54	1.20E-01
4-hydroxy-2-nonenal	12.54	8.37E-02	-1.31	5.11E-01
4-hydroxy-2-nonenal-[Cys-Gly] conjugate	5.36	2.51E-01	1.14	4.26E-01
4-hydroxybenzaldehyde	-1.21	7.95E-01	-1.01	9.62E-01
4-hydroxybenzoate	-1.18	5.54E-01	-1.42	1.47E-01
4-methyl-2-oxopentanoate	2.52	2.52E-01	-1.44	9.10E-02
4-methylphenol	8.47	2.72E-01	-1.08	4.95E-01
4-methylumbelliferyl glucoside	9.62	2.73E-02	-1.18	5.83E-02
4-tyrosol	8.25	1.28E-02	1.03	9.11E-01
5,6-dihydrouracil	1.06	8.52E-01	-1.58	1.59E-01
5-amino-1-(5-phospho-D-ribosyl)imidazole-4-carboxamide	11.42	1.53E-02	-2.13	1.42E-01
5-amino-4-imidazolecarboxyamide	7.29	1.12E-01	1.17	1.86E-02
5-amino-6-(D-ribitylamino)uracil	6.28	5.69E-02	1.09	4.84E-01
5-amino-levulinate	13.07	6.64E-02	-1.04	6.66E-01
5-aminopentanoate	21.98	7.05E-03	-3.00	8.35E-02
5-deoxy-α-ribose 1-phosphate	-7.19	2.28E-01	-4.59	2.59E-01
5-fluorocytosine	51.17	2.35E-02	-1.70	2.22E-01
5-hydroxyindole acetaldehyde	3.58	1.42E-01	1.02	8.74E-01
5-hydroxytryptophol	8.20	2.96E-02	-1.01	9.66E-01
5-methylcytosine	59.33	9.66E-02	1.03	7.58E-01
5-oxoproline	51.17	2.35E-02	-1.70	2.22E-01
6,7-dehydrobaicalein	11.34	1.99E-01	-1.50	3.02E-01
6-pyruvoyl tetrahydropterin	5.44	5.57E-02	1.09	6.64E-01
7,8-diaminopelargonate	-3.30	4.72E-02	-3.19	1.93E-02
7,8-dihydroneopterin	3.73	1.61E-01	-1.13	5.73E-01
8-amino-7-oxononanoate	9.69	1.24E-01	1.39	4.77E-02
9α-hydroxyandrosta-1,4-diene-3,17-dione	5.26	6.90E-02	1.89	3.59E-01
a (-)-ureidoglycine	2.99	5.34E-01	-2.93	1.71E-01
AAI	1.45	7.61E-01	-1.35	7.35E-01
acetyl phosphate	4.38	2.06E-01	1.12	8.85E-01
acrylamide	5.62	1.03E-01	1.87	4.07E-02
adenine	9.53	1.15E-01	-1.11	6.38E-01
adenosine	5.84	5.07E-02	1.14	4.68E-01
adenosine 3'-monophosphate	5.18	4.87E-03	1.09	6.81E-01
aldehydo-D-mannose	15.11	1.76E-01	1.16	1.69E-01
all-trans-retinol	33.97	1.43E-01	1.45	1.68E-01
androst-4-ene-3,17-dione	4.88	6.91E-02	1.21	1.83E-01

Supplementary Table 5 – CONTINUED

hypoxanthine	14.50	1.70E-01	-1.61	1.74E-01
indole	3.71	4.13E-02	1.03	8.53E-01
indole-3-acetamide	6.07	9.98E-02	-1.15	5.21E-01
indole-3-acetate	3.58	1.42E-01	1.02	8.74E-01
indole-3-acetonitrile	13.62	6.59E-02	1.70	3.73E-02
indole-3-glycol	8.20	2.96E-02	-1.01	9.66E-01
indole-3-glycol aldehyde	3.58	1.42E-01	1.02	8.74E-01
keto-D-fructose	15.11	1.76E-01	1.16	1.69E-01
keto-L-sorbose	15.11	1.76E-01	1.16	1.69E-01
L,L-diaminopimelate	11.15	1.47E-01	-1.12	6.34E-01
L-1-glycerophosphorylethanolamine	30.09	2.47E-02	-1.09	5.00E-01
L-2,4-diaminobutanoate	-1.65	2.96E-02	-2.16	2.01E-01
L-4-hydroxyglutamate semialdehyde	59.33	9.66E-02	1.03	7.58E-01
L-allo-threonine	73.19	2.42E-02	-1.51	4.82E-01
L-arginine	13.20	1.34E-01	-2.22	4.09E-01
L-ascorbate	-1.15	5.54E-01	-1.45	6.65E-02
L-asparagine	1.04	9.11E-01	-2.59	1.36E-01
L-aspartate	4.21	1.44E-01	-2.93	1.70E-01
L-aspartyl-4-phosphate	12.45	9.77E-03	-1.16	6.10E-01
L-canavanine	15.47	1.40E-01	-1.45	5.43E-01
L-citrulline	3.80	5.38E-02	1.31	4.90E-01
L-cystine	16.53	7.61E-02	1.16	2.87E-01
L-glutamate	59.33	9.66E-02	1.03	7.58E-01
L-glutamate-5-semialdehyde	13.07	6.64E-02	-1.04	6.66E-01
L-glutamine	20.08	4.92E-02	-1.18	7.63E-01
L-gulonate	4.99	1.72E-01	1.33	8.38E-02
L-histidine	-1.73	5.08E-01	-1.23	3.69E-01
L-homoserine	73.19	2.42E-02	-1.51	4.82E-01
L-homoserine lactone	38.78	6.15E-02	-1.57	3.70E-01
linamarin	45.57	6.96E-02	-1.30	5.05E-01
linoleate	1.78	3.15E-01	1.69	6.18E-01
linustatin	1.45	6.28E-01	1.64	2.36E-01
L-isoglutamine	20.08	4.92E-02	-1.18	7.63E-01
L-isoleucine	16.41	1.18E-01	-3.02	1.09E-01
L-kynurenine	3.49	2.50E-02	1.09	4.92E-01
L-leucine	16.41	1.18E-01	-3.02	1.09E-01
L-lysine	86.41	1.28E-01	-1.24	7.17E-01
L-methionine	9.91	1.57E-01	1.09	6.16E-01
L-ornithine	70.97	1.86E-02	-1.44	6.59E-01
lotaustralin	35.67	4.30E-02	-1.07	8.24E-01

Supplementary Table 5 – CONTINUED

L-phenylalanine	32.86	1.75E-01	1.18	5.50E-01
L-proline	49.09	5.53E-02	1.12	8.11E-01
L-serine	3.07	2.36E-02	-3.25	3.03E-02
L-sorbopyranose	15.11	1.76E-01	1.16	1.69E-01
L-threo-3-phenylserine	3.60	8.19E-02	-1.96	1.83E-02
L-threonine	73.19	2.42E-02	-1.51	4.82E-01
L-tryptophan	-1.07	8.49E-01	-1.95	4.90E-02
L-tyrosine	109.86	3.42E-02	-1.29	5.68E-01
L-valine	21.98	7.05E-03	-3.00	8.35E-02
L-α-amino-ε-keto-pimelate	75.32	8.79E-02	-1.16	4.52E-01
malonate semialdehyde	1.15	5.86E-01	-2.00	3.02E-02
maltose	3.09	8.95E-02	3.28	5.02E-01
menadiol	6.07	9.98E-02	-1.15	5.21E-01
meso-diaminopimelate	11.15	1.47E-01	-1.12	6.34E-01
methyl-1,4-benzoquinol	9.66	5.40E-02	1.00	9.69E-01
methyl-1,4-benzoquinone	5.48	2.91E-01	-1.19	4.54E-01
N,N'-diacetylchitobiose	3.01	3.52E-01	-1.71	1.06E-01
N,N-dimethylaniline	4.34	4.59E-02	1.16	1.47E-01
N,N-dimethylaniline-N-oxide	7.67	2.18E-02	1.14	5.95E-01
N,N'-dimethyl-p-phenylenediamine	42.10	2.23E-03	-1.00	9.99E-01
N1-acetylspermidine	32.95	2.58E-02	1.30	6.49E-02
N2-succinyl-L-ornithine	6.99	1.10E-01	1.07	4.11E-01
N5-formyl-N5-hydroxy-L-ornithine	3.55	3.75E-01	-1.24	7.16E-01
N5-hydroxy-L-ornithine	1.16	8.52E-01	-1.15	8.30E-01
N-acetyl-L-citrulline	1.52	3.25E-01	-1.80	1.04E-01
N-acetyl-L-glutamate	75.32	8.79E-02	-1.16	4.52E-01
N-acetyl-L-glutamate 5-semialdehyde	2.30	8.98E-02	1.11	5.97E-01
N-acetyl-L-ornithine	13.20	1.34E-01	-2.22	4.09E-01
N-acetylmuramate	17.16	4.63E-02	-1.28	5.12E-01
N-acetylputrescine	21.90	1.89E-01	-1.05	8.81E-01
N-acetyl-α-D-mannosamine	3.00	3.26E-01	1.41	6.59E-02
N-acetyl-β-D-galactosamine	3.00	3.26E-01	1.41	6.59E-02
N-acetyl-β-D-glucosamine	3.00	3.26E-01	1.41	6.59E-02
N-acetyl-β-D-glucosamine(anhydrous)-N-acetylmuramate	9.69	1.20E-01	-1.03	3.14E-01
n-butanoate	1.89	3.94E-01	-1.51	2.73E-01
N-carbamoyl-L-aspartate	-1.15	5.54E-01	-1.45	6.65E-02
N-carbamoylputrescine	16.41	1.18E-01	-3.02	1.09E-01
N-ethylammelide	13.62	6.59E-02	1.70	3.73E-02
N-ethylammelide	13.62	6.59E-02	1.70	3.73E-02

Supplementary Table 5 – CONTINUED

N-formylkynurenine	6.80	3.03E-01	-1.01	9.55E-01
N-formyl-L-glutamate	15.02	1.85E-02	-1.24	6.69E-01
nicotinamide	-1.21	7.95E-01	-1.01	9.62E-01
nicotinate	38.78	6.15E-02	-1.57	3.70E-01
nicotine-1'-N-oxide	13.67	1.95E-01	-1.01	9.67E-01
N-α-acetyl-L-methionine	31.03	1.38E-01	-1.14	6.90E-01
O-acetyl-L-serine	59.33	9.66E-02	1.03	7.58E-01
octanal	41.57	2.15E-02	-1.04	8.25E-01
octanoate	11.58	1.95E-02	1.18	2.64E-01
octanol	-3.21	1.20E-01	-2.02	2.16E-01
oleate	-1.18	6.16E-01	-1.05	9.10E-01
oxaloacetate	3.58	3.07E-03	1.00	9.99E-01
PAI-1	2.54	5.66E-02	1.47	1.50E-01
PAI-2	12.23	3.58E-02	-1.03	8.20E-01
palmitate	-4.79	1.35E-01	-3.12	8.29E-02
palmitoleate	3.42	4.64E-02	-1.36	6.96E-01
petroselinate	-1.18	6.16E-01	-1.05	9.10E-01
phenazine-1-carboxylate	8.66	6.91E-02	-1.05	6.04E-01
phosphocholine	1.53	3.58E-01	-1.20	8.32E-01
phosphonoacetaldehyde	2.93	8.81E-02	-1.19	4.27E-01
precorrin-3A	2.25	3.04E-01	5.60	2.48E-02
preQ0	15.02	1.85E-02	-1.24	6.69E-01
pristanate	-2.15	4.94E-01	2.08	2.46E-01
protoporphyrin IX	3.38	4.60E-02	1.01	9.81E-01
protoporphyrinogen IX	2.68	9.42E-02	1.87	3.41E-01
pseudouridine 5'-phosphate	1.22	8.30E-01	-2.07	2.23E-01
putrescine	6.08	1.71E-01	-1.04	8.76E-01
pyocyanin	3.43	3.16E-02	-2.66	5.00E-02
pyridoxal	5.40	1.23E-01	-1.32	3.98E-01
pyridoxamine	26.44	1.53E-01	1.01	9.42E-01
pyrroline-hydroxy-carboxylate	51.17	2.35E-02	-1.70	2.22E-01
pyruvate	1.15	5.86E-01	-2.00	3.02E-02
queuine	44.88	2.27E-02	-1.38	5.44E-01
riboflavin	13.17	6.90E-02	1.08	2.41E-01
S-adenosyl 3-(methylthio)propylamine	6.13	1.77E-01	1.01	9.18E-01
S-adenosyl-L-homocysteine	9.44	2.57E-03	1.11	3.67E-01
salicylaldehyde	-1.21	7.95E-01	-1.01	9.62E-01
salicylate	-1.18	5.54E-01	-1.42	1.47E-01
shikimate 3-phosphate	2.68	2.20E-01	1.07	8.89E-01
S-methyl-5'-thioadenosine	47.30	8.03E-02	1.05	8.54E-01

Supplementary Table 5 – CONTINUED

sn-glycerol 1-phosphate	-1.67	3.42E-01	-1.20	5.65E-01
sn-glycerol 3-phosphate	-1.67	3.42E-01	-1.20	5.65E-01
spermidine	38.96	1.10E-01	-1.93	5.61E-01
S-sulfo-L-cysteine	10.47	3.04E-02	1.15	1.78E-01
succinate	1.73	5.00E-01	-1.79	1.55E-01
sucrose	3.09	8.95E-02	3.28	5.02E-01
sucrose-6F-P	50.12	2.74E-02	1.09	2.74E-01
thiamin	127.48	1.18E-01	-1.08	7.00E-01
trans-4-hydroxy-L-proline	13.07	6.64E-02	-1.04	6.66E-01
trans-cinnamate	9.66	5.40E-02	1.00	9.69E-01
ubiquinol-6	-1.06	8.34E-01	-1.05	8.98E-01
UDP	8.50	1.88E-02	-1.43	3.59E-01
UDP-2,3-diacetamido-2,3-dideoxy-α-D-glucuronate	-6.03	2.54E-01	-1.41	6.99E-01
UDP-2,3-diacetamido-2,3-dideoxy-α-D-mannuronate	-6.03	2.54E-01	-1.41	6.99E-01
UDP-N-acetyl-α-D-glucosamine	2.11	5.26E-01	-2.21	3.28E-01
UDP-N-acetyl-α-D-mannosamine	2.11	5.26E-01	-2.21	3.28E-01
UDP-α-D-galactofuranose	-1.32	7.88E-01	-1.30	5.30E-01
UDP-α-D-galactopyranose, UDP-galactose	-1.32	7.88E-01	-1.30	5.30E-01
UDP-α-D-galactose	-1.32	7.88E-01	-1.30	5.30E-01
UDP-α-D-glucose	-1.32	7.88E-01	-1.30	5.30E-01
UMP	1.22	8.30E-01	-2.07	2.23E-01
uracil	-1.96	5.58E-03	-1.52	7.26E-02
uridine 2'3'-cyclic monophosphate	5.65	2.84E-02	1.13	6.84E-02
uridine 3'-monophosphate	1.22	8.30E-01	-2.07	2.23E-01
vernolate	-1.71	6.19E-01	1.46	7.84E-01
xanthine	16.38	2.82E-02	-1.54	4.80E-01
α,α-trehalose	3.09	8.95E-02	3.28	5.02E-01
α-D-glucose	15.11	1.76E-01	1.16	1.69E-01
α-linolenate	-2.00	2.11E-01	1.40	6.03E-01
α-ribazole	5.68	1.89E-01	1.07	7.01E-01
β-D-cellobiose	3.09	8.95E-02	3.28	5.02E-01
β-D-fructofuranose	15.11	1.76E-01	1.16	1.69E-01
β-D-mannose	15.11	1.76E-01	1.16	1.69E-01
β-D-ribosylnicotinate	1.82	2.28E-01	-1.82	5.82E-01
Δ1-piperideine-2-carboxylate	1.33	3.69E-01	-1.21	6.59E-01

APPENDIX B

SUPPLEMENTARY FIGURES

Supplementary Figure 1. Growth Curve of *P. aeruginosa* PAO1 in chronic wound medium. Each line represents growth of P. aeruginosa in separate batches of medium on different days. Growth rate (k) was measured at 1.01 $\pm$ 0.03 h^{-1}. Doubling time was calculated to be 41.8 $\pm$ 1.2 minutes.

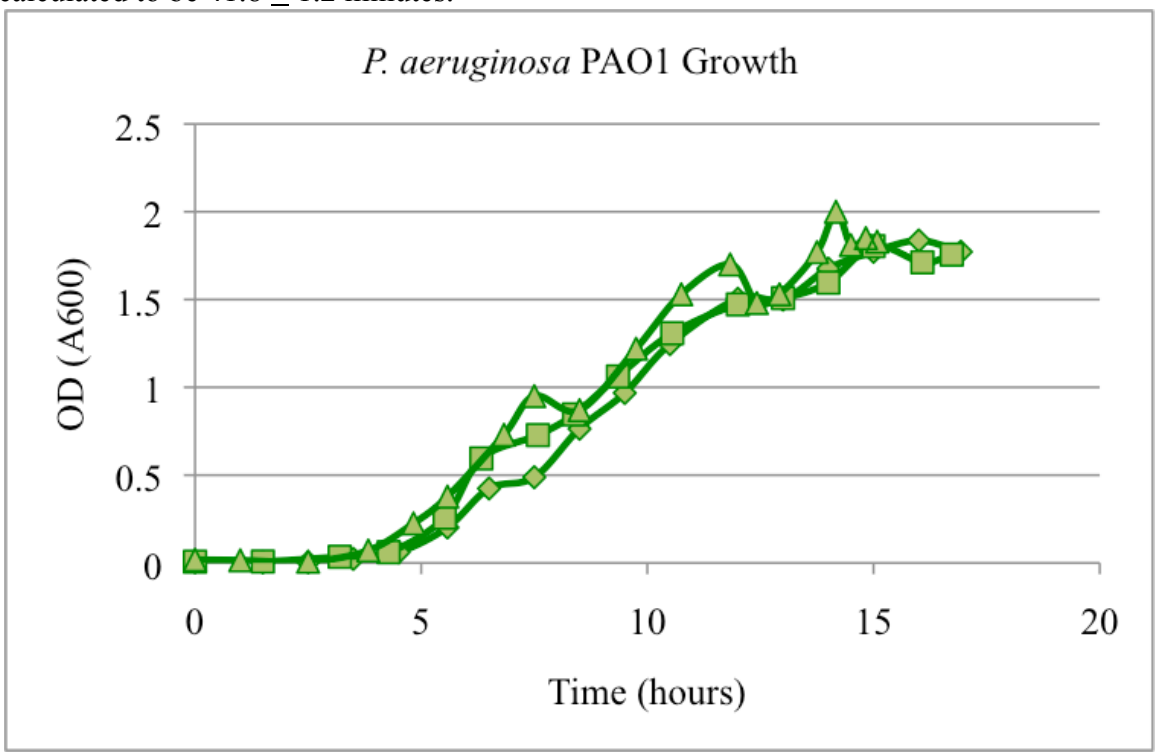

Supplementary Figure 2. MIC of ciprofloxacin was determined as 0.06 mg/L for *P. aeruginosa* PAO1 in chronic wound medium.

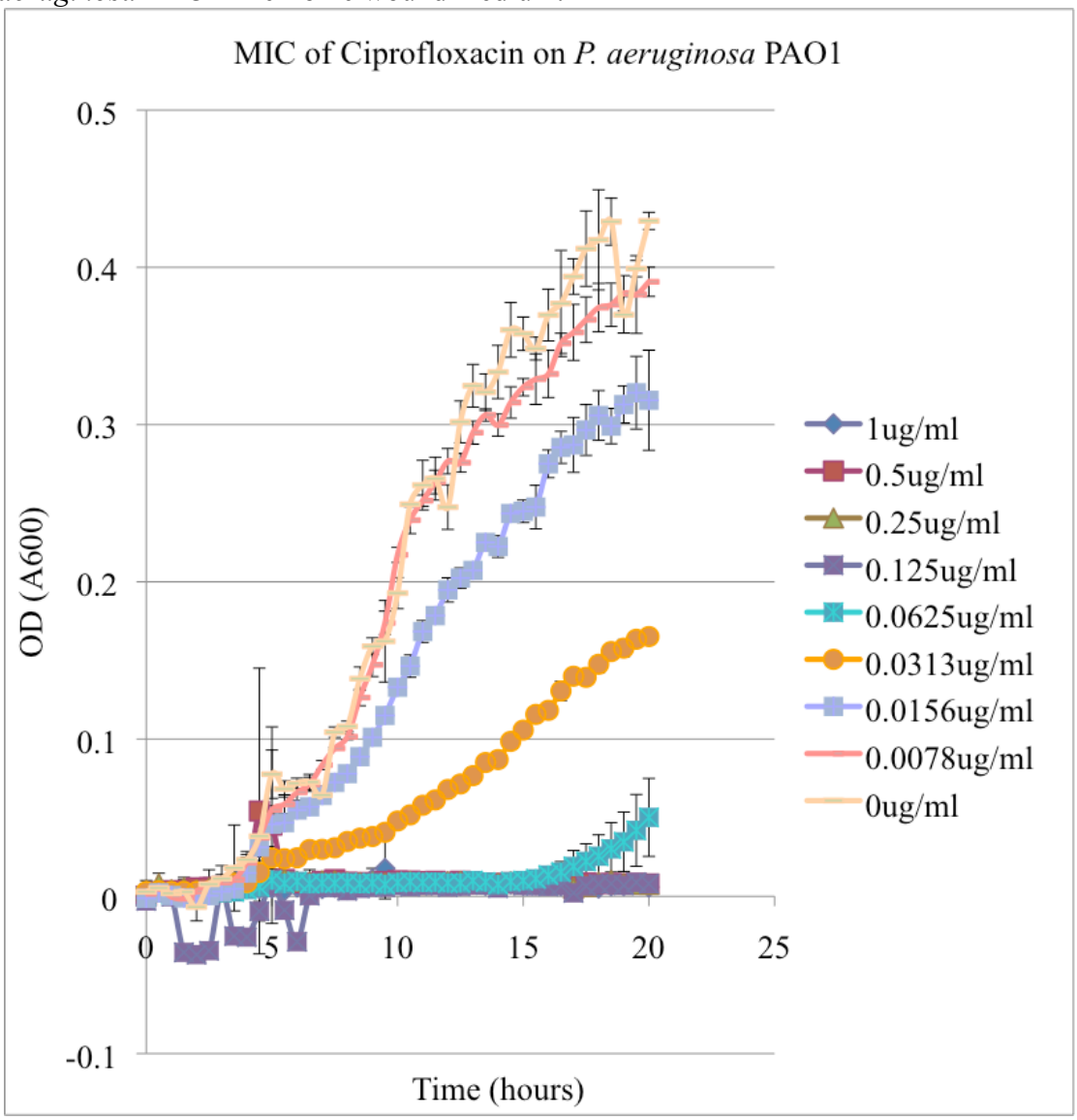

Supplementary Figure 3. Box plot of expression after GC-RMA normalization. All samples were normalized together. Samples from left to right are: Treated 2, Control 3, Treated 3, Planktonic 1, Planktonic 2, Planktonic 3, Control 1, Control 2, Treated 1. Figure was created in FlexArray version 1.6.3.

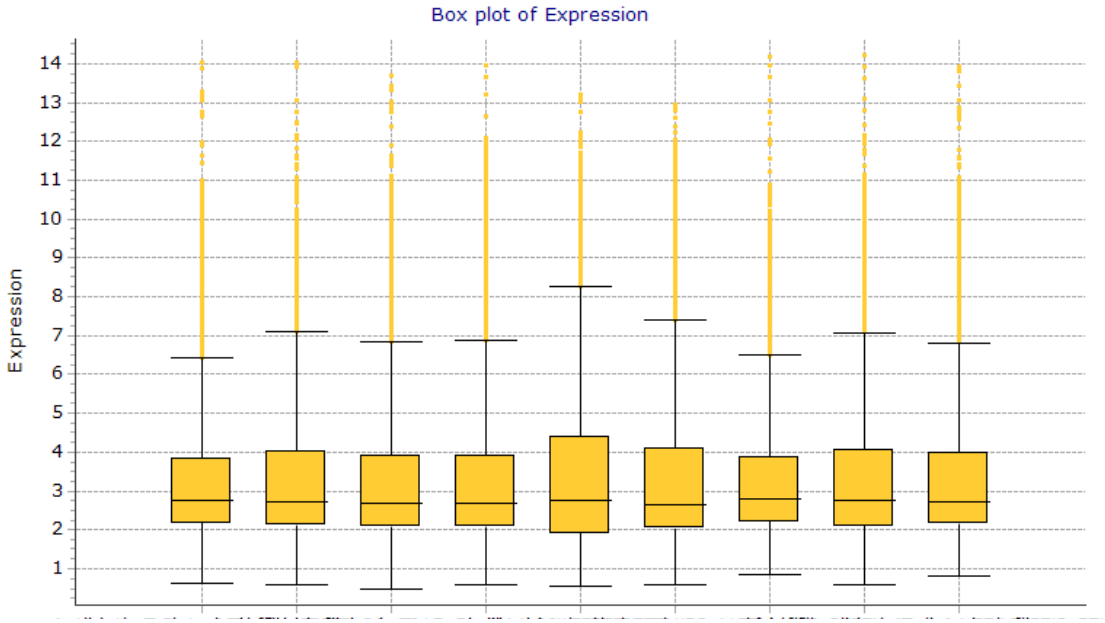

Supplementary Figure 4. Volcano plot of adjusted P values (Benjamini-Hochberg). Negative values on the X-axis represent transcripts up-regulated during biofilm growth and positive values represent transcripts down-regulated during biofilm growth. 2-fold change is indicated by solid vertical lines.

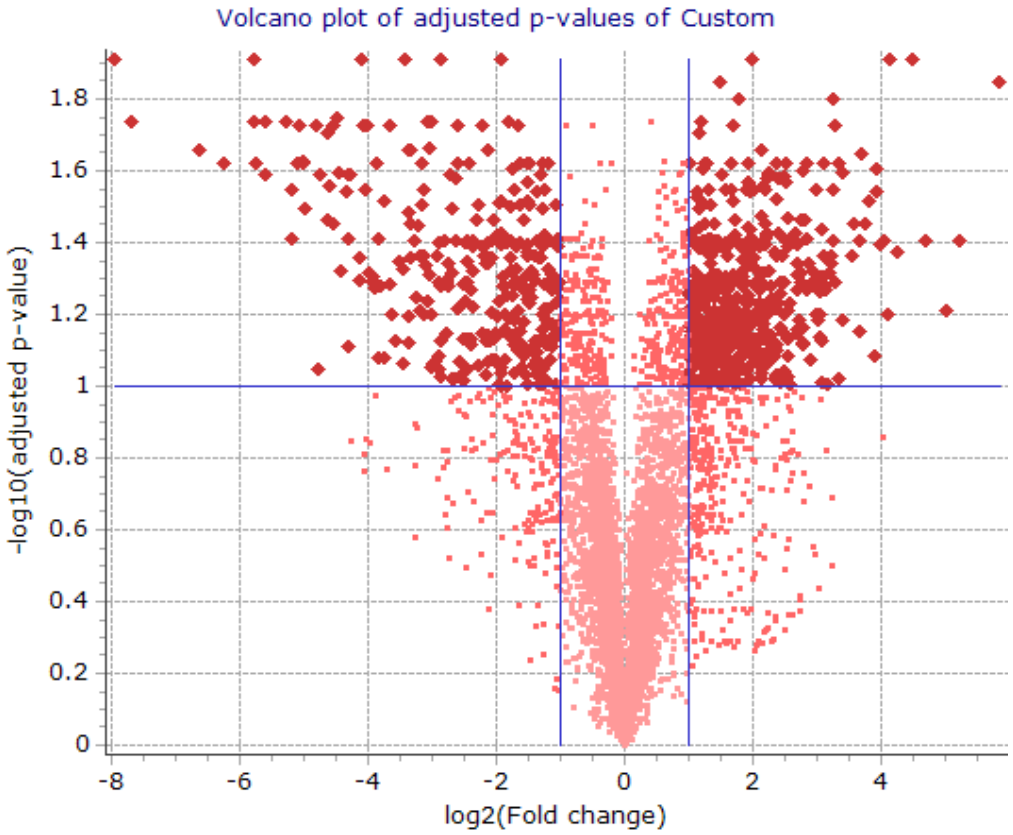

Supplementary Figure 5. Volcano plot of adjusted P values. Negative values on the X-axis represent transcripts down-regulated after ciprofloxacin treatment and positive values represent transcripts up-regulated by ciprofloxacin treatment. 2-fold change is indicated by solid vertical lines.

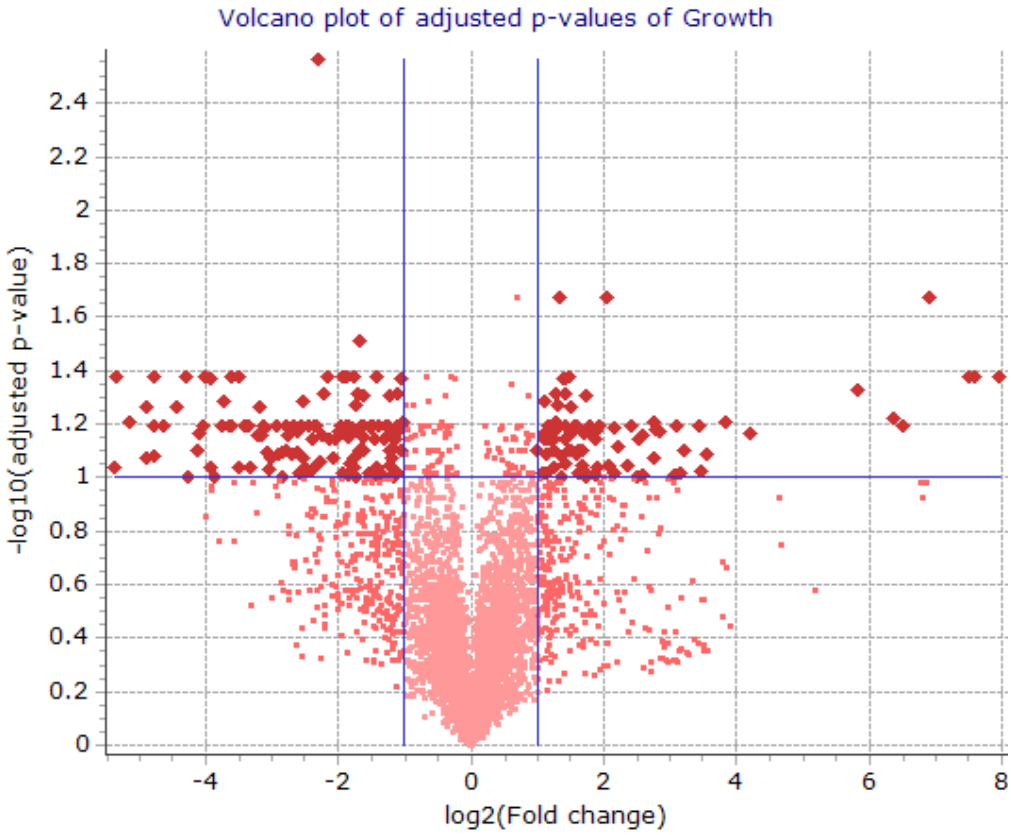

Supplementary Figure 6. Volcano plot of T6SS genes down-expressed and up-expressed in biofilms.

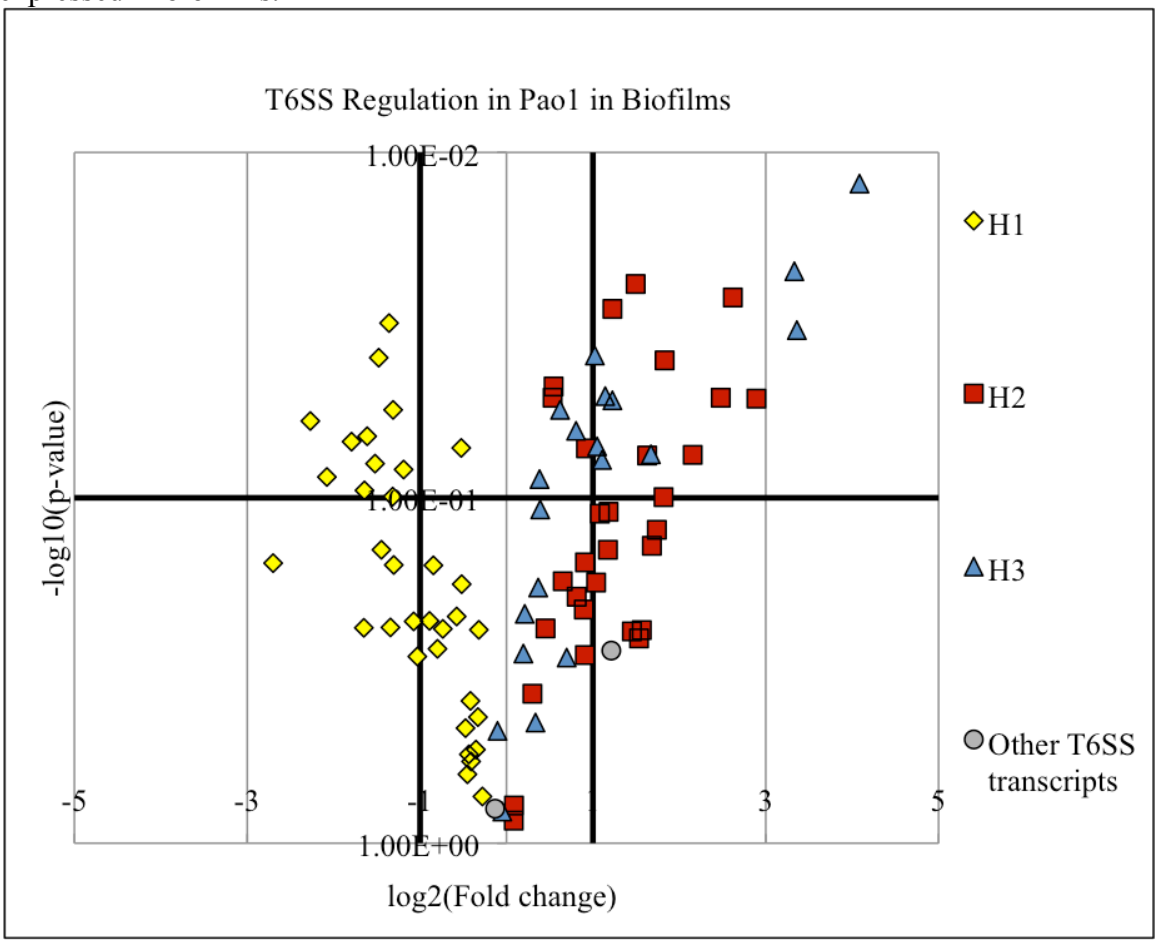
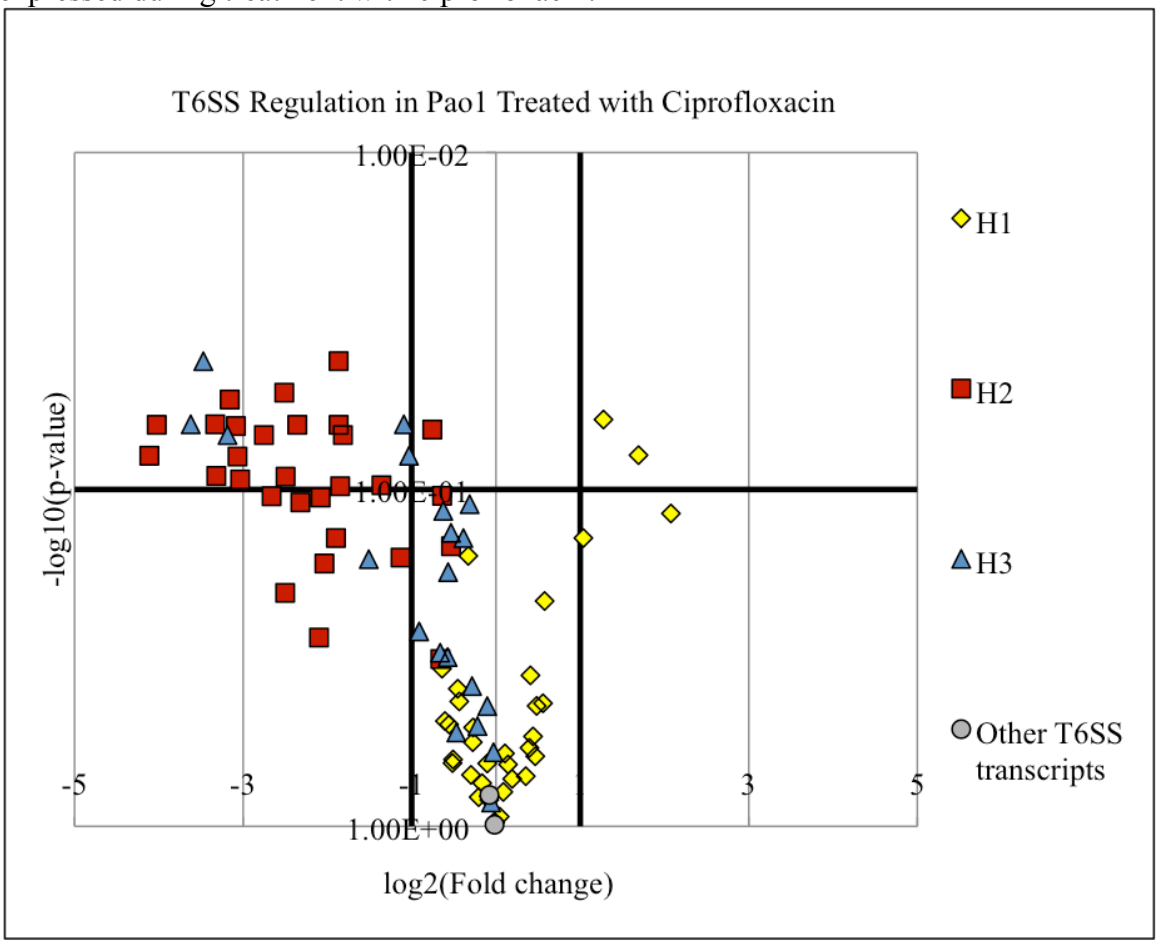
Supplementary Figure 7. Volcano plot of T6SS genes down-expressed and up-expressed during treatment with ciprofloxacin.